UNIVERSITY OF NAPLES FEDERICO II

DEPARTMENT OF PHARMACY

PhD program in Pharmaceutical Sciences

"Role of Transsulfuration pathway in vascular complications associated with Metabolic Syndrome: H_2S donors as a new potential therapeutic strategy".

PhD student:
Martina Smimmo

Coordinator
Prof. ROSARIA MELI

Tutor
Prof. MARIAROSARIA BUCCI

Co-tutor
Prof. ELISABETTA PANZA

XXXVI CYCLE (2021-2023)

Table of Contents

LIST OF ABBREVIATIONS

- **3-MST** (3-mercaptopyruvate sulfurtrasferase)
- **5HT** (Serotonin)
- **ACE** (angiotensin-converting enzyme)
- **Ach (**Acetylcholine)
- **ADA** (American Diabetes Associatiosh)
- **AHA** (American Heart Association)
- **ATP III** (Adult Treatment Panel III)
- **BAEC** (Bovine Aortic Endothelial Cells)
- **BSA** (Bovin Serum Albumin)
- **Ca-CAM** (Calcium- Calmodulin)
- **CAD** (Coronary Artery Disease)
- **CaM (**Calmodulin)
- **CaM** (calmodulin)
- **CAT** (Cysteine aminotransferase)
- **Cav-1** (Caveolin-1)
- **CBS** (cystathionine β-synthase)
- **CE** (Cholesteryl Ester)
- **Cer** (Ceramide)
- **cGKs** (cGMP-dependent protein kinases)
- **cGMP (**Cyclic guanosine monophosphate)
- **CHO** (Chinase Hamster Ovary cells)
- **CSE** (Cystathionine γ-liase)
- **CVD** (Cardiovascular Disease)
- **DASH** (Dietary Approches to Stop Hypertansion)

- **ECs** (Endothelial Cells)
- **EDHF** (Endothelium-Derived Hyperpolarizing Factor)
- **EDRF** (endothelial-derived relaxing factor)
- **eNOS (**Endothelial Nitric Oxide Synthase)
- **ER** (Endoplasmic Reticulum)
- **ET-1** (Endothelin)
- **ETHE1** (Persulfide dioxygenase)
- **FFA (**free fatty acids)
- **GLP-1 (**glucagon-like peptide-1)
- **GLUT (**Glucose transporter)
- **GTP (**Guanosine 5'-triphosphate)
- **H&E** (Hematoxylin and Eosin)
- **H2DFC**-DA (fluorescence probe 2',7'-dichlorofluorescein-diacetate)
- **H_2S** (Hydrogen Sulfide)
- **HDL** (High-Density Lipoprotein)
- **HG** (High Glucose)
- **IBVD** (Inflammatory Based Vascular Diseases)
- **IBVD (**Inflammatory-based vascular disease)
- **IDF** (International Diabetes Federation)
- **IFG** (impaired fasting glucose)
- **Iso (**Isoprenaline)
- **L-Cys** (L-cysteine)
- **L-NIO** (N5-(1-Iminoethyl)-L-ornithine dihydrochloride
- **LAD** (Left Anterior Ascending artery)
- **LDL** (Low-Density Lipoprotein)

- **MHC-II** (Major Histocompatibility complex class-II)
- **MLCK** (Myosin Light Chain Kinase)
- **MS** (Metabolic Syndrome)
- **NCEP** (Cholesterol Education Program)
- **NHLB1** (National Heart, Lung, and Blood Institute)
- **NO** (Nitric Oxide)
- **NOD mice (**Non-obese diabetic mice)
- **NOS** (Nitric Oxide Synthetase)
- **PDEs** (Phosphodiesterases)
- **PE** (Phenylephrine)
- **PFA** (paraformaldehyde)
- **PGI2** (Prostacyclin)
- **PLP** (Pyridoxal 5'-phosphate)
- **PPAR-γ** (Peroxisome Proliferator-Activated Receptor-γ)
- **ROS (**Reactive oxygen species)
- **S1P (**Sphingosine-1-Phosphate)
- **sGC (**soluble Guanylate Cyclase)
- **SGLT** (Sodium-glucose co-transporters)
- **SLs** (Sphingolipids)
- **SP** (Sodium Palmitate)
- **SPT (**Serine-Palmitoyl Transferase)
- **SPTLC1 (**Long chain base subunit 1)
- **SPTLC2 (**Long chain base subunit 2)
- **SQRLD** (Sulfide Quinone Oxidoreductase)
- **SUR-1** (Sulphonyl-Urea Receptor-1)
- **T1DM** (Type 1 Diabetes Mellitus)

- **T2DM** (Type 2 Diabetes Mellitus)
- **TAC** (Transverse Aortic Constriction)
- **TSP** (transsulfuration pathway)
- **TZD (**Thiazolidinedione)
- **VASP** (Vasodilator-stimulated phosphoprotein)
- **VDCCs** (Voltage-Dependent Calcium Channels)
- **VSMC** (Vascular Smooth Muscle Cells)

ABSTRACT

Embarking on a journey to unravel the intricate mechanisms underlying vascular complications in metabolic disorders, during my Ph.D. program I was devoted to a comprehensive exploration of Metabolic Syndrome (MS), Type 1 Diabetes (T1D), and coronary atherosclerosis. This ambitious endeavor was divided into three distinct but interconnected projects, each shedding light on novel aspects of these complex pathologies. I concluded my Ph.D. program at Neilos s.r.l company where I delved into the nutraceutical market, assessing the positioning of a potential nutraceutical product rooted in my research.

In the first part of my Ph.D. at University of Naples Federico II, by using *in vitro* and *ex vivo* approaches, I elucidated the impairment of the hydrogen sulfide (H_2S) pathway in vascular complications associated with Metabolic Syndrome. In the *in vitro* model simulating hyperlipidemic/hyperglycemic conditions, several hallmarks of endothelial dysfunction were observed, including eNOS/NO signaling impairment, ROS overproduction, and a reduction in CSE-derived H_2S. Transitioning to an *ex vivo* model using *db/db* mice, decreased CBS and CSE expression in the aorta were found, leading to reduced L-cysteine-induced vasorelaxation. Molecular analysis revealed altered eNOS/NO signaling with changes in the eNOS/Cav-1 ratio, along with reduced Ach- and Iso-induced vasorelaxation. *In vivo* treatment with the H_2S donors NaHS and Erucin ameliorated vascular dysfunction observed in *db/db* mice without impacting eNOS/NO signaling, further highlighting a specific action on smooth muscle component rather than the endothelium. In *db/db* aortas, reduced cGMP levels were also detected, implicating a defective sGC/cGMP signaling. NaHS and Erucin administration restored

cGMP content. This beneficial effect involves an increased sGC activity, due to enzyme persulfidation, coupled with PDE5 inhibition, demonstrated in sGC overexpressing cells. Collectively, these results demonstrate a pivotal role of reduced cGMP levels in impaired vasorelaxation in a murine model of MS involving an impairment of both H_2S and NO signaling.

In the second part of my Ph.D. at University of Naples Federico II, I shifted focus to Type 1 Diabetes (T1D) and its cardiovascular complications, using Non-Obese Diabetic (NOD) mice, which exhibit spontaneous type 1 diabetes. The characterization of vascular dysfunction was performed, noting a marked reduction in Ach- and L-cys induced vasorelaxation. Treatment with H_2S donors (Erucin and NaHS) positively impacted endothelial-dependent vasodilation, specifically targeting the eNOS/NO pathway. Remarkably, this positive effect on vascular function was achieved without altering blood glucose levels, underscoring the specific targeting of H_2S donors to endothelial pathways. Expanding the scope of our study, we investigated the immune profile in diabetic mice, finding elevated pro-inflammatory T-helper (Th) cells, specifically Th1 and Th17, in diabetic condition. Interestingly, treatment with H_2S donors effectively attenuated this immune imbalance, suggesting a broader immunomodulatory role for H_2S in Type 1 diabetes. The key findings emphasized the versatility of H_2S donors in ameliorating vascular dysfunction and influencing the immune profile, presenting a potential therapeutic way for both MS and T1D.

In the third part of my Ph.D., at Weill Cornell University of New York, I studied the role of sphingolipid pathway in the onset and progression of atherosclerosis. The ER membrane protein Nogo-B has been identified as a key negative regulator of SLs synthesis, however its role in macrophages

is unclear. Therefore, here, I investigated how the loss of Nogo-B impacts macrophage functions in atherosclerosis. *In vivo* data showed that the loss of Nogo-B specifically in macrophage cells, enhanced atherosclerotic lesions increasing necrotic core and plaque vulnerability elevating the risk of plaque rupture, a critical consequence in coronary artery disease (CAD). The *in vitro* model, using primary peritoneal macrophages isolated from Nogo-Bf/f ApoE$^{-/-}$ and NgKO-ApoE$^{-/-}$ mice, revealed that the absence of Nogo-B led to an accumulation of total ceramides and hexosilceramides, supporting Nogo-B's inhibitory role on serine palmitoyltransferase (SPT). Notably, lipidomic analysis indicated increased cholesterol ester (CE) levels in MΦ Nogo-B KO ApoE$^{-/-}$ macrophages, couple to a heightened expression of cholesterol biosynthetic genes. Linked to the specific depletion of Nogo-B in macrophages, an overactivation of the inflammasome, a key event in the inflammatory response associated with atherosclerosis, was observed. Intriguingly, this overactivation appeared to be independent of Nogo-B's canonical function as an SPT enzyme regulator. These findings unveil a novel and critical role of Nogo-B in macrophages during the development of atherosclerosis.

During the latter part of my Ph.D., I spent six months at Neilos S.r.l, where my focus was on positioning a novel formulation based on *Eruca sativa* Mill. extract as a supportive treatment for Metabolic Syndrome. Market analysis identified six existing formulations for MS, primarily targeting glucose and/or cholesterol management. In contrast to current formulations, which focus on glucose and cholesterol, *Eruca sativa* Mill. uniquely addresses cardiovascular complications, filling a critical gap in the market.

1. INTRODUCTION

1.1 Cardiovascular system

The cardiovascular system serves as a circulatory apparatus responsible for the transportation of blood and lymph to and from the tissues within the body. The components of these bodily fluids encompass cells, nutrients, metabolic byproducts, hormones, and antibodies. Comprising a central pump embodied by the heart and an intricate network of blood vessels, this physiological system establishes the conduit through which blood circulates throughout all of the body. The heart propels blood through the arterial system with substantial force, and its return to the heart occurs under reduced pressure, facilitated by the negative pressure within the thoracic cavity during inhalation and the contraction of veins by skeletal muscle. The vascular arrangement is such that blood emanating from the heart expeditiously reaches an intricate network of narrow, delicately walled vessels known as blood capillaries, situated either within or proximate to tissues throughout the entire body. Blood capillaries facilitate the exchange of fluid between blood and tissues. The fluid, known as blood filtrate, carries oxygen and metabolites and moves through the capillary wall. In the tissues, these molecules are traded for carbon dioxide and waste products. Most of the fluid returns to the distal or venous end of the blood capillaries, while the rest enters lymphatic capillaries as lymph. The lymph is then ultimately returned to the bloodstream through a network of lymphatic vessels. The blood vessels and heart form two pathways of circulation.

- Pulmonary circulation transports blood from the heart to the lungs and back to the heart.

- Systemic circulation carries oxygenated blood from the heart to the rest of the body and then returns deoxygenated blood back to the heart.

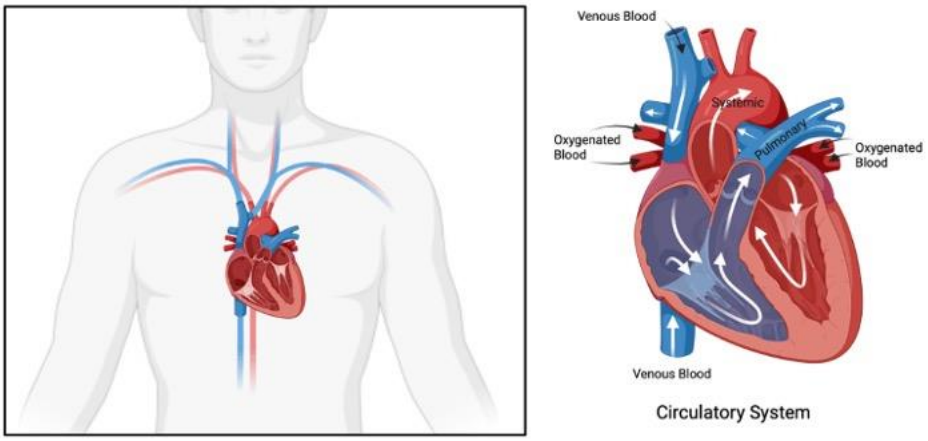

Figure 1. **The cardiovascular system.**

Blood vessels can be classified into three main types: arteries, veins, and capillaries. The main function of arteries is to transport blood to capillaries. The smallest arteries, known as arterioles, play a critical role in delivering blood to capillary networks and regulating the blood flow into these networks. Arterioles, capillary networks, and postcapillary venules form a microvascular bed that is specific to each tissue.On the other hand, veins collect blood from the microvascular bed starting from the postcapillary venule and transport it away. Arteries carry blood away from the heart, so their walls are designed to withstand the force exerted by each heartbeat. Therefore, artery walls are thicker and more robust compared to veins of similar diameter.

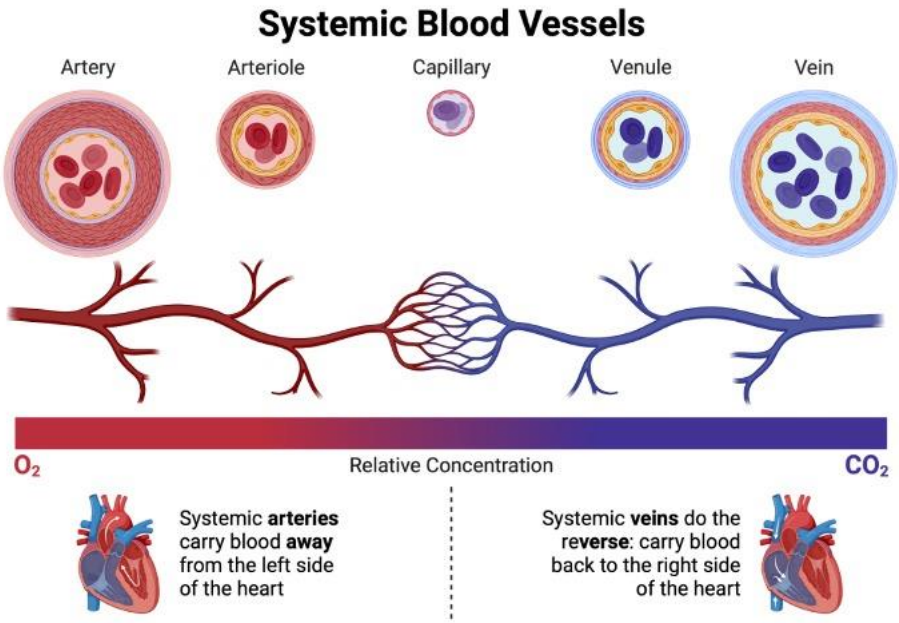

Figure 2. **Major structural features of blood vessels**

Blood vessels comprise three layers from the lumen outward. The tunica media is primarily composed of circumferentially arranged smooth muscle cells, extending from the internal to external elastic membranes. The innermost layer, tunica intima, consists of the endothelium, basal lamina, and subendothelial layer.The tunica adventitia is composed of longitudinally arranged collagenous tissue and elastic fibers. Large arteries and veins may contain vasa vasorum and nervi vascularis in the tunica adventitia. Throughout vessels, endothelial cells align parallel to blood flow, sensing shear stress, and facilitating substance diffusion. Smooth muscles in the media control vessel radius, separated from the endothelium by the internal elastic lamina. Arterioles have a single layer of smooth muscle cells, while larger vessels may have up to 20 layers. Arteries and

veins differ in the development of the media and adventitia, with arteries having a stronger and thicker media and more prominent elastic tissue.

1.1.1 Arteries general figures

Arteries are categorized into elastic and muscular types, with most arteries containing a combination of both tissues in their media. Elastic tissue allows arteries to distend and contract, aiding blood flow. Larger arteries near the heart have more elastic tissue, correlating with higher pressure. The aorta, for example, has more elastic tissue than the pulmonary trunk. Elastic tissue cushions pressure changes from the heartbeat and smoothens pressure drops by automatic recoil. In peripheral arteries, elastic tissue moderates pressure and reduces blood velocity, while smooth muscle, controlled by the autonomic nervous system, adjusts vessel caliber for blood flow regulation. Arterioles, with a media mostly composed of smooth muscle, play a crucial role in blood pressure control and regional blood flow distribution through vascular resistance effects [1]. According to Poiseuille's law, changes in the radius (lumen diameter) of a vessel result in significant changes in resistance, as vessel resistance is inversely proportional to the fourth power of the radius [2]. The diameter of resistance arteries depends on vasomotor tone and vessel structure. Vasomotor control, primarily through vasoconstriction by vascular smooth muscle cells (VSMC), rapidly adapts vessel diameter. Structural changes, initially adaptive but later maladaptive, occur in response to chronic hemodynamic variations, leading to vascular remodeling. This process contributes to vascular diseases, including hypertension. Both intrinsic and extrinsic mechanisms regulate vessel diameter. Circulating mediators like angiotensin II and catecholamines, along with locally released autonomic

nervous system mediators, provide extrinsic regulation. Intrinsic regulation involves shear stress sensing on the endothelium, leading to vasodilator release, and stretch sensing by smooth muscle cells, causing vessel lumen narrowing, known as myogenic tone. [2][3][4] [5].

1.1.2 Regulation of vascular tone by endothelium and smooth muscles cells (VSMCs)

In the human body, the circulatory system consists of about 60,000 miles of vessels of varying sizes, all lined with a simple squamous epithelium called endothelium. This endothelium is a continuous layer of flattened, elongated, and polygonal cells that are aligned in the direction of blood flow. Traditionally seen as a passive, cellophane-like membrane, the endothelium is vital for maintaining vessel wall permeability in the circulatory system [1], however, subsequent research has shifted the perspective on the endothelium, depicting it as a dynamic, diverse, dispersed organ with essential secretory, synthetic, metabolic, and immunologic functions. Along the luminal surface, endothelial cells express various adhesion molecules and receptors, playing a crucial role in blood homeostasis. The functional attributes of these cells adapt to diverse stimuli, a phenomenon referred to as endothelial activation, implicated in the pathogenesis of numerous vascular diseases. Endothelial cells actively engage in interactions between the blood and underlying connective tissue, contributing to various vessel properties:

- The maintenance of a selective permeability barrier allows for the movement of mediators between the blood and tissues. Small hydrophobic molecules, like oxygen and carbon dioxide, pass through the lipid bilayer via simple diffusion. However, water and

hydrophilic molecules (e.g., glucose, amino acids) require active transport across the plasma membrane via the transcellular or paracellular pathway. Transcellular transport involves pinocytic vesicles and receptor-mediated endocytosis for specific molecules. Fenestrations in some blood vessels facilitate the transport of larger molecules.

- The endothelium maintains a non-thrombogenic barrier by producing anticoagulants (e.g., thrombomodulin) and antithrombogenic substances (e.g., prostacyclin [PGI2] and tissue plasminogen activator). Normal endothelium prevents platelet adherence and thrombus formation, while damaged endothelial cells release prothrombogenic agents.
- The secretion of vasoconstrictors (endothelin, angiotensin-converting enzyme [ACE], prostaglandin H2, thromboxane A2) and vasodilators (nitric oxide [NO], prostacyclin) modulate blood flow and vascular resistance.
- The immune response is regulated by the interaction between lymphocytes and the endothelial surface. This interaction is mainly achieved through the expression of adhesion molecules and their receptors on the endothelial surface, as well as through the secretion of three classes of interleukins (IL-1, IL-6, and IL-8).
- Lipoproteins, particularly LDLs that contain high levels of cholesterol, and very low-density lipoproteins (VLDLs), are oxidized by reactive oxygen species (ROS) produced by endothelial cells. The modified LDLs are then quickly taken up by

macrophages and transformed into foam cells, which are a defining feature in the development of atherosclerotic plaques.

The endothelium not only acts as a structural barrier between the circulation and surrounding tissue, but it also secretes mediators that influence vascular hemodynamics. These autacoids, including nitric oxide (NO), prostacyclin (PGI2), endothelin 1 (ET-1), endothelium-derived hyperpolarizing factor (EDHF), and reactive oxygen species (ROS), play a role in regulating blood pressure and blood flow. NO and PGI2 contribute to vessel dilation: Nitric oxide (NO) triggers the activation of soluble guanylyl cyclase (sGC), resulting in the relaxation of smooth muscles. This process elevates the concentration of cyclic guanosine monophosphate (cGMP) within the cell, which in turn, activates G kinase. Ultimately, this leads to a decrease in the concentration of calcium ions (Ca^{2+}) within the smooth muscle cells, resulting in their relaxation. Prostacyclin (PGI2) binds to receptors present on smooth muscles, which stimulates the activation of cAMP-activated protein kinase A (PKA). This, in turn, leads to the phosphorylation of myosin light chain kinase (MLCK) and prevents the activation of the calcium-calmodulin complex. Additionally, endothelium-derived hyperpolarizing factor (EDHF) acts on Ca2+-dependent potassium channels, resulting in the hyperpolarization of smooth muscle cells and their subsequent relaxation. ET-1 is a potent vasoconstrictor that binds to ETA receptors on vascular smooth muscles. This causes the vessels to narrow, increasing vascular resistance and raising systemic blood pressure. Vascular smooth muscle cells (VSMCs) play a crucial role in the upkeep of blood vessels, ensuring their structural integrity and proper functioning. These cells preserve contractile tone

through a well-structured arrangement of contractile/cytoskeleton proteins and related regulatory elements within the cellular cytoplasm. They also contribute to vessel distensibility by creating, secreting, and organizing extracellular matrix (ECM) components endowed with elastic recoil and resilience properties [2]. Vascular smooth muscle contraction requires the phosphorylation of myosin light chains by myosin light chain kinase (MLCK), which is activated by Calcium-Calmodulin (Ca-CAM) before shortening can occur. The maintenance of tension in vascular smooth muscle occurs in a graded manner, without the presence of twitch tension. This allows the blood vessels to generate and sustain tension throughout their entire length. The unique ability of vascular smooth muscle to sustain tension with relatively low ATP consumption is due to a mechanism known as the "latch". The latch mechanism allows the vessel's cross bridges to stay attached under tension without being phosphorylated. This results in a slowly cycling bridge that requires approximately seven times less ATP to maintain tension at a constant length. Thin filament proteins like caldesmon and calponin also influence the phosphorylation mechanisms for tension generation. Regulatory proteins and mechanisms play a crucial role in controlling tension in vascular smooth muscle. They are responsible for regulating both the length and the rate of shortening of the muscle and ensure that it is tightly controlled by various factors. However, when these control mechanisms fail, it can lead to vascular pathologies [3]. When the mechanical stress on adult arterial walls changes, certain contractile proteins present in these walls begin to disappear gradually. These proteins include smooth muscle myosin heavy chain isoforms, alpha-actin, h-caldesmon, and calponin. Conversely, non-muscle myosin heavy chain, which is primarily expressed in fetal vessel

walls, is re-expressed in activated VSMCs [4]. As a result of this modulation, a prominent structural reorganization occurs, which leads to the loss of myofilaments and the formation of an extensive endoplasmic reticulum, as well as a large Golgi complex referred to as the synthetic phenotype. Due to increased mechanical stress caused by high blood pressure, the smooth muscle cells (SMCs) in the arterial walls lose their ability to contract, secrete more proteins, and become more responsive to growth factors produced by neighbouring SMCs. This, in turn, further stimulates hypertrophy of the medial SMCs and/or intimal hyperplasia, leading to thickening of the arterial walls [3].The condition is causing a reduction in the width of the inner space of the tube or vessel. Not only the magnitude of vasoconstriction but also the structural characteristics of the vessel wall influenced by vascular remodeling processes govern the lumen diameter of resistance arteries [5]. Remodeling involves changes in the organization of the cytoskeleton, cell-to-cell connections, and growth, apoptosis, senescence, calcification, and rearrangement of vascular smooth muscle cells (VSMCs) at the molecular and cellular levels [6]. Remodeling at the extracellular level is impacted by changes in matrix protein composition and reorganization of various proteins [6]. These include proteoglycans, fibronectin, collagens (type I and III) that provide tensile strength, and elastin, which is responsible for vascular elasticity [7]. It is still not clear whether increased pressure or other factors are responsible for the initiation of vascular remodeling. However, the endothelium likely plays a vital role. It acts as a sensor of hemodynamic and humoral factors and moderates signals to the underlying VSMCs that are critically involved in the remodeling process [8]. Arteries remodel to adapt to an increased pressure load, which is beneficial under normal conditions. Pathological

remodeling results in stiff vessels, commonly seen in hypertension. The mechanisms involve multiple cell types, signaling pathways, and factors.

1.1.3 The L-arginine/NO/cGMP/PKG pathway in the regulation of vascular tone

Endothelial-derived relaxing factor (EDRF) was discovered as a compound causing blood vessel relaxation in endothelial cells. Despite being difficult to characterize chemically for years, It is now understood that the vascular effects of EDRF are largely due to nitric oxide (NO) and its related compounds. These compounds are released by endothelial cells in various types of blood vessels. It has been demonstrated that nitric oxide (NO) is a critical gaseous signaling molecule for both the cardiovascular system and the brain [9]. NO regulates a variety of cellular functions, including the regulation of blood vessel diameter. It is synthesized in ECs by endothelial nitric oxide synthase (eNOS) and acts as an endogenous vasodilatory gas. In response to receptor-dependent agonists (bradykinin, acetylcholine, ATP) and physicochemical stimuli (shear, stretch), nitric oxide synthase catalyzes the oxidation of one of the terminal guanidine groups of L-arginine to produce NO, with the stoichiometric production of L-citrulline [10]. NOS isoenzymes are categorized into three types: nNOS, iNOS, and eNOS. nNOS is present in both the central and peripheral nervous systems, as well as in several non-neuronal cell types. iNOS is expressed by almost all nucleated cells when exposed to appropriate stimuli. Endothelial-derived NO diffuses to the neighboring smooth muscle, where it interacts with various receptor molecules, of which the soluble guanylyl cyclase (sGC) is the most well-characterized and the most important one concerning the regulation of vessel tone [10], sGC contains

heme iron in the ferrous (II) state, which is required for the binding and interaction with NO to cause enzyme activation. When NO binds with certain molecules in the body, there is a significant increase in the formation of cyclic guanosine monophosphate (cGMP). This increase in cGMP activates a protein called cGMP-dependent kinase I, which then leads to an increase in the open probability of Ca^{2+}-activated K^+ (BK)-channels. This causes smooth muscle cells to hyperpolarize, which in turn inhibits the influx of Ca^{2+} induced by agonists (figure 3), cGK-Iβ enzyme phosphorylates two substrates: IRAG and VASP. IRAG inhibits Ca2+ release and smooth muscle contraction [11]. VASP is phosphorylated at serine 239, which can monitor the activity of the NO-cGMP pathway [11]. Over the last few years, it has become apparent that cGMP kinases are involved in regulating certain cellular circuits. The cGMP-dependent protein kinases (cGKs) are part of the serine/threonine kinase family and can be found in various eukaryotes [12], [13]. The enzymes have a rod-like structure and are activated at submicromolar to micromolar concentrations of cGMP [12], [14]. The subject in question consists of three distinct functional domains: an N-terminal (A) domain, a regulatory (R) domain, and a catalytic (C) domain. The regulatory domain possesses two cGMP-binding sites that interact allosterically and bind cGMP with both high and low affinity. When both binding sites are occupied, it causes a significant change in the domain's secondary structure [15]. The catalytic domain of cGKs have the MgATP- and peptide- binding pockets. The peptide-binding domain transfers the γ phosphate from ATP to a serine/threonine residue of the target protein. The N terminus of cGKs performs three major functions: (1) dimerization - cGKs are homodimers held together by a leucine zipper present in the N terminus, (2)

activation/inhibition - cGMP binding to both sites in the R domain causes a conformational change that releases the inhibition of the catalytic center by the N terminus and allows phosphorylation of substrate proteins. Autophosphorylation of the N terminus may precede activation of heterophosphorylation. It increases the spontaneous activity of cGKI and cGKII [16], [17] and is initiated by the binding of low cGMP concentrations to the high affinity site of cGKI [18]; Smooth muscle, including uterus, vessels, intestine, and trachea, highly express the Iβ isozyme along with the Iα isozyme [19]. Smooth muscle tone is regulated by Ca2+. Deletion of cGKI did not affect cAMP-induced relaxation of vascular smooth muscle. This supports the conclusion that cAMP and cGMP use different signaling pathways in smooth muscle. Contraction is initiated by receptor-mediated generation of IP3 that releases Ca^{2+} from intracellular stores followed by an influx of extracellular Ca^{2+} through voltage-dependent Ca^{2+} channels [20]. The increase in Ca2+ triggers contraction by activating the Ca2+/calmodulin-dependent MLCK. This in turn phosphorylates RLC, leading to the activation of myosin ATPase. A decrease in Ca2+ deactivates MLCK and causes MLCP to dephosphorylate RLC. Smooth muscle contraction is modulated also at constant Ca^{2+} by changing the sensitivity of contraction to Ca^{2+} [21].

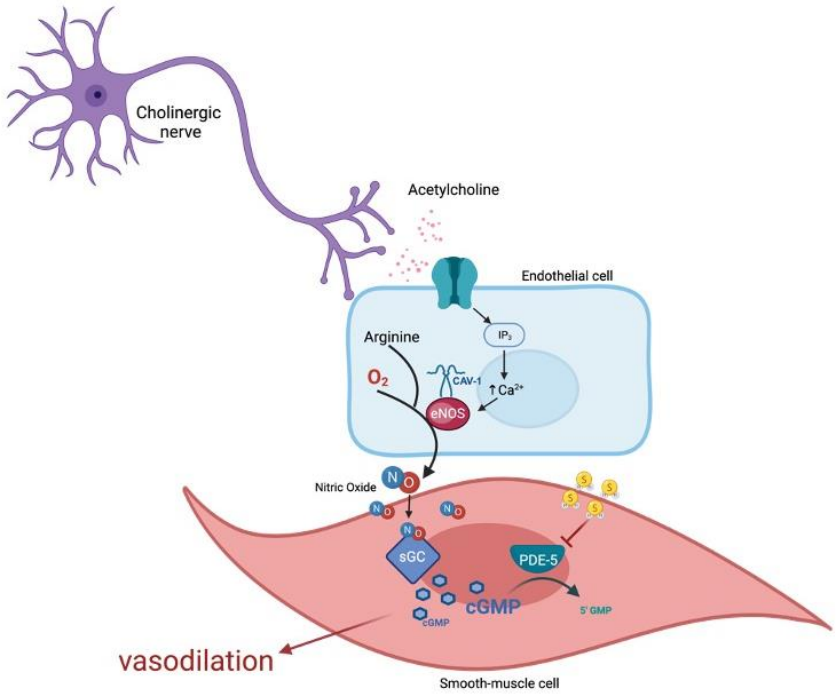

***Figure 3*. L-arginine/NO/cGMP pathway in the regulation of vascular tone.**

1.1.4 Regulation of NO production

The nitric oxide synthase found in the vascular endothelial cells is a multi-domain enzyme that consists of an N-terminal oxygenase domain. This domain includes binding sites for heme and L-arginine (Glu361) [22] and tetrahydrobiopterin (BH_4), and a reductase domain (amino acids 492–1205) containing binding sites for FMN, FAD, NADPH and calmodulin (CaM) [23]. The endothelial nitric oxide synthase (eNOS) is expressed constitutively and regulated by Ca2+/calmodulin (CaM) and phosphorylation, which activates the enzyme. On the other hand, the protein Caveolin-1 (Cav1) inhibits the enzyme activity by opposing CaM binding. Although eNOS is a constitutive enzyme, it can be affected by numerous physical (receptor-independent agonists) and chemical

(receptor-independent agonists) stimuli in vitro and in vivo. When agonists activate endothelial cells receptors, it triggers a burst of nitric oxide production that is usually 15-20 times higher than the basal production. The intensity of this sudden increase reaches its maximum in few seconds of stimulation. Despite continuous agonist presence, production returns to baseline within minutes. These responses occur with changes in Ca2+ and are eliminated by removing or chelating extracellular Ca2+. When endothelial cells are exposed to fluid shear stress, their production of NO is doubled and maintained while the stimulus lasts. Although applying shear stress to static endothelial cells increases NO production, it is not as significant as when fluid shear stress is applied, [Ca^{2+}] [24]. Activation of phosphatidylinositol 3-kinase is crucial for regulating NO production in endothelial cells stimulated mechanically. It subsequently activates serine kinases Akt and protein kinase A, which in turn phosphorylate a serine residue in the reductase domain of eNOS, this phosphorylation increases eNOS activity [25]. Although this process, which also involves the formation of an eNOS signaling complex and the association of heat shock protein 90 with eNOS [26], has been referred to as the Ca^{2+}-independent activation of eNOS. Chelating intracellular calcium ions eliminates the increase in endothelial nitric oxide synthase (eNOS) activity, which is induced by shear stress. This suggests that the production of nitric oxide (NO) still depends on the presence of calcium ions, but eNOS can now be activated even at resting calcium ion levels. Wall shear stress not only increases eNOS activity but also modulates its expression by enhancing transcription and prolonging mRNA stability [27]. In general, arterial levels of laminar shear stress (4–20 dynes/cm) are reported to increase expression of eNOS, whereas low or oscillatory shear stresses do the

opposite.[28] [29]. Endothelial cells can differentiate between various hemodynamic forces and react to them differently. Unidirectional shear stress boosts eNOS mRNA expression through a transcriptional mechanism, whereas oscillatory shear stress regulates eNOS expression through post-transcriptional events. However, cyclic stretch has little to no impact on eNOS expression.

1.2 Metabolic Syndrome (MS)

The word ‘syndrome’ originates from the Greek ‘συνδρομον’, with the meaning ‘coexistence’. In a medical context, Metabolic Syndrome is a cluster of interconnected risk factors that increase the likelihood of developing cardiovascular diseases, type 2 diabetes, and other health complications [30]. This complex and multifaceted condition is characterized by a combination of factors, including obesity, high blood pressure, elevated blood sugar levels, abnormal lipid profiles, and insulin resistance [30]. Over the past two decades, there has been a significant surge in the incidence of MS, largely attributed to the global epidemics of diabetes and obesity. According to current estimates, around 20-25% of the world's population is affected by Multiple Sclerosis (MS). [31]. Individuals with MS are twice as likely to face a heightened risk of mortality and three times more prone to heart attacks or strokes. To address this intricate health issue, precise diagnosis is essential and requires the involvement of healthcare experts. Several diagnostic criteria, which are subject to frequent revisions, assist in the management of this complex syndrome [30] [31], .

1.2.1 Clinical diagnosis and Criteria for MS

During the past decade, several different sets of criteria have been proposed for the diagnosis of metabolic syndrome. In 2001, the National Cholesterol Education Program (NCEP) Adult Treatment Panel III (ATP III) introduced straightforward diagnostic criteria based on common clinical measures. These measures include waist circumference, triglycerides, HDL-cholesterol, blood pressure, and fasting glucose levels. A diagnosis of the metabolic syndrome is established when defined abnormalities are present in any 3 of these 5 measures.

The ATP III criteria for the MS have gained broad acceptance in both clinical practice and epidemiological studies. One key advantage of these criteria is their avoidance of overemphasis on a single causative factor. The American Heart Association (AHA) and the National Heart, Lung, and Blood Institute (NHLBI) support the continued use of these criteria with minor modifications and clarifications (*Table 1*).

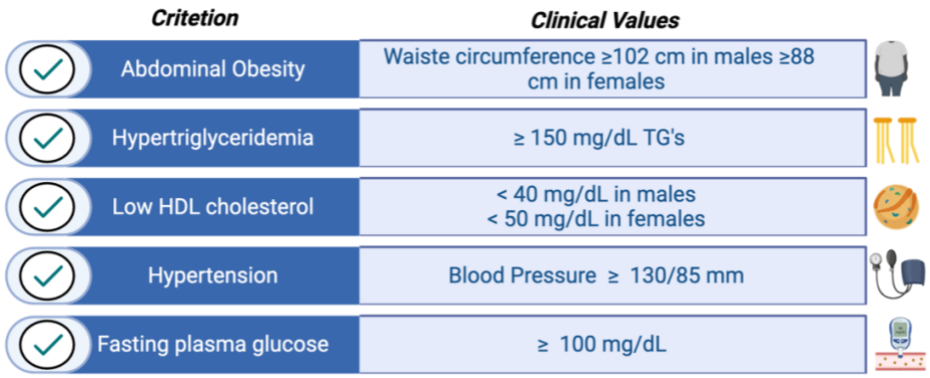

Table 1. **Diagnostic Criteria for Metabolic Syndrome**

These modifications include flexibility in waist circumference thresholds, accounting for individuals or ethnic groups with insulin resistance tendencies. They also consider triglycerides, HDL-C levels, and blood

pressure as abnormal, even when individuals are under drug treatment for these factors. The definition of elevated blood pressure has been clarified as surpassing the threshold for either systolic or diastolic pressure. The threshold for identifying elevated fasting glucose has been adjusted from ≥110 mg/dL to ≥100 mg/dL, aligning with the revised definition of impaired fasting glucose (IFG) by the American Diabetes Association (ADA). The International Diabetes Federation (IDF) has proposed clinical criteria like the updated ATP III criteria. The key difference is that the IDF recommends adjusting waist circumference thresholds for different ethnic groups due to varying relationships between waist circumference and metabolic risk factors in different populations. The updated AHA/NHLBI diagnostic criteria maintain ATP III waist circumference thresholds for Americans, except for those who are particularly prone to insulin resistance, such as Asian Americans. The IDF emphasizes increased waist circumference as a required element for diagnosing MS, as it combines both obesity and insulin resistance concepts. This facilitates the rapid identification of potential MS candidates. In the U.S. population, updated ATP III and IDF criteria identify the same individuals as having MS and Recommendations for its clinical management are nearly identical in updated ATP III and IDF reports.

Insulin resistance:

Insulin resistance occurs when cells become less responsive to insulin signals. As a result, more insulin is required to transport glucose into cells. Initially, the pancreas compensates by producing extra insulin to maintain normal blood glucose levels. However, over time, the pancreas may

struggle to keep up, leading to elevated blood glucose levels and the potential development of metabolic syndrome [32].

Central obesity:

Central obesity, also known as abdominal obesity, is a prominent feature of metabolic syndrome. It involves the accumulation of excess fat around the abdomen, particularly in the visceral adipose tissue. It is typically assessed using waist circumference measurements. In most guidelines, central obesity is defined as a waist circumference of 102 cm (40 inches) or more in men and 88 cm (35 inches) or more in women [33].

Hyperlipidemia:

Hyperlipidemia in metabolic syndrome refers to abnormal lipid profiles, particularly elevated triglycerides and low high-density lipoprotein cholesterol (HDL-C) levels. The criteria for hyperlipidemia often include triglyceride levels above 150 mg/dL and HDL-C levels below 40 mg/dL in men or 50 mg/dL in women. These lipid abnormalities contribute to atherogenic dyslipidemia, which is associated with an increased risk of atherosclerosis and cardiovascular events.

Hyperglycemia:

Hyperglycemia, or elevated blood sugar levels, is a key criterion in metabolic syndrome and often indicates impaired glucose metabolism or insulin resistance. Fasting blood glucose levels of 100 mg/dL (5.6 mmol/L) or higher are commonly used as the threshold for hyperglycemia. Hyperglycemia is a precursor to type 2 diabetes and is a major contributor to the progression of metabolic syndrome.

Hypertension:

Hypertension, or high blood pressure, is a prevalent component of MS and is closely associated with insulin resistance and obesity. Blood pressure criteria for MS often include levels of 130/85 mm Hg or higher. Individuals with a history of hypertension or taking antihypertensive medication may meet this criterion. Hypertension significantly increases the risk of cardiovascular disease and other complications associated with MS. Understanding the intricate nature of these criteria is essential for diagnosing and managing MS effectively.

1.2.2 Clinical Management and Therapeutic Approaches for MS

The primary goal of clinical management for MS is to mitigate risk of clinical cardiovascular disease and type 2 diabetes mellitus and it involves a multifaceted approach, focusing on lifestyle modifications, pharmacological interventions, and targeted risk factor control.

Lifestyle Modifications:

Dietary Interventions: A cornerstone of managing metabolic syndrome involves adopting a heart-healthy diet. Emphasis is placed on reducing saturated fats, trans fats, and refined sugars while increasing the consumption of fruits, vegetables, whole grains, and lean proteins. The DASH (Dietary Approaches to Stop Hypertension) and Mediterranean diets are often recommended [34] .

Regular Exercise: Physical activity plays a crucial role in managing MS. Regular exercise can help improve insulin sensitivity, reduce abdominal obesity, and lower blood pressure. The American Heart Association

recommends at least 150 minutes of moderate-intensity exercise or 75 minutes of vigorous-intensity exercise per week [35].

Weight Management: Achieving and maintaining a healthy body weight is vital. Weight loss can significantly improve metabolic syndrome risk factors. Even modest weight loss can lead to substantial health benefits.

Smoking Cessation: Quitting smoking is essential, as smoking is associated with insulin resistance and worsens MS components.

Pharmacological Interventions

Pharmacological treatment is a part of a complex management strategy and it is used when non-medical interventions are ineffective. One of the primary challenges in MS therapy is the inherent variability among individuals. Recognizing and respecting these individual differences is crucial for tailoring therapeutic interventions to the specific needs of each patient. The pharmacological approach can thus address this pathology from various perspectives, depending on the patient's needs or clinical indications [36].

Anti-obesity drugs

Obesity is increasingly recognized as the principal cause of the growing global burden of common diseases, such as metabolic syndrome, diabetes, cardiovascular diseases, and tumors. In this regard, in 2021, the European Commission published a document defining obesity as a chronic relapsing disease, serving as a gateway to a series of other pathologies. To date, the European Medicines Agency (EMA) has approved three drugs for the

treatment of obesity: orlistat, the combination of extended-release naltrexone/bupropion, and liraglutide.

- **Orlistat** is a specific inhibitor of pancreatic lipase with prolonged action. This drug selectively inhibits lipase, reducing the absorption of fatty acids introduced by the diet by 30%. In the presence of bile salts, lipase hydrolyzes dietary triglycerides, releasing fatty acids from glycerol. The inhibition of lipase results in a reduced degradation of triglycerides, leading to a consequent decrease in their absorption. The unabsorbed triglycerides pass through the intestinal tract and are eliminated with the feces. In several trials lasting up to 2 years, orlistat was more effective than diet alone for weight reduction and maintenance of lost weight. The primary adverse effects typically associated with orlistat are gastrointestinal, commonly occurring early during the therapy. Due to the potential reduction in the absorption of vitamins by orlistat, it is recommended to supplement a standard daily multiple-vitamin [37].
- In 2015, the EMA and FDA granted a marketing authorization for **Mysimba,** a combination of bupropion (an antidepressant also used in smoking cessation) and naltrexone (an antagonist of μ-opioid receptors, clinically used for the treatment of opioid and alcohol dependence). Bupropion is a monoamine reuptake inhibitor that enhances the synthetic activity of dopamine and norepinephrine. It also stimulates hypothalamic POMC neurons that reduce appetite and increase energy expenditure. Following its release, POMC is degraded into α-MSH and β-endorphin, which

activates negative effects on appetite. Naltrexone, an opioid antagonist, blocks the orexigenic effects of beta-endorphin [38] .

- **Liraglutide** is a peptide analog of glucagon-like peptide-1 (GLP-1), which acts as an agonist of the GLP-1 receptor. Initially approved for the treatment of type 2 diabetes at a dose of 1.8 mg/day, it has recently been approved for the treatment of obesity at a dose of 3 mg/day. GLP-1 exhibits diverse physiological effects, positioning it as a promising option for Type 2 Diabetes Mellitus (T2DM) treatment. When it binds to its specific receptor (GLP-1R), GLP-1 stimulates insulin secretion and inhibits glucagon secretion, but this occurs only when glucose levels are elevated [39], [40], [41]. This unique mechanism holds the promise of lowering plasma glucose levels while mitigating the risk of hypoglycemia. Despite the great potential of GLP-1 as a therapeutic for T2DM, the peptide is rapidly degraded and inactivated by the enzyme dipeptidyl peptidase-4 (DPP-4), which results in a short in vivo half-life of about 1.5 min. Consequently, the native peptide is only effective if administered via continuous infusion and is therefore impractical as a diabetes medication. Hence, efforts toward therapeutic targeting of GLP-1R have focused on GLP-1 peptide mimetics resistant to enzymatic degradation, and with prolonged plasma half-life. Liraglutide shares 97% homology with human GLP-1, incorporating two specific modifications . The initial alteration involves substituting lysine with arginine at position 34, while the second modification entails attaching a 16-carbon acyl group to the side chain of lysine-26 via a γ-glutamic acid spacer. This appended fatty acid

component facilitates binding to serum albumin, thereby slowing down renal excretion. Consequently, liraglutide exhibits a half-life of approximately 13 hours in humans. In 2020 also **semaglutide** was approved by US FDA and EMA, its dose for weight management is 2.4 mg injected subcutaneously [42].

Insulin sensitizers

- **Thiazolidinedione (TZD)** is a synthetic ligand of peroxisome proliferator-activated receptor-γ. The first TZD approved by the FDA was troglitazone; however, it was later withdrawn from the market about five years after its approval due to reports of hepatotoxic events. As of today, the only TZD on the market is pioglitazone, as rosiglitazone was also withdrawn from the market due to negative cardiovascular effects. Pioglitazone is administered orally and typically prescribed in combination with metformin. It is an activator of PPAR-γ, a nuclear receptor that, when stimulated, acts as a transcription factor, controlling the expression of a series of genes involved in insulin sensitivity, including: GLUT-4, acylCoA synthesis and AKT.

Metformin

Metformin has been a crucial drug in managing type 2 diabetes (T2D) for many years. It is the most used oral antihyperglycemic agent. As of now, it is recommended as the first-line therapy for people who are recently diagnosed with T2D as per the American Diabetes Association (2014). Metformin, chemically known as N, N-dimethylbiguanide, belongs to the biguanide class of antidiabetic medications, characterized by two

interconnected guanidine rings. Its origin traces back to galegine (isoamylene guanidine), a guanidine derivative discovered in the French lilac Galega officinalis. In comparison to other biguanides developed for diabetes treatment, such as phenformin and buformin, metformin exhibits a superior safety profile and high tolerance. The withdrawal of phenformin and buformin in the early 1970s was prompted by the associated risks of lactic acidosis and increased cardiac mortality.

The incidence of lactic acidosis with therapeutic doses of metformin is rare, occurring in less than three cases per 100,000 patient-years, and is comparable to or lower than non-metformin therapies. Over the past five decades, metformin has been widely utilized in the treatment of T2D, proving to be both safe and effective as monotherapy and in combination with other oral antidiabetic agents and insulin. One notable clinical advantage of metformin is its ability to manage hyperglycemia without inducing hypoglycemia or weight gain, while also demonstrating remarkable cardiovascular safety. Beyond its application in T2D, there is growing interest in utilizing metformin for conditions such as polycystic ovary disease, diabetic nephropathy, and gestational diabetes. Additionally, metformin has been associated with a reduced risk of cardiovascular complications and improved cancer prognosis. Despite being in use in Europe for hyperglycemia treatment since 1957 and gaining FDA approval in the USA in 1994, the precise molecular mechanisms underlying metformin's therapeutic action remain elusive and unclear [43], [44].

Lipid lowering agents

Lipid-lowering drugs are useful for treating metabolic syndrome with dyslipidemia. A combination of statins and fibrates is recommended to manage atherogenic dyslipidemia in MS.

The intestinal absorption of cholesterol mainly occurs in the proximal part of the small intestine, where the solubilization of cholesterol micelles introduced through the diet takes place. Cholesterol is first transferred from micelles to the surface of the enterocyte membrane and then to the cytoplasmic compartment. From there, it moves into the endoplasmic reticulum where it can be converted into cholesterol esters by acyl-CoA: cholesterol acyltransferase (ACAT). Both free and esterified cholesterol form chylomicrons, which are secreted into the lymphatic duct. Once in circulation, lipoprotein lipase (LPL) acts on chylomicrons and their remnants, which are rapidly metabolized by the liver. By inhibiting the absorption of cholesterol, there is a decrease in cholesterol release to the liver, a reduction in cholesterol stored in hepatocytes, and a decrease in LDL synthesis, resulting in an increase in their clearance.[45].

- **Ezetimibe** is approved by regulatory authorities worldwide, including the FDA and the European Medicines Agency; it addresses the need for effective management of dyslipidemia, particularly elevated low-density lipoprotein cholesterol. Ezetimibe functions by selectively inhibiting the intestinal absorption of dietary and biliary cholesterol at the brush border of the small intestine. It targets the Niemann-Pick C1-Like 1 (NPC1L1) protein, a key mediator of cholesterol absorption. By disrupting this process, ezetimibe reduces the influx of cholesterol into enterocytes, leading to decreased delivery of cholesterol to the

liver and subsequently lowering circulating LDL-C levels. Numerous clinical trials, including the IMPROVE-IT study, have demonstrated the efficacy of ezetimibe in combination with statins, showcasing its ability to provide incremental LDL-C lowering beyond what statins achieve alone. This dual approach addresses both cholesterol synthesis and absorption, offering a comprehensive strategy for managing dyslipidemia [46].

- **Statins**, a class of drugs hailed for their remarkable impact on cardiovascular health, represent the cornerstone of pharmacological interventions in lipid management. Widely prescribed, statins play a pivotal role in reducing cholesterol levels and mitigating the risk of cardiovascular events. Statins primarily act by inhibiting 3-hydroxy-3-methylglutaryl-coenzyme A (HMG-CoA) reductase, a key enzyme in the cholesterol biosynthetic pathway. By suppressing cholesterol synthesis in the liver, statins induce an upregulation of hepatic LDL receptors, leading to increased clearance of circulating low-density lipoprotein cholesterol (LDL-C) and a subsequent reduction in LDL-C levels. Commonly prescribed statins include atorvastatin, simvastatin, rosuvastatin, pravastatin, and lovastatin. Each exhibits distinct pharmacokinetic properties and potency, allowing for personalized treatment strategies based on patient characteristics and lipid profiles.
- **Fibrates** are an important class of lipid-lowering drugs. This class of drugs is composed of numerous compounds, of which, to date, the ones approved in Europe are: bezafibrate, clofibrate, fenofibrate, and gemfibrozil. They all derive from phenoxyacetic

acid and are particularly effective in reducing triglyceride levels. The mechanism of action of fibrates on lipoprotein metabolism involves activating peroxisome proliferator-activated receptors (PPAR alpha) at the molecular level [47] .

- **PCSK9 inhibitors**, a revolutionary class of drugs, have reshaped the landscape of lipid management by providing a highly targeted approach to lower levels of low-density lipoprotein cholesterol (LDL-C). Amid the intricate network of cholesterol metabolism, PCSK9 has emerged as a pivotal player, and therapeutic interventions targeting this protein hold significant promise in reducing cardiovascular risk. PCSK9 inhibitors, exemplified by evolocumab and alirocumab, monoclonal antibodies that exert their effects by binding to circulating PCSK9 molecules. By doing so, these inhibitors disrupt PCSK9's interaction with LDL receptors on hepatocytes. This interference enhances the recycling of LDL receptors, facilitating an increased clearance of LDL-C from the bloodstream. The net result is a powerful and specific reduction in LDL-C levels [48], [49].

In summary, the management of MS is a comprehensive and multifaceted approach that combines lifestyle modifications, pharmacological interventions, and targeted control of risk factors. Patients with MS benefit from individualized treatment plans designed to reduce cardiovascular risk and improve overall health.

Anti-hypertensive agents

- **Angiotensin-Converting Enzyme (ACE) inhibitors**, such as enalapril and lisinopril, play a pivotal role in managing hypertension by blocking the conversion of angiotensin I to angiotensin II, stimulating the dilation of blood vessels. Studies have indicated that ACE inhibitors may offer additional benefits beyond blood pressure control, including improvements in insulin sensitivity and a reduction in central adiposity [48], [49] .
- **Angiotensin II Receptor Blockers (ARBs)**, exemplified by losartan and valsartan, selectively antagonize the effects of angiotensin II. These agents have shown promise in ameliorating insulin resistance and reducing oxidative stress in metabolic syndrome, thus contributing to an overall improvement in cardiovascular outcomes [48], [49], [50].

1.3 Diabetes

Glucose is a crucial cellular energy player, and its plasma concentration reflects dietary intake, metabolism and endogenous biosynthesis. These processes are primarily regulated by the coordinated actions of two pancreatic hormones: insulin and glucagon. While insulin is a hypoglycemic hormone, glucagon exerts a hyperglycemic effect by moving glucose from stores and increasing its synthesis and hepatic production. Insulin and glucagon respond to plasma glucose levels and pancreatic activity, using molecular mechanisms ATP-dependent potassium channels, influencing depolarization of pancreatic β cell membranes, opening voltage-dependent calcium channels, and stimulating insulin release. Insulin regulates intracellular glucose transport and

function, key point for cellular energy. Glucose entry into the cells is mediated by GLUT transporters, with GLUT-2 predominant in liver and pancreas and GLUT-4 in skeletal muscle and adipose tissue. GLUT-2 acts independently of insulin and is activated only by extracellular glucose concentration, while GLUT-4 translocation from cytosol to the cellular membrane is insulin-dependent. Alongside GLUT, there are sodium-glucose co-transporters (SGLT1 and SGLT-2) mainly expressed in the kidneys and heart, ensuring glucose reabsorption [51].

Diabetes Mellitus (DM) is primarily categorized into two prominent types:

- Type 1 diabetes mellitus (T1DM), also known as insulin-dependent diabetes mellitus (IDDM), is a condition where hyperglycemia is caused by a complete absence of insulin in the body..
- Type 2 diabetes mellitus (T2DM), also known as non-insulin-dependent diabetes mellitus (NIDDM), is characterized by high blood glucose levels due to insufficient insulin production and/or resistance to insulin in peripheral tissues.

The choice of drug treatment varies depending on the type of diabetes. In the case of type 1 diabetes, insulin replacement therapy is a mandatory option. Conversely, for type 2 diabetes, the primary approach involves the use of oral hypoglycemic drugs, which are considered the gold standard therapy.

1.3.1 Type 1 Diabetes Mellitus (T1DM)

Type 1 diabetes is usually diagnosed in children and young adults. According to the International Diabetes Federation, an estimated 10% of all diabetes cases are of type 1. The global incidence of T1D is rising, particularly in Western countries [52]. The cause of T1D is not fully

clarified, but it is believed to be a combination of genetic and environmental factors. Individuals with a family history of T1D have a higher risk of developing the condition. Certain viral infections, such as enteroviruses, may also trigger an autoimmune response leading to T1D in genetically predisposed individuals [53].

Type 1 diabetes is a chronic autoimmune disease characterized by the destruction of insulin-producing β-cells in the pancreas. When β-cells are absent, insulin is not produced or released. This results in a gradual decrease of insulin levels in the body until it completely disappears. In this condition, the body's tissues are unable to efficiently take in and store glucose, amino acids, and lipids from the blood, even if their levels are high. Furthermore, glycogenolysis and gluconeogenesis continue unchecked in the liver, promoting the release of glucose into the bloodstream. Simultaneously, muscle tissue breaks down proteins, releasing amino acids that travel to the liver to serve as fuel for gluconeogenesis. Conversely, in adipose tissues, triglycerides break down and are released into the circulation. The resulting fatty acids are then transported to the liver, where they promote gluconeogenesis and release ketone bodies, which accumulate in the plasma, increasing blood acidity. This, in turn, leads to symptoms such as unexplained weight loss, nausea, vomiting, blurred vision, and eventually coma. These events culminate in a significant increase in blood glucose concentration, reducing glucose reabsorption in the kidneys, resulting in osmotic diuresis and the characteristic "sweetening" of urine. This phenomenon causes the well-known symptoms of polyuria (excessive urination) and subsequent polydipsia (excessive thirst).

1.3.1.1 Type 1 Diabetes therapy

Insulin replacement

Type 1 diabetes is a chronic disease that ultimately leads to the complete depletion of insulin due to the destruction of β pancreatic cells. Consequently, the primary approach for treating T1D is primary insulin replacement therapy. The use of exogenous insulin as a treatment for T1D was initially documented by Banting and Best in 1921, who employed crude extracts from animal pancreas to achieve blood sugar-lowering effects. However, challenges were encountered regarding the pharmacokinetics of insulin, mainly attributable to insulin absorption. These issues hindered the attainment of sustained glycemic control and the prevention of diabetic complications[50] .

Subsequently, a variety of humanized insulin analogs have emerged, which not only mimic the biological functions of native insulin but also have improved pharmacokinetic profiles. Nevertheless, clinical observations over the past few decades have underscored the limitations of insulin replacement therapy, particularly its inability to fully replicate the biological actions of endogenous insulin. Concurrent with the increasing incidence of T1D cases, there is a paramount necessity to identify innovative therapeutic strategies for reestablishing normoglycemia. The current treatment for Type 1 Diabetes focuses on combining intensive dietary treatments with lifelong exogenous insulin administration, either through multiple daily injections or insulin pumps. In addition, there have been advances in the development of genetically modified insulin analogues (aspart, lispro, and Delgludec insulins), which are fast acting and long acting. These provide a more physiological glycometabolic control compared with traditional insulins. The conventional insulin-

focused treatment for T1D makes patients prone to hypoglycemia, insulin resistance, and other long-term health conditions, in addition to requiring a lifetime of dependence on exogenous insulin and increasing the likelihood of mild obesity and psychiatric disorders. Developing alternative strategies is highlighted to restore glycemic control and achieve insulin independence. The use of self-monitoring devices to measure blood glucose and non-enzymatically glycosylated hemoglobin A1C (HbA1c) has facilitated the therapeutic application of commercial insulin preparations. As a result, a variety of insulin analogues have been developed with different onset times and durations. These modified insulins are classified as rapid-acting (biological activity begins within 4 minutes and lasts for 30 minutes), short-acting (regular insulin-biological activity beginning from 30 minutes and lasting for 4 hours), intermediate-acting (Insulatard, Insuman-with peak onset from 4 to 6 hours), long-acting (Glargine and Detemir-with biological activity from 24 to 36 hours), and ultra-long acting (Degludec-with onset from 30 to 90 minutes and lasts until 42 hours)[54]. However, delivery systems such as syringes, glucose sensor-augmented insulin infusion pumps, and supersonic injectors are necessary for these preparations. [55], the use of these traditional delivery systems involves an invasive procedure and treatment fails to provide long-term insulin independence. Consequently, research is being carried out to identify alternative means of insulin replacement therapy. A new method for administering insulin orally involves using a self-orienting millimeter-scale applicator that can be ingested.(SOMA) [56]. The device autonomously positions itself to engage with gastro-intestinal tissue and realise directly through the gastric mucosa while avoiding perforation. The results obtained from diabetic rodent studies demonstrate stable plasma

insulin levels comparable with those achieved with subcutaneous administration. Such approach has potential to enhance the clinical outcomes of exogenous insulin replacement therapies.

Immune therapies

The increasing prevalence of Type 1 Diabetes (T1D) cannot be attributed solely to genetic factors. It is widely acknowledged that a complex interplay between genetic susceptibility and environmental influences triggers the activation of self-reactive immune cells. Consequently, the pathogenesis of T1D involves a multifaceted interaction between β cells and components of both the innate and adaptive immune systems. This activated immune response leads to the destruction of β cells through various cell types and multiple pathways, prompting the exploration of numerous immunomodulatory strategies for T1D treatment [57] [54]. The identification of specific components of the autoimmune response has facilitated the implementation of various immunomodulatory therapies, including the chimeric anti-CD3 monoclonal antibody, otelixizumab. It is directed against the chain of the CD3 T-cell membrane receptor, reducing the deterioration in insulin production. Several studies have been conducted to assess the safety profile of otelixizumab [57], but despite the positive results from Phase I and II, those from Phase III are currently contradictory. Other immunosuppressants, such as teplizumab and abatacept, represent promising therapies in slowing the progression of type 1 diabetes (TD1) in specific patient subpopulations, although their current use is characterized by adverse events. Currently, however, combination therapy seems to be the best choice in ensuring a lasting brake on the autoimmune response for patients with TD1. Current research is focused

on developing the next generation of immunotherapies. Clinical trials are underway to investigate agents like anti-IL-21, which offers a potential alternative to modulate the activity of regulatory T cells (Tregs). Tregs, known for their negative modulation of other immune cells, have shown promise in enhancing islet graft survival in preclinical studies and human trials. Another innovative strategy is to expose the immune system to nanoparticles coated with pancreatic peptides bound to major histocompatibility complex class-II (MHC-II) proteins. This approach selectively targets the pancreas-specific immune response while sparing the rest of the immune system, offering potential benefits for T1D treatment. In summary, ongoing research aims to advance immunotherapies for T1D by addressing the complex immune interactions that lead to the destruction of β cells and exploring innovative strategies for long-term glycemic control and improved patient outcomes [57].

1.3.2 Type 2 Diabetes

Type 2 diabetes mellitus (T2DM), often referred to as adult-onset diabetes, is a prevalent chronic metabolic disorder characterized by high blood sugar levels. According to data provided by the International Diabetes Federation (IDF), the year 2021 witnessed an estimated 463 million individuals living with diabetes, with projections indicating that this number will burgeon to a staggering 700 million by 2045. This disconcerting prevalence underscores the prominence of diabetes as one of the most prevalent non-communicable diseases on a worldwide scale.

1.3.2.1 T2DM therapy

The pharmacological treatment of patients with type 2 diabetes currently encompasses a broad array of medications, including some recently approved ones. The drugs available to date include:

- Direct insulin secretagogues (sulfonylureas) and indirect ones (incretin system drugs).
- Anti-hyperglycemic agents (metformin and glucosurics).
- Insulin sensitizers.
- Inhibitors of intestinal glucose absorption.

These drugs collectively form a diverse arsenal aimed at managing type 2 diabetes, offering a range of approaches to address different aspects of the condition.

Sulfonylureas

Sulfonylureas increase insulin secretion from pancreas. Sulfonylureas interact with a receptor called SUR-1 (Sulphonyl-Urea Receptor-1) which is associated with K^+ ATP-dependent channels present on β cells membranes. When sulfonylureas bind to the receptor, it causes the channel to shut down. This results in depolarization, which allows calcium ions to enter the cell. As a result, vesicles containing insulin are mobilized. They also reduce the secretion of glucagon. Sulfonylureas are classified into different generations, with increased potency and reduced side effects, including hypoglycemia, hot flashes, and sometimes hematological toxicity.

Tolbutamide, Chlorpropamide and Tolazamide belong to the first generation, while Gluburide, Glibenclamide and Glipizide are part of the second generation. Glibenclamide is currently the most widely used sulfonylurea (SU) in the treatment of type 2 diabetes, despite recent

attention being focused on a side effect characterized by cardiovascular complications (ischemia). In an effort to overcome these cardiovascular complications, the third generation of SUs has emerged, with glimepiride being a prominent member. Glimepiride, to date, exhibits fewer adverse reactions on the cardiovascular system. It is distinguished by a longer duration of action and glucose-dependent insulin secretion, allowing for once-daily administration. Glimepiride, indeed, forms a less stable bond with pancreatic beta cells compared to other molecules in the same family. It demonstrates better responsiveness when blood glucose levels are higher. The dual hepatic and renal elimination of the drug also permits its use in elderly patients [58], [59].

Incretin mimetic drugs

Incretin mimetic drugs represent a significant advancement in the pharmacological management of type 2 diabetes mellitus (T2DM). Derived from the physiological actions of incretin hormones, particularly glucagon-like peptide-1 (GLP-1), these medications offer a unique approach to blood glucose control. Incretin mimetic drugs primarily target the GLP-1 receptor, aiming to replicate the actions of endogenous GLP-1. GLP-1 is an incretin hormone released by the intestine in response to nutrient ingestion, stimulating insulin secretion in a glucose-dependent manner. Additionally, GLP-1 suppresses glucagon release, slows gastric emptying, and promotes satiety, collectively contributing to improved glycemic control. They can be divided into 2 major classes [60]:

- **GLP-1 receptor agonists**: Exenatide, liraglutide, dulaglutide, and semaglutide are examples of GLP-1 receptor agonists. Administered via subcutaneous injection, these drugs activate the

GLP-1 receptor, enhancing insulin secretion and reducing postprandial glucose levels. They also exhibit weight loss benefits and have been associated with cardiovascular benefits in some cases.

- **Dipeptidyl Peptidase-4 (DPP-4) Inhibitors**: sitagliptin, saxagliptin and linagliptin belong to the class of DPP-4 inhibitors. Unlike GLP-1 receptor agonists, these oral medications work by inhibiting the degradation of endogenous GLP-1. By preventing the enzymatic breakdown of GLP-1, DPP-4 inhibitors prolong the action of incretin hormones, leading to improved insulin secretion and reduced glucagon release.

Anti-hyperglycemic drugs

These are drugs that regulate blood glucose by counteracting hyperglycemic mechanisms. Among them, the main ones used in therapy are metformin, as previously described, and the SGLT2 inhibitors. In euglycemic conditions and with proper renal function, urine should be devoid of glucose. Indeed, glucose, after being filtered by the glomerulus, is entirely reabsorbed at the tubular level through the coordinated activity of co-transporters, uniporters belonging to the SGLT families. Specifically, SGLT1 and SGLT2 actively transport glucose against its concentration gradient, secondarily to the facilitating effect exerted by the binding with sodium, whose concentration in the renal system is very high. Based on these molecular foundations, the pharmacological induction of glycosuria has become a new therapeutic strategy for patients with type 2 diabetes, with prospects for imminent use also in type 1 diabetes and in obese patients. In fact, the inhibition of SGLT2 leads to the appearance of

massive glycosuria. This therapeutic approach represents a groundbreaking development in diabetes treatment and is considered a paradigm shift, translating a clinical manifestation of diabetes (glycosuria) into a therapeutic effect [61]. Selective SGLT2 inhibitors, belonging to the class of gliflozins, are now available in 32 countries worldwide. Dapagliflozin was the first gliflozin approved by the EMA in 2012 [62]. It is a selective, long-lasting inhibitor, as the glycosuric effect and thus glycemic control persist for 18 hours after a single dose. In 2020, dapagliflozin received approval for marketing for the treatment of chronic symptomatic heart failure with reduced ejection fraction in adults and chronic kidney disease, regardless of the presence of diabetes [62]. Following the introduction of dapagliflozin, empagliflozin, ertugliflozin, and sotagliflozin have also been approved. The only known side effect of glifozins to date is the diuretic effect.

1.4 Cardiovascular complications associated with metabolic diseases.

Diabetes is a chronic disease causing high blood sugar. Medical care involves various treatments to manage blood sugar levels. Diabetes treatment aims to prevent tissue damage from hyperglycemia. The importance of protecting the body from hyperglycemia cannot be overstated; the direct and indirect effects on the human vascular tree are the major source of morbidity and mortality in both type 1 and type 2 diabetes. Generally, the injurious effects of hyperglycemia are separated into macrovascular complications (coronary artery disease, peripheral arterial disease, and stroke) and microvascular complications (diabetic nephropathy, neuropathy, and retinopathy) (figure 4).

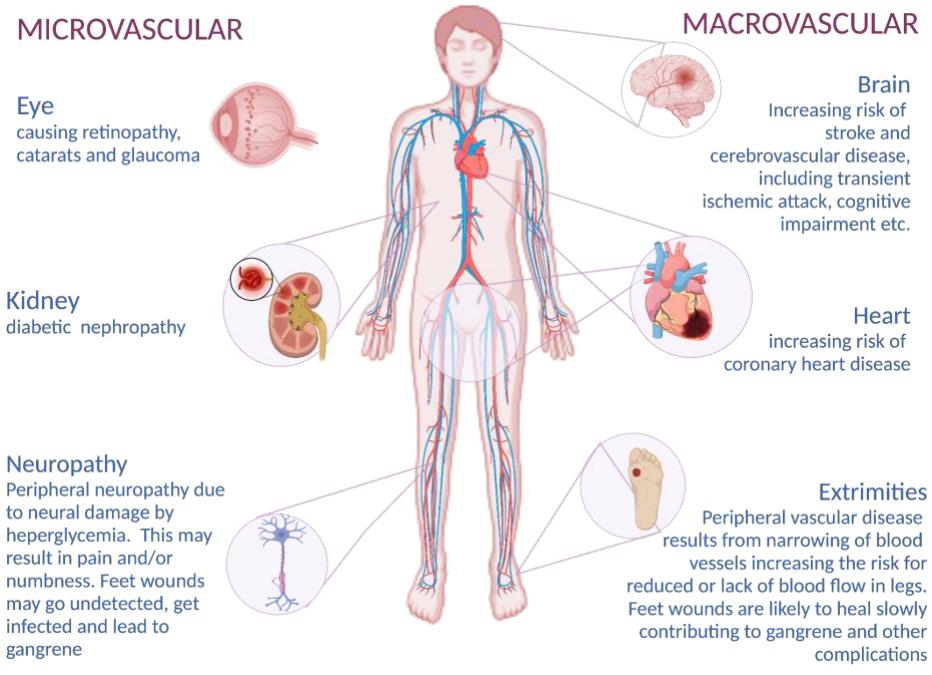

Figure 4. **Macro-and micro-vascular complication associated with type 1 diabetes**

1.4.1 Nephropathy

Diabetic nephropathy is distinguished by proteinuria exceeding 300 mg/24 h, elevated blood pressure, and a gradual deterioration in renal function. In its most severe manifestation, diabetic nephropathy culminates in end-stage renal disease necessitating dialysis or transplantation. However, in the initial stages, overt disease follows a preliminary phase known as incipient nephropathy (or microalbuminuria). During this phase, the urine contains minute protein amounts that are undetectable through conventional dipstick testing. The pace of glomerular filtration rate decline varies considerably among individuals. Nevertheless, antihypertensive therapy significantly retards the deterioration of renal function and enhances the life expectancy of diabetic nephropathy patients. In cases of type 1 diabetes complicated by diabetic nephropathy, angiotensin-converting enzyme inhibitors have nephroprotective effects beyond blood pressure reduction. These benefits are evident even in normotensive patients and ameliorate other associated microvascular complications such as retinopathy. For individuals with type 2 diabetes, effectively managing blood pressure takes precedence over the choice of antihypertensive medication, although angiotensin-converting enzyme inhibitors are the preferred initial treatment, often requiring combination therapy.

1.4.2 Neuropathy

The most common type of diabetic neuropathy is a progressive peripheral polyneuropathy that affects the feet. It primarily affects the patient's sense

of touch and is often symptomless. This condition is present in 40-50% of all individuals with diabetes. A monofilament test can detect reduced sensation, and patients with sensory neuropathy, as well as other high-risk factors, should receive advice on foot care to reduce the risk of developing ulcers[63].

1.4.3 Retinopathy

Diabetic retinopathy is a progressive condition categorized by various clinical abnormalities, and it stands as the leading cause of blindness among individuals aged 30-69. The damage to the retina results from a combination of microvascular leakage and occlusion, which can be precisely observed through fluorescein angiography. Remarkably, a significant proportion of individuals newly diagnosed with type 2 diabetes already exhibit signs of retinopathy. In contrast, vision-threatening retinopathy is seldom encountered in the first five years following a diagnosis of type 1 diabetes or before puberty. However, after approximately 15 years, nearly all type 1 diabetes patients and two-thirds of type 2 diabetes patients develop background retinopathy. Vision-threatening retinopathy typically arises from neovascularization in type 1 diabetes and maculopathy in type 2 diabetes. Maculopathy can be classified into three types based on whether leakage or capillary occlusion is the primary cause. The three types are exudative maculopathy, which is characterized by the presence of hard exudates in the macular area; ischemic maculopathy, which is identified by clusters of hemorrhages resulting from capillary occlusion; and edematous maculopathy, which is caused by extensive leakage leading to macular edema. Maculopathy can

be classified into three types based on whether leakage or capillary occlusion is the primary cause [63].

1.4.4 Atherosclerosis

Diabetes, both type 1 and type 2 and MS significantly amplifies the risk of atherosclerosis. Prolonged high blood sugar levels in diabetes can damage blood vessels' inner lining, leading to inflammation and endothelial dysfunction. This creates an ideal environment for plaque formation and accelerates atherosclerosis progression. Atherosclerosis is a chronic inflammatory disease caused by an imbalance in lipid metabolism and a maladaptive immune response driven by the accumulation of cholesterol-leden macrophages in the artery wall. The pathogenesis of atherosclerosis is a multistep process that begins with endothelial dysfunction. The normal artery is composed of three layers; the intima, tunica media, and adventitia. Under normal conditions, the intima's endothelial monolayer does not attract blood leukocytes. When activated by stimuli related to cardiovascular risk factors such as smocking, hypertension, diabetes hypercholesterolemia, endothelial cells can express adhesion molecule, the endothelium starts having lower tight junctions that allow LDL to enter the tunica intima. Monocytes normally circulate in the blood stream but once the endothelium starts being damaged monocytes are recruited into the arterial wall. The monocytes release free radical to defend the organism but when this free radical come in contact with LDL, oxidation occurs this form of LDL further stimulate the white blood cell to phagocyte them and to produce even more immune cells to modify the LDL. Macrophages in the intima starts eating those LDL oxidized and also smooth muscle cells starts engulfing LDL creating the beginning of the plaques. All the detritus

just formed try to be removed leaving also dead cells giving rise to the necrotic core. Monocytes differentiate in macrophages foam cells leading to a maladaptive inflammatory response resulting in subendothelial expansion with neointimal proliferation, inflammatory cell recruitment, lipid and matrix accumulation. The lesion can progress and manifest a necrotic core covered by a thin layer of matric and smooth muscle cells called fibrous cap. These lesions are defined "vulnerable" because they can disrupt allowing contact of blood coagulation factors with thrombogenic material (principally the potent procoagulant tissue factor) within the plaque, thereby triggering an acute thrombotic vascular event, manifesting in myocardial infarction, stroke, and sudden death [64], [65].

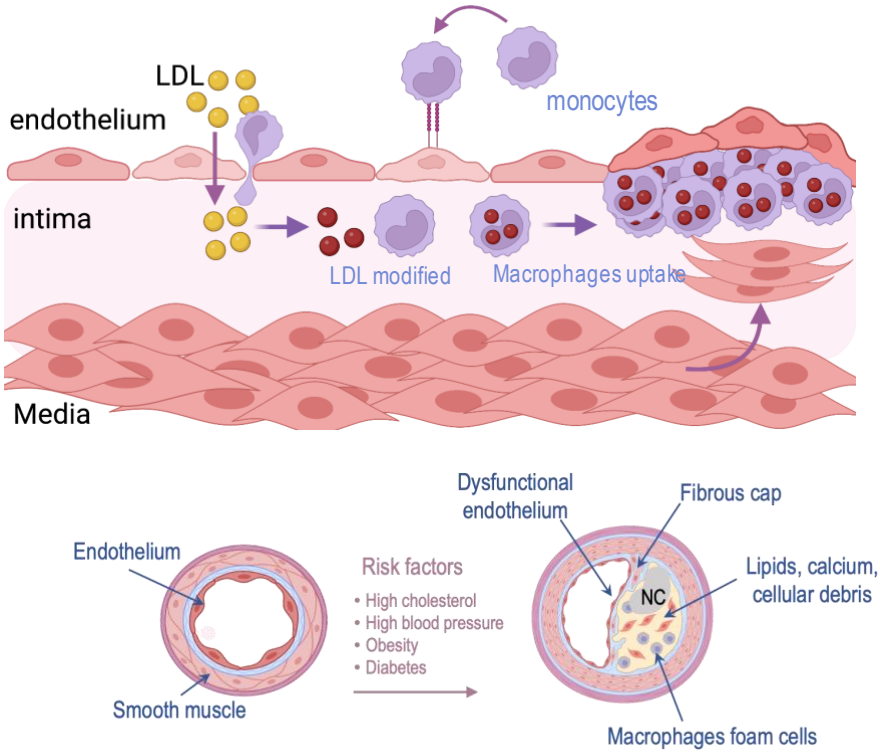

Figure 5. **Onset and progression of atherosclerotic plaque.**

1.4.5 Coronary artery disease

Coronary artery disease (CAD), a prevalent cardiovascular condition, is the leading cause of heart-related morbidity and mortality worldwide. Its pathogenesis is intricate, involving several key mechanisms that contribute to the development and progression of atherosclerotic lesions in the coronary arteries. Atherosclerosis causes vascular remodeling, leading to the thickening of the arterial walls. Over time, these arterial segments may become stenotic, narrowing the lumen and restricting blood flow. This narrowing can lead to ischemia in the myocardium and subsequent angina pectoris. One of the most critical events in CAD pathogenesis is plaque rupture. Vulnerable plaques with thin fibrous caps are prone to rupture, exposing the lipid-rich core to the bloodstream. Platelets aggregate at the site of rupture, leading to thrombus formation. A thrombus can occlude the coronary artery, causing acute myocardial infarction (heart attack) and myocardial damage [66]

1.4.6 Endothelial dysfunction

Endothelial dysfunction is a critical pathological condition characterized by impaired function of the endothelium. This condition plays a pivotal role in the development and progression of many cardiovascular diseases, including atherosclerosis, hypertension, and coronary artery disease. It is characterized by an overproduction of free radical oxygen species (ROS) coupled to an impairment of eNOS/NO signaling (defined eNOS uncoupling), with a consequent reduction in vasodilating properties, pro-coagulability and arterial stiffness [67]. Physiologically, reactive oxygen species (ROS) serve as signaling molecules intricately involved in vascular

homeostasis being crucial in regulating oxygen sensing, apoptosis, cell proliferation, defense against microbial injury, and inflammatory reactions.[68]. Endothelial, smooth muscle cells and adventitia utilize various enzymatic systems, including mitochondrial enzymes, xanthine oxidase, lipoxygenase, and NADPH oxidase, to produce these molecules in the vessels. Notably, vascular tissues maintain an antioxidative defense mechanism that consistently counteracts the formation of reactive oxygen species (ROS). Enzymes like superoxide dismutase, catalase, thioredoxin peroxidase, glutathione peroxidase, and heme oxygenase actively engage in exerting antioxidant effects. In instances where ROS production overwhelms the innate antioxidant system, the body succumbs to oxidative stress. A shared characteristic in inflammatory-based vascular diseases (IBVD) is the presence of oxidative stress, with the endothelium being the primary target. Oxidative stress can impair the production of nitric oxide (NO) by eNOS, which is a critical factor for the endothelium. When the levels of Reactive Oxygen Species (ROS) are high, the eNOS co-factor BH4 can be oxidized which causes eNOS uncoupling. This uncoupling results in the generation of O^{2-} instead of NO. Due to the increased oxidative stress observed in vascular disease, NO is degraded more quickly due to its reaction with $O^{2-\cdot}$. On the other hand, oxidative stress can also convert eNOS from a NO-producing enzyme to an enzyme that generates $O^{2-}\cdot$, which is known as eNOS uncoupling. Mechanisms implicated in eNOS uncoupling include oxidation of the critical NOS cofactor BH_4, depletion of L-arginine, and accumulation of endogenous methylarginines. More recently, S-glutathionylation of eNOS has been proposed as another mechanism leading to eNOS uncoupling. This finding has been verified in individuals having heart failure with preserved ejection fraction,

establishing a connection between the oxidation of BH_4 in BH_2 and the uncoupling of eNOS. The compromised generation of NO adversely affects various facets of vascular function. Under normal conditions, NO not only enhances vessel dilation but also mitigates the oxidation of low-density lipoproteins (LDL), lowers platelet reactivity, and reduces leukocyte adhesion, thus exerting a protective effect on the vasculature. As a result, the hindered release of NO due to endothelial dysfunction induces vasoconstriction, pro-coagulability, and arterial stiffness that sustain the vicious IBVD circle. Another factor contributing to the impairment of NO biosynthesis associated with IBVD is the presence of the protein caveolin-1 (CAV-1). Under resting conditions, eNOS is bound to CAV-1, a resident protein of caveolae that maintains eNOS in a low-activated state. When intracellular Ca^{2+} levels rise, the Ca^{2+}-calmodulin complex binds to eNOS and, together with hsp90, displaces eNOS from the negative control of CAV-1, leading to the enzyme activation. Several studies have demonstrated that, in IBVD, the reduced production of NO is due to an increase of CAV-1 expression that retains the eNOS in a less active state. Indeed, CAV-1 over-expression has been identified in hyperlipidemia diabetes, atherosclerosis and pulmonary hypertension [67]

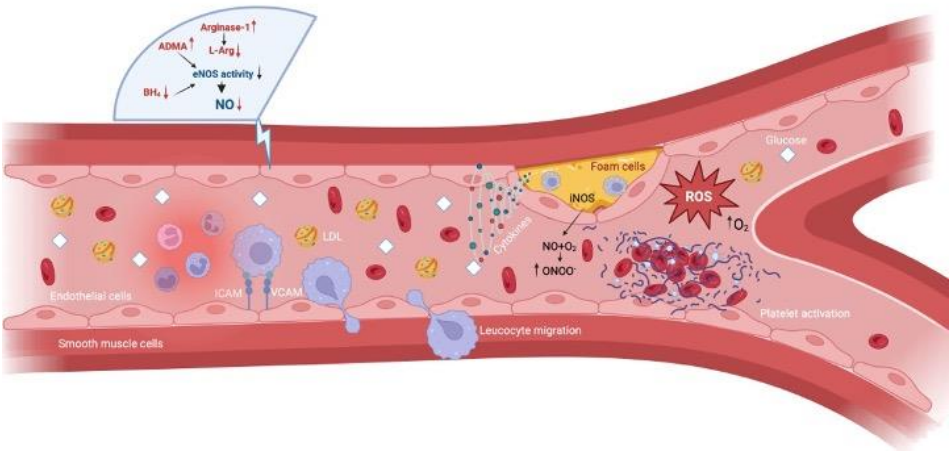

Figure 6. **Main features of endothelial dysfunction**

1.5 H_2S: Hydrogen sulfide

Svetonio in his biography of Cesare Augusto, the first emperor of the Roman Empire, recounts Imperator's struggle with arthritis, rheumatism, and hypertension. He found great benefit in the thermal bath of the Aquae Albulae often referred to as "white waters" due to their distinctive white hue, which stemmed from a high sulfate content [69]. Centuries have elapsed and the therapeutic effects of sulfur' water have remained associated with the realm of the thermal spa. The groundbreaking concept that a gas could have a role within the body as a mediator namely nitric oxide (NO) lead to the Nobel Prize in 1998. The gasotransmitters are small, labile molecules biosynthesized in the body by enzymic reactions with a very short half-life, ranging from seconds to minutes. Being a gas, these molecules freely permeate the cell membranes without specific transporters, reaching molecular targets relatively far from the site of their biosynthesis [69]. This characteristic unveils a new concept: the biological effect triggered by the gasotransmitters is not necessarily due to the interaction with a single specific target. This concept, apparently obvious,

has changed radically the classical idea of ligand–receptor interaction in pharmacology and have autocrine and paracrine effects. The three most well-known gasotransmitters are carbon monoxide (CO), nitric oxide (NO), and hydrogen sulfide (H_2S). Due to their unique chemical nature, once produced, freely travel through the cells, interacting with many different molecular structures. It would take several years before H_2S would be recognized as the third endogenous mediator [69]

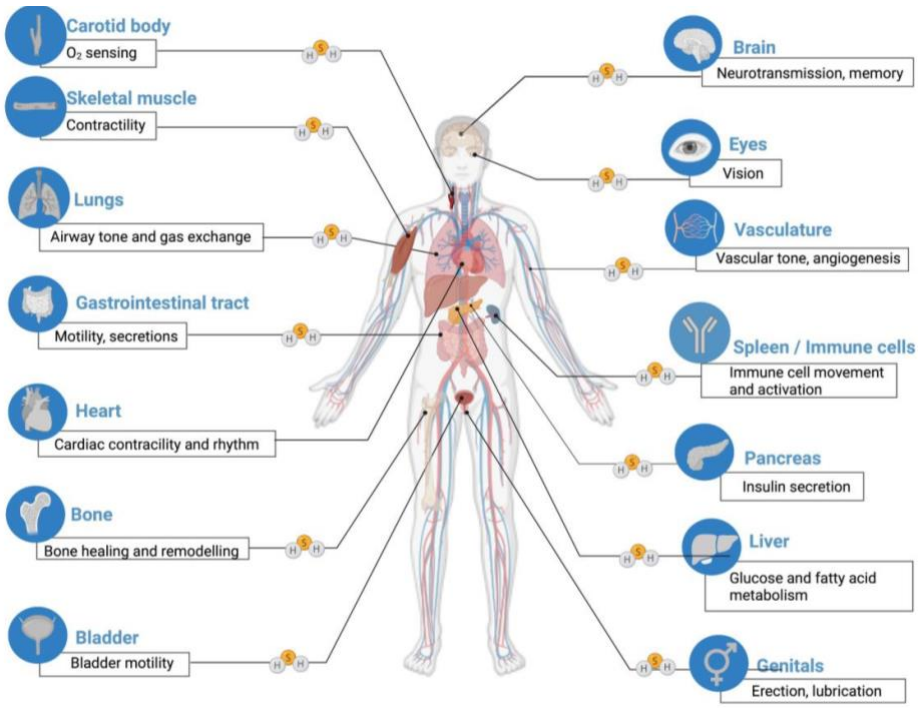

Figure 7. **The physiological roles of H_2S** *(From Cirino et.al Physiological Reviews 2023)*

Hydrogen sulphide is a colorless, flammable, water-soluble gas with the characteristic smell of rotten eggs. For many decades, H_2S received attention primarily as a toxic gas and as an environmental hazard, but it is also produced in mammals including humans, and it can be detected in

significant amounts [70]. Its molecular structure is like that of water, but instead of an oxygen atom, it contains a sulfur atom, which is less electronegative than oxygen, making the molecule less polar. H_2S has a boiling point of -60.7 °C and is weakly acidic. In an aqueous solution, it dissociates into an H^+ ion and a hydrogen sulfide ion (HS^-) (Ka1= 1.310-7 M), which, in turn, further dissociates into a sulfide ion (S2-) and H+ (Ka2= 110-19 M).

In the plasma, under physiological conditions, one-third of hydrogen sulfide exists as undissociated, primarily as H_2S. The completely dissociated form, S^{2-}, is not appreciably present, as the dissociation of the HS- species only occurs at high pH values [71]. Hydrogen sulfide, at concentrations below 1000 ppm, can have toxic effects characterized by some symptoms such as eye irritation, sore throat, dizziness, nausea, breathing difficulties, and chest tightness. At concentrations exceeding 1000 ppm, it can lead to severe detrimental effects, particularly affecting the central nervous system and the respiratory system, resulting in respiratory paralysis and pulmonary edema, which in severe cases can be fatal. The mechanism through which these effects manifest is not yet fully understood. Most likely at millimolar concentrations, H_2S targets mitochondria, where it reversibly inhibits cytochrome c oxidase [72] [73]. In previous years, hydrogen sulfide (H_2S) played a minor role; however, it has now been reevaluated and recognized as the third endogenous gaseous mediator. In addition to sharing similar beneficial properties with nitric oxide (NO), H_2S does not trigger the formation of reactive oxygen species

(ROS). On the contrary, it is able to prevent their formation, thus demonstrating antioxidant activity [74].

1.5.1 H_2S synthesis and metabolism

In mammalian tissues, H_2S can be produced through both enzymatic and non-enzymatic pathways, with the enzymatic pathway being the primary source of H_2S in the human body. H_2S is endogenously synthesized starting from the aminoacid L-cysteine (L-Cys) by the action of different enzymes. L-cysteine, an essential aminoacid, can be acquired through dietary intake or synthesized from L-methionine. In a transmethylation reaction, methionine is converted into the intermediate homocysteine, which subsequently undergoes transsulfuration. This transsulfuration process leads to the production of L-cysteine. It is important to note that this transsulfuration reaction initiates the transsulfuration pathway (TSP), which involves the transformation of homocysteine into L-cysteine and the subsequent synthesis of numerous sulfur metabolites, including, among others, H_2S. Notably, this pathway also gives rise to taurine and glutathione, two of the most significant endogenous antioxidants [75]. The main enzymes involved in TSP are: cystathionine β-synthase (CBS), cystathionine γ-lyase (CSE) ,two pyridoxal-5'-phosphate-dependent enzymes, and MPST (3-MST). These three constitutive enzymes are widely distributed throughout the body displaying tissue specificity: CBS is predominantly expressed in the CNS [76], [77], CSE is mostly present in the cardiovascular environment [78] [79], [80], meanwhile 3-MST is ubiquitous [81], [82]

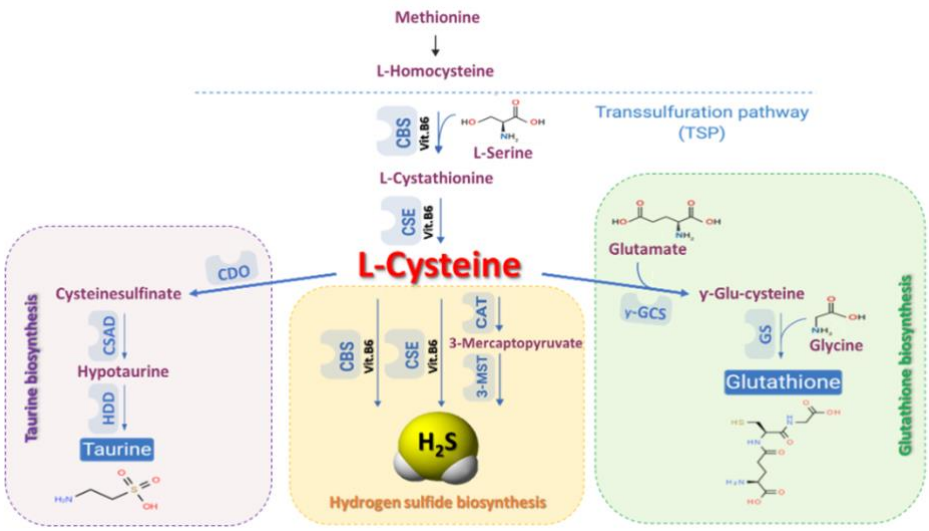

Figure 8. **Trans-sulfuration pathway** *(From Panza et.al Redox Biology 2021)*

CBS was first identified in 1969 by Braunstein *et al.* [83].In presence of L-cysteine, CBS generates H_2S *via* a β-replacement reaction along with the production of L-serine. CBS is also well known to catalyze the condensation of homocysteine and L-serine, which results in the formation of L-cystathionine and H_2O [84], [85]. This reaction is a key step for the biosynthesis of L-cysteine, which can be further used as an H_2S-producing substrate. CBS is principal H_2S synthase enzyme in the central nervous system, although its expression has also been observed in other organs such as kidney, liver, lymphocytes, uterus, placenta, and pancreas islets [76] CSE, similar to CBS, utilizes homocysteine as a substrate to generate H_2S along with α-ketobutyrate and ammonia. Alternatively, CSE can also catalyze L-cysteine to produce H_2S and other byproducts such as pyruvate, and ammonia [86]. The activity of CSE is known to be influenced by intracellular Ca^{2+} concentration [87]; low levels of intracellular Ca^{2+} induce the production of H_2S by CSE whereas CSE activity is suppressed

on the rise of intracellular Ca^{2+} by cell stimulation even in the presence of PLP. 3MST is the most recently discovered H_2S-producing enzyme [81]. To take this way, L-cysteine must be first converted into 3-mercaptopyruvate (3MP) by cysteine aminotransferase (CAT). Thereafter, 3MST transfers a sulfur atom from 3MP onto itself, which leads to the formation of persulfide. H_2S is then released from the persulfide in the presence of a reductant such as thioredoxin [88] [89]. Recently, another source of 3MP was found in mammals by Shibuya et al., d-cysteine [81]. Specifically, d-cysteine is transformed into 3MP by peroxisome-located d-amino acid oxidase (DAO). Metabolite exchanges between peroxisome and mitochondria can import 3-MP into mitochondria where it is further catalyzed into H_2S by 3MST. Distinct from CBS and CSE, the activity of 3MST appears to be regulated intrinsically by its redox state rather than interactions with other factors. Based on its crystal structure, three redox-sensitive cysteines (Cys154, Cys247, Cys263) have been identified on its catalytic site [90]. In line with this, oxidative stress significantly suppresses the activity of 3MST and, therefore, H_2S production probably by oxidation of these protein thiols[91], [92]Moreover, modulation of CAT or DAO activity can also apparently affect the generation of H_2S by 3MST. Within mammalian cells, 3MST is mainly located in mitochondria, although a detectable level of 3MST has also been reported in the cytoplasm [89].

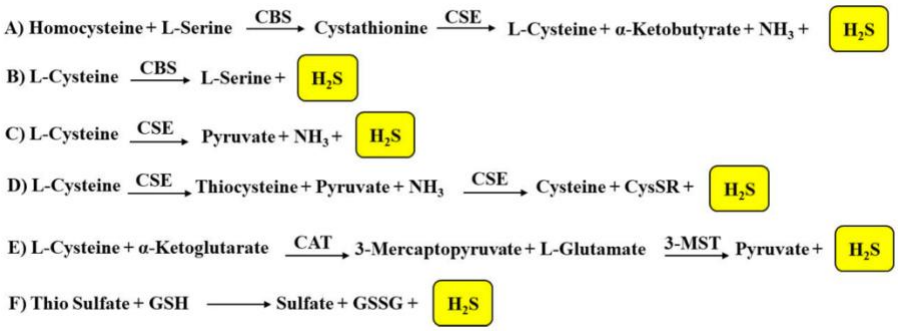

Figure 9. **H_2S biosynthesis.**

As previously reported, H_2S is also involved in non-enzymatic reactions. In particular, the non-enzymatic reduction of elemental sulfur leads to a minor endogenous source of hydrogen sulfide; this reaction occurs using reducing equivalents obtained from the oxidation of glucose in erythrocytes [93]. Human erythrocytes can obtain H_2S in the presence of elemental sulfur or inorganic polysulfides. Non-enzymatic oxidation sulfides provide thiosulfate and these can be converted to sulfite by enzymatic reactions with thiosulfate reductase in the liver, kidney, or brain, or by thiosulfate sulfur-transferase in the liver.

The catabolism of hydrogen sulfide includes non-enzymatic and enzymatic reactions. In the first reaction of a catabolic pathway, H_2S is rapidly oxidized, mainly in the mitochondria and in a non-enzymatic manner, to thiosulfate; subsequently, through an enzymatic reaction, thiosulfate is converted to sulfate and/or sulfite by TST (thiosulfate cyanide sulfur-transferase) [94].. Sulfite obtained by this reaction is then rapidly oxidized to sulfate; the latter is the major end-product of H_2S catabolism under physiological conditions [94]. Another catabolic pathway of H_2S is represented by the methylation to methanethiol and dimethyl sulfide mediated by TSMT (thiol-S-methyltransferase). This latter catabolic

pathway occurs in the cytosol of different cells of the gastrointestinal tract [94], [95]The last catabolic reaction of H S involves the methemoglobin that is able to bind to 25 of 52 endogenous gases (for example CO and NO); moreover, it is able to bind H_2S to give sulfhemoglobin [96]. The catabolism of H_2S in the mitochondria is related to the coupled activity of sev- eral mitochondrial enzymes (SQR, ETHE1, SO, of which the initial one (SQR) is oxygen- independent) and their substrates (CoC, GSH glutathione, O2). In order to form thiosulfate, H_2S is initially processed by SQR and GSH to form glutathione persulfide (GSSH) that serves as a substrate for both sulfite and thiosulfate formation. Alternatively, H_2S can be processed by SQR and sulfite to form thiosulfate. Most of the catabolic reactions regarding H_2S in mitochondria are enzymatic [97]

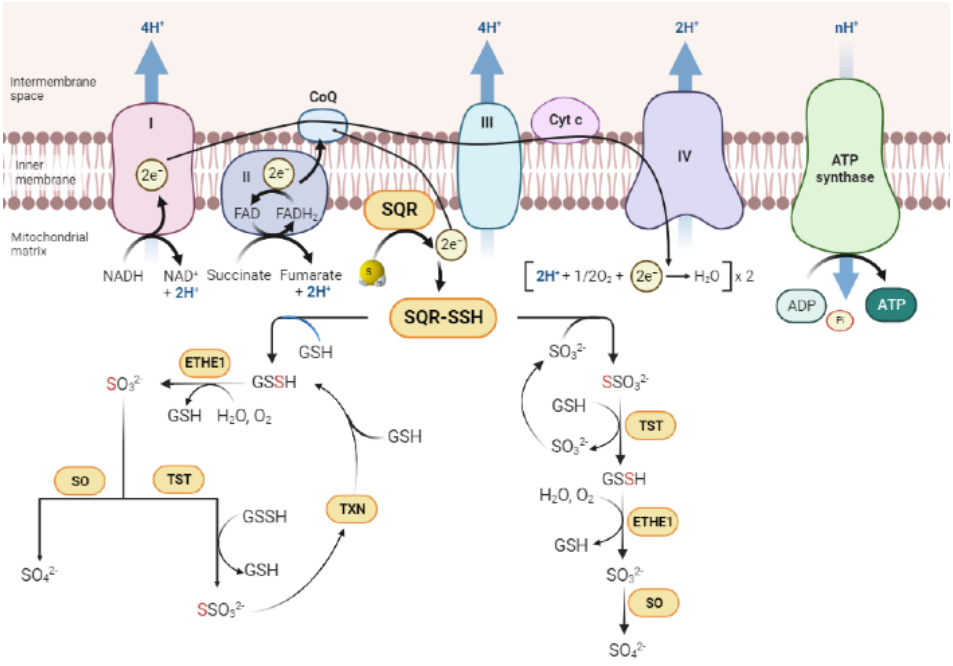

Figure 10. **H_2S catabolism**

1.5.2 H_2S molecular targets

H_2S participates in the homeostatic regulation of numerous biological systems. It acts as a vasoactive agent, modulating vascular tone and consequently, blood pressure. Furthermore, it is implicated in the homeostasis of various systems, including the neuronal, gastrointestinal, respiratory, renal, hepatic, and reproductive systems. It serves a protective function in atherosclerosis and inflammatory responses. Thanks to its high lipophilicity, H_2S easily reaches its molecular targets by crossing the plasma membrane, cytosol, or intracellular organelles. Due to its chemical reactivity, H_2S interacts with numerous macromolecules in various types of cells, using H_2S as a specific, selective, and potent signaling molecule. To date, the most recognized molecular targets of this gas-trasmitter are : ATP-sensitive potassium channels, voltage-gated channels and phosphodiesterases. Many cellular effects of H_2S are due to its interactions with ion channels expressed on the cytoplasmic membrane. The ATP-sensitive potassium channel (K_{ATP}) has been the first identified H_2S molecular target [98], [99]. This channel is ubiquitously expressed in the organism and is involved in numerous biological functions. It has a complex structure, consisting of 96 transmembrane domains, and exhibits a heterooctameric structure composed of two types of transmembrane subunits: Kir and Sur. H_2S-induced activation of K_{ATP} channels has been observed in the cardiovascular, endocrine, respiratory, nervous, and gastrointestinal systems. It appears that multiple subunits of K_{ATP} channels are modified by H_2S. It has been demonstrated that H_2S specifically acts on the SUR1 subunit (or sulfonylurea receptor 1 or ABCC8) of the K_{ATP} channel by binding to the amino acid residues Cys6 and Cys26 of the N-terminal region of SUR1 [100]. As for the voltage-gated potassium

channels, the prominent one seems to be the Kv7. It is involved in stabilizing the membrane potential, returning it to resting values to counteract electrical excitability in various cell types, including skeletal muscles. Martelli and colleagues have demonstrated that the use of XE-991, a selective inhibitor of the Kv7 channel, inhibits the vasodilatory effect induced by an exogenous H_2S donor (NaHS). Furthermore, exposure of rat aortic smooth muscle cells to NaHS induces membrane hyperpolarization similar to that observed with Retigabine, a selective activator of the Kv7 channel. Moreover, some very recent studies suggest that the persulfidation of the mitochondrial Kv7.4 channels contributes to the cardioprotective effect of H_2S against ischemia/reperfusion injury [101], [102] Voltage-dependent calcium channels (VDCCs) have also been identified as potential targets of H_2S. The interaction of H_2S with these channels inhibits VDCC currents [103]. The effects of H_2S on voltage-dependent channels appear to be tissue-specific. In recent years, studies of vascular physiology have identified H_2S as an endothelium-derived hyperpolarization factor (EDHF) [104]. This mediator is responsible for the activation of calcium-dependent potassium channels, SKCa and IKCa. This effect has been confirmed by a recent study conducted on smooth muscle of the endothelium and mesenteric arteries in mice. The co-administration of charybdotoxin and apamin, two selective blockers of IKCa and SKCa channels, is unable to block the vasodilatory effects of EDHF, suggesting an indirect activation linked to H_2S. However, the interaction of H_2S is not limited to the aforementioned channels, and H_2S does not only have the role of activation, as ionic channels differ in their amino acid composition, voltage dependence, opening mechanisms, ion selectivity, and sensitivity to various endogenous signaling molecules.

Therefore, the responses of these channels to hydrogen sulfide exposure can vary. It has been demonstrated, for example, that delayed-rectifier potassium channels in murine gastric muscle cells are inhibited by H_2S [105], while 4-aminopyridine (4-AP)-sensitive potassium channels in smooth muscle cells of the rat coronary artery can be activated by H_2S [106]. It has also been observed that H_2S activates chloride channels, voltage-dependent sodium channels, and transient receptor potential channels TRPV1 and TRPA1, sensitive to cation potential in different tissues [107] . Although hydrogen sulfide can act directly on target proteins without the involvement of second messengers, this gaseous transmitter also influences the levels of many known second messengers. The inhibition of phosphodiesterases (PDEs) [108] by H_2S leads to reduced degradation of cyclic GMP and cyclic AMP, consequently increasing cGMP and cAMP levels. Free intracellular calcium is another second messenger that plays a critical role in cellular signal transduction. Through its effects on plasma membrane ion channels and calcium reserves, H_2S can increase intracellular calcium levels in vascular endothelial cells by stimulating calcium entry or releasing calcium from an ATP-activatable intracellular reserve [109]. The increase in intracellular calcium levels activates many signal transduction pathways and calcium-dependent enzymes, affecting endothelial proliferation and functionality. In addition to these actions, H_2S also plays a role as an antioxidant. It is well-established that redox balance is a dynamic state in which levels of oxidants and antioxidants are balanced; an increase or decrease in antioxidant capacity disrupts redox balance, causing damage to molecules and cells.

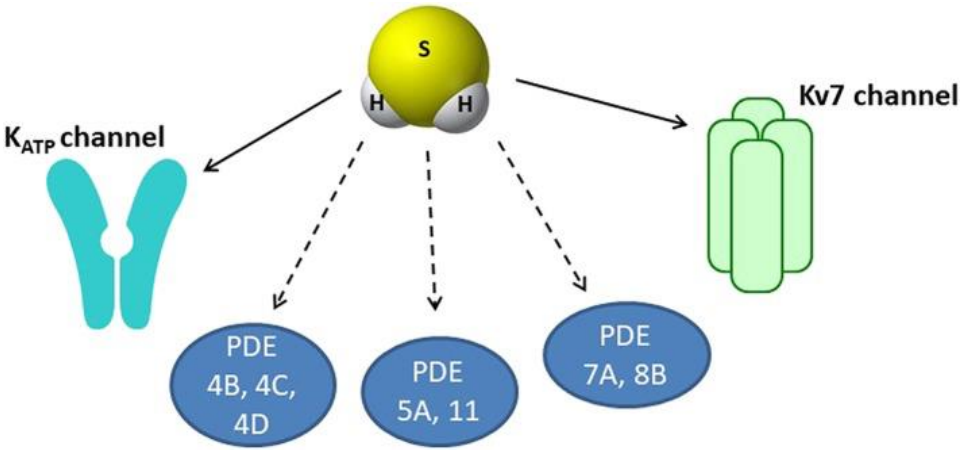

Figure 11. **H_2S molecular targets**

1.5.3 S-persulfidation

At appropriate concentrations, hydrogen sulfide, a well-known gasotransmitter, plays important roles in both physiology and pathophysiology. Increasing evidence suggests that modifying thiol groups of specific cysteines in target proteins via sulfhydration or persulfidation is one of the important mechanisms responsible for the biological functions of hydrogen sulfide [69]. A variety of key proteins of different cellular pathways in mammals have been reported to be sulfhydrated by hydrogen sulfide to participate and regulate the processes of cell survival/death, cell differentiation, cell proliferation/hypertrophy, cellular metabolism, mitochondrial bioenergetics/biogenesis, endoplasmic reticulum stress, vasorelaxtion, inflammation, oxidative stress, etc. Moreover, *S*-sulfhydration also exerts many biological functions through the cross-talk with other post-translational modifications including phosphorylation, *S*-nitrosylation and tyrosine nitration [110]. For example, the Kelch-like ECH-associated protein 1 (KEAP1) is a negative regulator of the activity

of the nuclear erythroid factor Nrf2 [111]. Sulfhydration induced by hydrogen sulfide on KEAP1 at the Cys-151 level facilitates the dissociation of Keap1 from Nrf2, thus leading to an enhancement of Nrf2-mediated antioxidant responses [111]. Post-translational modification of the nuclear factor κB (NF-κB) represents another example of the difference in functional effects induced respectively by S-nitrosylation and S-sulfhydration. NF-κB is a transcription factor that regulates the expression of many genes activated in response to inflammation or apoptosis. S-nitrosylation of the Cys38 residue of the p65 subunit of NF-κB inhibits the binding of NF-κB to cysteine-responsive sites in the promoter region of the gene encoding for the inducible nitric oxide synthase (iNOS), causing reduced expression [109]. S-sulfhydration of the same cysteine residue enhances the binding of NF-κB to the ribosomal protein S3, increasing the transcriptional activity of p65 in the nucleus [109]. As a result, cellular apoptosis is largely inhibited. For the regulation of the signal transduction process, both "turn-on" and "turn-off" mechanisms are required. For example, the removal of NO from S-nitrosylated proteins occurs through the denitrosylation process. S-nitrosoglutathione reductase (GSNOR), a denitrosylation enzyme, reduces the product of protein S-nitrosylation, GSNO, to glutathione hydroxysulfonamide [112]. The enzymes involved in protein desulfhydration reactions are still poorly understood. It has been demonstrated that mitochondrial persulfide dehydrogenase (ETHE1) catalyzes the in vitro conversion of persulfide to glutathione (GSSH) to sulfite. This process has important implications for sulfur metabolism in mitochondria and the balance of redox reactions [113]. However, the physiological substrate of ETHE1 is not known, although the binding with persulfide in the active site of the sulfide quinone oxidoreductase peptide

could be a candidate. Furthermore, little is known about the desulfhydration of S-sulfhydrated proteins in the cytosol or non-mitochondrial organelles. It can be assumed, however, that S-sulfhydrated proteins can be desulfhydrated in the presence of an excess of reducing agents, and therefore, the oxygen level is an important factor in desulfhydration processes.

1.5.4 H_2S and Cardiovascular System

The importance of hydrogen sulfide (H_2S) in the cardiovascular system and the rest of the body is well-recognized physiologically and biomedically. In blood vessels, cystathionine γ-lyase (CSE) is a major H_2S-producing enzyme expressed in both smooth muscle and endothelium as well as periadventitial adipose tissues. Regulation of H_2S production from CSE is controlled by a complex integration of transcriptional, post-transcriptional, and posttranslational mechanisms in blood vessels. In smooth muscle cells, H_2S regulates cell apoptosis, phenotypic switch, relaxation and contraction, in endothelial cells, H_2S controls cell proliferation, cellular senescence, oxidative stress, inflammation, etc. H_2S interacts with nitric oxide and acts as an endothelium-derived relaxing factor and an endothelium-derived hyperpolarizing factor. Extensive evidence has demonstrated the beneficial roles of the CSE/H_2S system in various blood vessel diseases, such as hypertension, atherosclerosis, and aortic aneurysm. The important roles signaling in the cardiovascular system merit further intensive and extensive investigation. H_2S-releasing agents and CSE activators will find their great applications in the

prevention and treatment of blood vessel-related disorders. Different enzymes are involved in the production of H_2S from both vascular smooth muscle cells (SMCs) and endothelial cells (ECs). Cystathionine β-synthase (CBS) is critical for the trans-sulfuration of homocysteine to generate cystathionine and then to H_2S. Similar to CBS, cystathionine γ-lyase (CSE) is also a pyridoxal-phosphate-dependent H_2S-generating enzyme. In the cardiovascular system, the transformation of L-cysteine to H_2S is mainly catalyzed by CSE with ammonium and pyruvate. The regulation of CSE gene expression mostly occurs at the CSE promotor site. The specific protein 1 (Sp1) transcription factor, nuclear factor erythroid-2-related factor-2 (Nrf2), and farnesoid X receptor (FXR) ligand can all bind to the CSE promotor, stimulating CSE transcription [114] [115], [116]. This mechanism explains how microRNA 21 (miR-21) directly repressed Sp1 expression, which inhibited CSE expression. [117]. TNF-α, a protein that plays a role in inflammation, increases CSE expression by binding to the CSE promoter through a protein called Sp1. On the other hand, Nrf2 protein mediates targeted gene transcription by binding to an antioxidant-responsive element (ARE) in the nucleus. Hassan et al. showed that PDGF-BB-induced CSE expression in mesangial cells is inhibited by co-treatment with antioxidants or by Nrf2 knockout. Furthermore, stabilization of Nrf2 protein upregulated CSE protein expression [115]. The evidence for the interaction of FXR with the CSE promotor was derived from HepG2 cells. The human CSE gene contains an FXR-responsive element in its 50-flanking region. Treatment of HepG2 cells with an FXR ligand increased CSE expression and mutation of FXR blocks FXR ligand- induced CSE expression [116]. Cysteine aminotransferase (CAT) and 3-mercaptopyruvate sulfurtransferase (MST) are other two enzymes

involved in H_2S pathway in the cardiovascular system [81]. Whereas CAT uses PLP as its cofactor, zinc is the cofactor of MST. The sequential reactions catalyzed by CAT and MST lead to the transformation of cysteine to 3-mercaptopyruvate (3-MP) to sulfane sulfur. This bound sulfur will need to be released or reduced to free H_2S [119]. CAT protein was found in vascular ECs, and MST protein was localized in both ECs and SMCs of rat thoracic aorta [81]. 3-MST protein was also localized in bovine pulmonary artery [120]. H_2S-induced vasorelaxation is a well-known vascular event, and the most widely characterized cellular target for H_2S in SMCs is the ATP-sensitive K^+ (K_{ATP}) channels. In the vascular system, specifically in SMCs, K_{ATP} channels contribute significantly toward vasodilation in response to various vasoactive substances. The opening of K_{ATP} channels hyperpolarizes cell membrane and inactivates voltage-dependent L-type $Ca2^+$ channels, leading to cell relaxation and blood vessel dilation by reducing intracellular free Ca^{2+} concentration[119]. It has been previously shown that H_2S at physiologically relevant concentrations induced the relaxation of rat aortic tissue and transient reduction of blood pressure, and these vascular effects of H_2S were mediated by a direct stimulation of K_{ATP} channels and subsequent hyperpolarization of aortic SMCs [99], [121], [122], [123]. Using the whole-cell and single-channel patch-clamp technique, Tang et al. demonstrated that H_2S activates K_{ATP} channels and hyperpolarized cell membrane in rat mesenteric artery SMCs [124], [125]. H_2S enhanced the amplitude of whole-cell K_{ATP} currents and increased the open probability of single K_{ATP} channels. Furthermore, inhibition of endogenous H_2S production with PPG reduced whole-cell K_{ATP} currents. H_2S also causes the relaxation of human airway SMCs via stimulating sarcolemmal K_{ATP}

channels [126] . Other studies proved that H_2S interacts with the SUR subunits of the K_{ATP} channel complex to cause the channel to open, and the sulfhydryl groups located on the extracellular surface of the SUR subunits are potential targets for H_2S S-sulfhydration [127]. The deletion of extracellular cysteine 6 or 26 of SUR1 subunits caused the loss of channel sensitivity to H_2S. It appears that H_2S firstly breaks the disulfide bond between cysteine 6 and cysteine 26 and then caused their S-sulfhydrations. In addition to K_{ATP} channels, H_2S is reported to activate Kv7 voltage-gated potassium channels (particularly the Kv7.4 subtype) in SMCs, and the activation of Kv7 channel mediates a significant part of the vasorelaxing effects of H_2S [101]. H_2S may induce SMC relaxation by altering intracellular pH. H_2S has been shown to decrease intracellular pH in a dose-dependent manner. Ionic exchangers, including Na^+/H^+ and Cl/HCO_3 and Ca^{2+} ATPase, maintain the resting pH in SMCs between 7.1 and 7.2. Preincubation of SMCs with a selective inhibitor of Cl/HCO_3, but not Na^+/H^+ exchanger inhibitor, prevented the drop of intracellular pH and vasorelaxation caused by H_2S, suggesting that Cl/HCO_3 exchanger is involved in H_2S-induced relaxation in SMCs [128]. Intracellular acidosis could activate K_{ATP} channel in SMCs and decrease vascular tone. As such, H_2S- induced opening of K_{ATP} channels may be partially triggered by intracellular acidification [129]. H_2S may cause vasorelaxation by increasing cGMP in SMCs. Incubation of rat aortic SMCs with NaHS increased cGMP concentration.The NaHS-induced rise in cGMP was evident as early as 1 min, reached a maximum at 3 min, and remained elevated for at least 10 min. Blockade of CSE activity by PPG or BCA or knockdown of CSE mRNA by siRNA resulted in a significant reduction of cGMP accumulation [130]. In contrast, overexpression of CSE elevated

intracellular cGMP level. Intracellular cGMP levels reflect the balance between the rate of cGMP synthesis via guanylyl cyclases and breakdown by phosphodiesterases. Further studies showed that H_2S acts as an endogenous inhibitor of phosphodiesterase. In a cell-free assay, Bucci et al. demonstrated that NaHS at 10–30 nM significantly inhibits phosphodiesterase activity and causes a reduction in the breakdown of 50-GMP [130]. H_2S also ameliorated the reduction in cGMP levels brought about by overexpression of phosphodiesterase 5A [79], [130]. The effect of H_2S on SMC relaxation is biphasic depending on its concentration [131] [129]. At higher level, H_2S produces vasorelaxation effect, while it induces vasoconstriction at lower concentration [132]. The researchers found that the application of NaHS in the concentration range of 10-100 μM can reverse the vasodilation caused by isoprenaline, salbutamol (two β-adrenoceptor agonists), and forskolin (a selective adenylyl cyclase activator) in rat aortic rings pre-contracted with phenylephrine, in a concentration-dependent manner.[133] . The authors have suggested that the contractile effect of hydrogen sulfide (H_2S), observed in isolated rat aorta, is linked to a reduction in cyclic adenosine monophosphate (cAMP) levels in smooth muscle cells (SMCs). Furthermore, H2S may react with nitric oxide (NO) to form a compound, possibly nitrosothiol, which ultimately results in a decrease in NO bioavailability. [74].

1.5.5 H_2S donors

Numerous scientific studies demonstrate the pathophysiological role of H_2S, making the use of compounds able to deliver H_2S a viable therapeutic approach. Over the past few years, several H_2S donors have been identified, driven by the challenge posed by the gaseous nature of

hydrogen sulfide. The gas nature make it hard to raises concerns about safety. Hence, recently, the scientific community focused on the development of hydrogen sulfide (H_2S) donors with different characteristics. These donors are classified according to their source, either synthetic or natural, and based on their cynetic release, categorized as either fast or slow. In the category of fast-release donors, we can find sulfide salts such as sodium hydrosulfide (NaHS) and sodium sulfide (Na2S). Commonly employed in biological studies, these salts provide direct access to biologically relevant forms of sulfide (H_2S and HS^-). Despite their role in establishing H_2S as a gasotransmitter and assessing therapeutic potential, sulfide salts have drawbacks. They hydrolyze immediately upon dissolution, leading to an equilibrium that decreases H_2S concentration. Air oxidation and lack of targeting capabilities pose challenges, requiring high doses in systemic delivery. These limitations drive the search for H_2S donors allowing controlled release [134]. Among these synthetically derived, slow-release H_2S donors morpholin-4-ium 4-methoxyphenyl(morpholino) phosphinodithioate (GYY4137) is emerging. This water-soluble compound, when administered intraperitoneally (ip) or intravenously (iv) to rats, elevates plasma H_2S concentration from approximately 32 μmol/l to about 80 μmol/l within 30 minutes. These heightened levels persist for 2 hours [135].

Another exemplary synthetic donor is the 4-thiocarbamoyl phenyl ester of 2-(6-methoxynaphthalene-2-yl)-propionic acid (ATB-346), a derivative of naproxen. This compound is proficient in H_2S release and, concurrently, exhibits significant anti-inflammatory activity by inhibiting cyclooxygenase (COX) activity, currentely under evaluation in clinical

trials [135]. Natural sources also contribute to slow-release H_2S donors, such as garlic extracts (DATS and DADS), sulforaphane, and Erucin. Among these, allicin (diallyl thiosulfinate), extracted from garlic, stands out as one of the most effective natural H_2S donor to date. Upon dissolution in water, allicin decomposes into several compounds, including diallyl disulfide (DADS) and diallyl trisulfide (DATS). A study demonstrated that DATS, with the highest sulfur atom count, produced substantial H_2S upon reacting with natural thiols like GSH, cysteine, homocysteine, and N-acetylcysteine. In contrast, DADS released a comparatively lower amount of gas-transmitter, indicating that DADS is a less efficient H_2S donor compared to DATS [135]. Additional natural donors have been sourced from the *Brassicaceae* family, a botanical group rich in metabolites with intriguing bioactivity. The most extensively studied compounds within this family include glucosinolates and their breakdown products, specifically isothiocyanates and indoles. Among the natural isothiocyanates, erucin emerges as a promising candidate. It can be derived either from *Eruca sativ*a Mill. or through the inter-conversion of sulforaphane, an isothiocyanate found in *Brassica oleracea* L., occurring in vivo. Erucin has demonstrated considerable oral bioavailability in both experimental mouse models and humans [136]. It possesses the characteristics of a slow H_2S donor with thiol-dependent release. Indeed, studies have revealed that erucin incubation, in the presence of L-cysteine, leads to stable and sustained H_2S production [137]. The gradual and sustained release of the gas-transmitter by exogenous H_2S donors is likely more dependable than other compounds (e.g., inorganic salt sulfide) in accurately replicating endogenous H_2S production. In 2020, Martelli and colleagues were the

first to demonstrate the properties of erucin, attributing to it a protective role against vasodilation and an antihypertensive effect in SHR rats [138].

Chapter 1

“ROLE OF TRANSSULFURATION PATHWAY IN VASCULAR COMPLICATIONS ASSOCIATED WITH METABOLIC SYNDROME: H_2S DONORS AS A NEW POTENTIAL THERAPEUTIC STRATEGY”.

2. AIM OF THE STUDY I

The relevance of H_2S signaling within the vasculature is demonstrated by the finding that plasmatic levels of H_2S are significantly reduced in diabetes and in hypertension, in human and animal models [139], [140], [141], [142]. Moreover, in rat aortic endothelial cells treated with high concentrations of glucose and palmitate, there is a reduction of both CSE expression and H_2S production coupled with an increase in ROS production and mitochondrial apoptosis [143]. Starting from these findings, this first part of my PhD aimed to assess a possible involvement of H_2S pathway in MS-associated vascular dysfunction and to evaluate the potential beneficial action of H_2S donors supplementation on MS-associated vascular dysfunction in a genetic murine model of MS (db/db mice). In particular, our attention focused on Erucin, a diet-derived H_2S slow-donor, present in *Eruca sativa* Mill., commonly known as rocket salads, and NaHS, an inorganic salt, a H_2S fast-donor.

3. MATERIALS AND METODHS I

3.1 Animal model: db/db (C57BL/BKS) mice

Animal care and experimental procedures in this study follow specific guidelines of the Italian and European Council law for experiments involving animals. All procedures were approved by the local animal care office (Centro Servizi Veterinari, University of Naples, Federico II) and carried out following ARRIVE guidelines (Percie du Sert et al., 2020) and EU recommendations (Directive 2010/63/EU) for experimental design and analysis in pharmacology care. The procedure was authorized by Ministero della Salute (prot. n. 97/2020). For this study, male db/db mice or their lean

db/+ littermates of 5 weeks of age were purchased from Charles River Laboratories (MI, Italy). All mice were housed in pathogen-free cages (three mice per cage) with a 12 h light-dark cycle (temperature 23 ± 2 °C, humidity 60%) and free access to dry feed and water. *Db/db* mice are used as animal model of diabetes type II and obesity. This strain is characterized by a spontaneous homozygous mutation on the gene coding for the leptin receptor ($Lepr^{db}$). Leptin is a hormone produced by the adipose tissue that plays a crucial role in regulating calorie expenditure, appetite, and metabolism, for that reason *db/db* mice demonstrate morbid obesity which begins at three to four weeks of age, severe hyperglycemia, pancreatic beta cells atrophy and insulin resistance.

3.2 Glycemia measurement

Animals were deprived of food for 2h to normalize glucose plasma levels. Then, glycemia was measured on the blood drop from tail vein following a superficial incision.

3.3 H_2S donors' treatments

Starting from 6 weeks to 10 weeks of age *db/db* mice were treated daily with NaHS or Erucin (3mg/Kg) or vehicle (potassium phosphate buffer pH 7.4) by oral gavage administration. Animal belonging to each cage were randomly assigned to different experimental gourps. Each experimental group included at least five mice.

3.4 Vascular reactivity on aortas rings

Once at 10 weeks of age, *db/db* mice were anesthetize with enflurane (5%) and then killed in a CO_2 chamber (70%) . The thoracic aortas were rapidly harvested from db/db and WT C57BL/6J mice and adherent connective and fat tissue were removed. Rings of 1–1.5 mm length were cut and placed in organ baths (3.0 mL) filled with oxygenated (95% O2–5% CO2) Krebs' solution. The rings were connected to an isometric transducer (7006, Ugo Basile, Comerio, Italy) and changes in tension were continuously recorded with a computerized system (PowerLAb, ADInstrument). The rings were initially stretched until a resting tension of 1.5 g was reached and then were allowed to equilibrate for at least 45 min; during this period the tension was adjusted, when necessary, to 1.5 g and the bath solution was periodically changed. In each set of experiments, rings were firstly challenged with phenylephrine (PE, 1μM, Sigma-Aldrich) until the responses were reproducible. To verify the integrity of the endothelium, cumulative concentration-response curves to ACh (10 nM–30 μM) were performed with PE pre-contracted rings. Then, Isoprenaline (Iso, 10 nM-30 μM), NaHS (10 nM -300 μM), Erucin (10 nM - 300μM). In interest of evaluating the NO pathway contribution, the ring was pre-contracted with a submaximal dose of PE (300 nM) and once stable tone was reached N5-(1-Iminoethyl)-L-ornithine dihydrochloride (L-NIO; 10 μM; a selective inhibitor of eNOS) was administrated and rings incubated for 20 minutes. In these experiments we also used L-cysteine to investigate the H_2S contribution. In particular H_2S release from L-cysteine is correlated to enzymatic activity of both CBS ans CSE. L-cysteine cumulative concentration-response curves (10 nM-3 μM) were performed on PE- precontracted rings. The composition of Krebs solution was as

follows (in mM): NaCl 118, KCl 4.7, MgSO4 1.2, KH2PO4 1.2, CaCl2 2.5, NaHCO3 25 and glucose 11.

3.5 Cell culture experiments

3.5.1 Endothelial cells (BAEC) in high glucose and high palmitate concentration environment

Bovine aortic endothelial cells (BAEC) were used between passages 3-8. BAEC were cultured and grown in medium supplemented with 2mmol/l glutamine, 10% heat inactivated FBS, 50U/ml penicillin/streptomycin. Cells were grown until they reached 90% confluence and then were serum starved overnight. BAEC were incubated for 3 hours in 50 mM (high glucose) D-glucose (HG) solution plus 100 μM sodium palmitate (SP) solution to mimic hyperglycemic and hyperlipidemic (HG+SP) environment. Then cells were stimulated with insulin (100 nM, 15 min). Following that time, pellets were collected and used for Western blot analysis and H_2S content, while supernatants were used for nitrite/nitrate (NOx) assay.

3.5.2 soluble Guanylyl Cyclase (sGCα1β1) overexpressing cells

Chinase Hamster Ovary (CHO) cells overexpressing subunit α1β1 of sGC were furnished by Bayer, Leverkusen, Germany. Cells were cultured and grown in DMEM/F12 (HAM) supplemented with 2 mmol/L glutamine, 10% heat-inactivated fetal bovine serum, 1 mM sodium pyruvate, 0.9 mM sodium bicarbonate, 50 U/mL penicillin/streptomycin, 2.5 μg/ml Amphotericin B, 1mg/ml genetic, 0.25 mg/ml zeocin (Wunder et al; 2005).

Cells were incubated for 2 hours with Erucin 1μM and then collected for persulfidation assay.

3.5.3 Sodium palmitate preparation

A stock of 10 mM Sodium Palmitate /1.66 mM BSA solution (6:1 FA: BSA) was prepared. 69,54 mg of Sodium palmitate (Sigma-Aldrich, Milan, Italy) were solubilized in 10 ml of 150 mM NaCl solution under shaking at 70°C. Simultaneously 2,26 g of BSA-free fatty acid (EMD Millipore; Darmstadt, Germany) were dissolved in 10 ml of 150 mM solution at 37°C under slow stirring. Then 8 ml of Sodium Palmitate solution was added into 10 ml of BSA solution and mixed by stirring at 37°C for 1 hour until the conjugate solution became clear and pH was adjusted to 7.4. The palmitate-BSA stock was filtered using a 0.22 μm low-protein binding filter (Millipore, USA).

3.6 Nitrite/nitrate (NOx) assay

Cellular supernatants (120 μl) were incubated in a microplate with cadmium (Sigma-Aldrich; 50 mg/well) for 1 h to convert the inorganic anion nitrate (NO_2^-) to nitrite (NO_3^-) and then centrifuged at 12000 rpm at 4°C for 15 minutes. NOx was fluorometrically determined in microtiter plates by Promega Glomax explorer (Madison, WI) and calculated against a standard curve of sodium nitrite ($NaNO_2$, 50–2000 nM; Sigma-Aldrich). Each independent experiment was performed in duplicate.

3.7 Intracellular ROS Measurement

The generation of ROS was evaluated using the fluorescence probe 2′,7′-dichlorofluorescein-diacetate (H2DCF-DA). BAEC (1×10^4 cells/well) were plated in 96-multiwell black plates (Corning, USA). At the end of the previously described treatments, cells were incubated with H2DCF-DA (10 μM) for 30 minutes at 37 °C. Fluorescence generation was measured using a fluorescent microplate reader (excitation 485 nm and emission 538 nm; GloMax®-Multi Detection System, Promega: Madison, WI, USA). The intracellular ROS levels were expressed as relative fluorescence intensity (RFI).

3.8 H_2S assay

H_2S determination was performed using methylene blue-based assay. Briefly, BAEC were homogenized in a lysis buffer (100 mM potassium phosphate buffer, pH = 7.4, sodium orthovanadate 10 mM and a cocktail of protease inhibitors 1% v/v) and the protein concentration was determined using the Bradford assay (Bio-Rad Laboratories, Milan, Italy). The lysates were added to a reaction mixture (total volume 500 μL) containing pyridoxal 5′-phosphate (2 mM, 20 μL), l-cysteine (10 mM, 20 μL) and saline (30 μL). The reaction was performed in parafilm-sealed Eppendorf tubes and initiated by transferring tubes from ice to a 37 °C water bath. After 40 min incubation, zinc acetate 1% (ZnAc; 250 μL) was added to trap any H_2S emitted followed by trichloroacetic acid 10% (TCA; 250 μL). Subsequently, N,N-dimethylphenylendiammine sulphate 20 μM (DPD; 133 μL) in 7.2 M HCl and $FeCl_3$ (30 μM, 133 μL) in 1.2 M HCl were added. After 20 min, absorbance values were measured at a

wavelength of 668 nm. All samples were assayed in duplicate, and H_2S concentration was calculated against a calibration curve of NaHS (3.12–250 μM). Results were expressed as nmol/mg protein per min.

3.9 Protein extraction and Western-Blot analysis

Cells and tissues were homogenized in modified RIPA buffer (50-mM Tris–HCl pH 8.0, 150-mM NaCl, 0.5% sodium deoxycholate, 0.1% sodium dodecyl sulfate, 1-mM EDTA, 1% Igepal; Roche Applied Science, Monza, Italy), protease inhibitor cocktail (Sigma-Aldrich) and sodium orthovanadate (10 mM). Protein concentration was determined by Bradford assay using bovine serum albumin as standard (Bio-Rad Laboratories, Milan, Italy). Denatured proteins (40μg) were separated on 8-10% SDS-polyacrylamide gel and transferred to PVDF membrane with Turbo Trans-blot (Biorad). Membranes were then blocked in PBS containing 0.1% v/v Tween-20 and 5% w/v non-fat dry milk for 45 minutes, followed by overnight incubation at 4°C with the following antibodies: : mouse monoclonal anti-eNOS (1:1000, BD Biosciences, Milan, Italy), mouse monoclonal anti-CSE (CSE, 1:500, Proteintech; Manchester, UK), rabbit polyclonal anti-CBS (1:1000, Proteintech, Manchester, UK), rabbit polyclonal anti-Caveolin-1 (Cav-1; 1: 1000; Elab Science; Houston, Texas, USA) rabbit polyclonal anti-3MST (1:1000, Novus Biological, USA), rabbit polyclonal anti-PDE5A (1:1000, ElabScience; Houston, Texas, USA), rabbit polyclonal anti-soluble guanylyl cyclase α1 (sGCα1 1:1000, Merck, Milan, Italy), rabbit polyclonal anti-SQRLD (1:1000, Proteintech; Manchester, UK), rabbit polyclonal anti-ETHE-1 (1:1000, Invitrogen; Waltham, Massachusetts, USA), GAPDH (1:3000; Elabscience) and mouse monoclonal anti-β-actin

(1:3000, Merck, Milan, Italy). Membranes were washed in PBST prior to incubation with horseradish-peroxidase conjugated secondary antibody for 2h. Following incubation, membranes were washed and developed by using chemiluminescence assay. Images were obtained by using Chemidoc chemiluminiscent detection system and densitometrically analysed using ImageJ and optical density (arbitrary units) was reported.

3.10 cGMP determination

Aorta obtained from WT, db/db mice treated or not with Erucin were homogenized in 8 volumes of buffer containing 5% trichloroacetic acid per gram of tissue. Cells overexpressing sGC α1β1 treated with Erucin or with vehicle were lysed in 200µl of PBS containing 10 µl of 3.3M HCl. cGMP was extracted and measured using a commercially available enzyme immunoassay kit (Cayman Chemical, Michigan, USA) following the manufacturer's instructions.

3.11 Persulfidation assay

Persulfidation was detected using a modified biotin switch assay. sGC overexpressed CHO cells were precipitated with 20% trichloroacetic acid and then washed with 10% and 5% trichloroacetic acid. Following centrifugation, the pellets were resuspended in HENS buffer containing methanethiosulfonate (20 mM). Acetone precipitation was performed, then the pellets obtained were resuspended in lysis buffer containing 50-mM iodoacetyl–PEG2–biotin, and 2.5-mM dimedone, and then incubated for 2 hr at room temperature in the dark. Lysates (500 µg) were precipitated and resuspended in 50-µl Tris–HCl (50 mM, pH 8.5) containing

guanidinium chloride (GdmCl 6 mM), and incubated at 95°C for 5 min. A negative control was generated for each sample by adding DTT (1 mM) during biotin cross-linking. 10% of the sample was immediately boiled at 95°C and used for the identification of the levels of sGCα1 among the samples (input). 90 % of the samples were used for biotin immunoprecipitation overnight (4°C) using a high-capacity streptavidin resin. Persulfidated proteins were detected by SDS-PAGE and Western blotting with a specific antibody against sGCα1.

3.12 Data Analysis

All data were reported as mean ± SEM and the number of the replicated experiments for all data sets is at least n=3 except for the ex vivo experiments n=5. The relaxation data have been reported as % of relaxation calculated against the maximal contraction to phenylephrine-induced tone. Statistical analysis has been performed by using one-way or two-way analysis of variance (ANOVA) where appropriate, followed by the Bonferroni or Dunnett posthoc test, where applicable. Data were analyzed by using Prism Graphpad 8.0. Data sets were considered statistically significant when a value of $p < 0.05$ was reached.

4. RESULTS

4.1 CSE/H_2S pathway is defective in BAEC exposed to high concentrations of both sodium palmitate and glucose (SP+HG).

Firstly, we have assessed if in our in vitro model of BAEC exposed to hyperlipidemic and hyperglycemic conditions, endothelial dysfunction occurs. As shown in figure 12A, NOx content, an indirect index of eNOS/NO pathway activation, was significantly reduced in SP+HG-exposed BAEC compared to cells placed in normal conditions (fig. 12 A). This reduction was coupled to an increase in ROS levels (fig. 12 B) confirming that, in our experimental setting, endothelial dysfunction takes place. Starting from these findings, we have then assessed the involvement of the H_2S pathway by measuring H_2S levels and the H_2S-generating enzymes expression in SP+HG-exposed BAEC. As shown in figure 12 C, in cell lysate of BAEC placed in SP+HG environment, lower levels of H_2S were detected, when compared to a normal environment. In details, the basal production of H_2S in cells undergoing SP + HG treatment was not significantly different from cells exposed to vehicle, even though showed an overt trend of reduction. However, when we performed the same measurement, following the addition of L-cysteine, the endogenous substrate for H_2S biosynthesis, we observed a significant increase in both vehicle and SP+HG-exposed BAEC, however, the H_2S production was significantly reduced in SP+HG exposed BAEC compared to the vehicle. In line with the attenuated H_2S content, a reduction in the expression of CSE was detected in SP+HG exposed BAEC (fig. 12 D). Conversely, no change in both CBS and 3MST expression (the other two H_2S-producing enzymes) was observed, in both experimental groups (fig. 12 E-F).

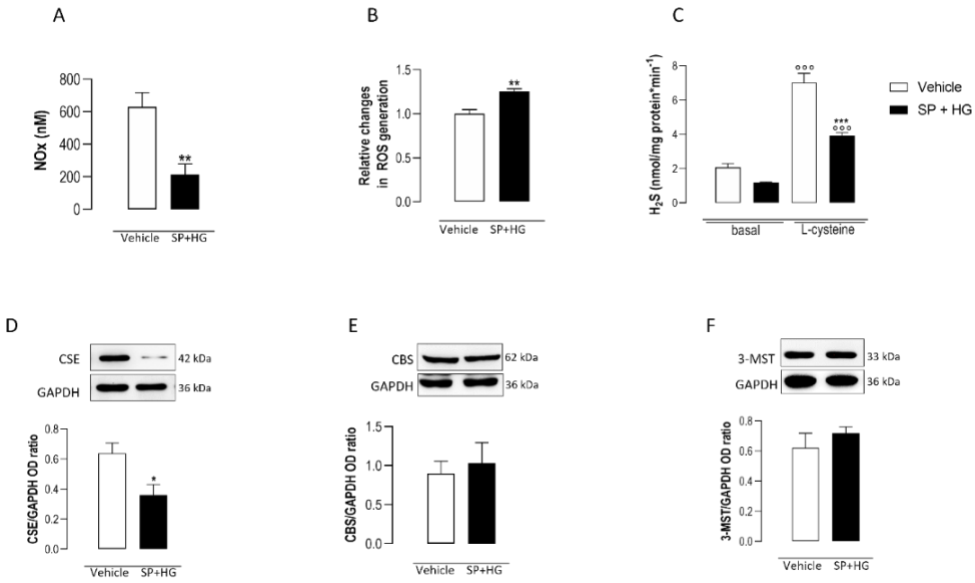

Figure 12. **Evaluation of CSE/H_2S pathway in BAEC exposed to high concentrations of both sodium palmitate and glucose (SP+HG).**

(A) Total NO levels (expressed as total nitrate/nitrite, NOx) in BAEC exposed to SP+ HG (100 µM and 50 mM, respectively) environment (3h) or vehicle (BSA/NaCl) and then stimulated with insulin (100 nM; 15 min). Data were expressed as mean ± SEM of n=4 for each group. Statistical analysis was conducted by using Student's T-test, **p<0.01 vs vehicle. **(B)** Concentration of intracellular ROS levels in BAEC exposed to SP+HG environment or vehicle and then stimulated with insulin. Data were expressed as fold change compared to the levels of ROS detected in the vehicle, taken as 1 (n= 4). Statistical analysis was conducted by using Student's T-test **p<0.01 vs. vehicle. **(C)** Levels of H_2S in the total cell lysate of BAEC exposed to SP+HG environment or vehicle and then stimulated with insulin. Data were expressed as mean ± SEM of n=3 for each group. Statistical analysis was conducted by using one-way ANOVA followed by Bonferonni's for multiple comparisons, °°°p<0.01 vs. own basal; ***p<0.01 vs. vehicle. **(D-F)** Representative western blots of at least three separate experiments with similar results. Quantification of CSE **(D)**, CBS **(E)** and 3MST **(F)** protein levels in cell lysates of BAEC exposed to SP+HG environment or vehicle, and then stimulated with insulin. Data were normalized to GAPDH. Values were presented as mean ± SEM. Statistical analysis was conducted by using Student's T-test. *p<0.05 vs vehicle.

4.2 L-cys/CSE pathway is disrupted in db/db mice contributing to vascular dysfunction coupled to MS.

To verify if the MS-associated vascular dysfunction could involve a defective CSE/H_2S pathway, we carried out *ex vivo* and molecular experiments on aorta harvested from *db/db* mice at 10 weeks of age. Firstly, a concentration–response curve to L-cys on PE-stable tone was performed. As shown in Figure 13 A, the vasorelaxation induced by L-Cys was strongly impaired in *db/db* isolated aorta rings in comparison with WT. A dysregulation in the expression of the H_2S-generating enzymes was also found in db/db mice. Indeed, CSE and CBS expression were significantly lower (fig. 13 B-C), meanwhile 3-MST expression was robustly increased compared to the WT (Fig. 13 D). The degrading H_2S enzymes expression was also evaluated, as shown in figure 13 E-F, and no significant change of ethylmalonic encephalopathy 1 protein (ETHE1), and sulfide quinone reductase (SQRLD), was observed (Fig. 13 E-F). Taken together these results indicate that in MS-associated vascular dysfunction, there is an altered pattern of expression of H_2S-generating enzymes characterized by a significant impairment of L-cys/CSE/H_2S pathway. To assess whether the impairment of endogenous H_2S production was coupled to a reduced activity of downstream signaling, we evaluated the acute relaxing effect of H_2S-donors, i.e., NaHS and Erucin, on PE-precontracted aortic rings harvested from *db/db* and WT mice (fig. 13 G-H). Interestingly both NaHS and Erucin concentration-response curves were markedly impaired in aorta harvested from db/db mice indicating an alteration in the downstream pathways activated by H_2S, essential for the vascular function.

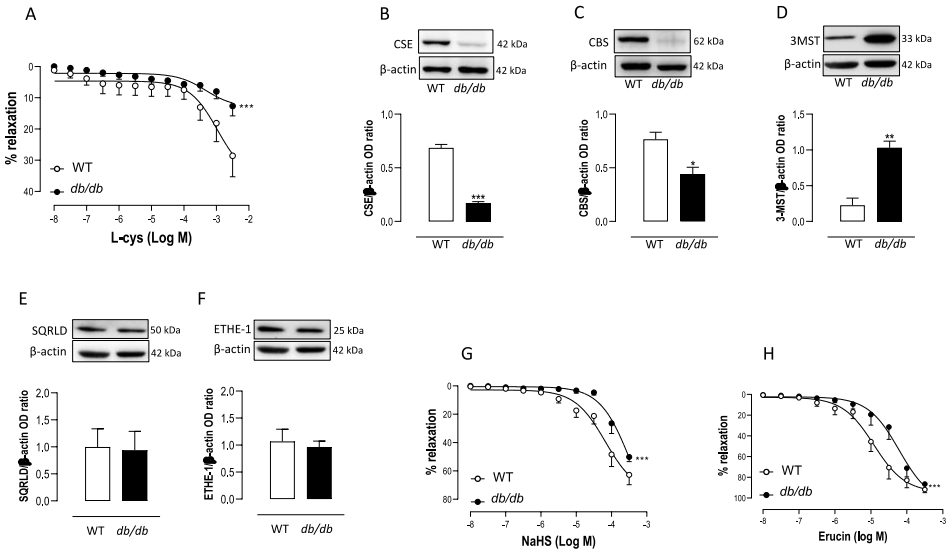

Figure 13. **Evaluation of H_2S signaling in isolated aortic rings of db/db mice.** **(A)** Concentration-response curve of L-cysteine (10 nM-3 mM)- on a stable tone of phenylephrine (PE 1 μM) in aorta rings harvested from *db/db* and WT mice at 10 weeks of age. Values were expressed as mean values ± SEM of n=6 for each group and expressed as % relaxation. Statistical analysis was performed by using two-way ANOVA followed by Bonferroni's for multiple comparisons. ***p<0.001 vs. wt. **(B-F)** Representative western blots of three separate experiments with similar results. Quantification of CSE **(B)**, CBS **(C)**, 3MST **(D),** SQRLD **(E)** and ETHE-1 **(F)** protein levels in aorta lysates of db/db and WT mice at 10 weeks of age. Data were normalized to β-actin. Values were presented as mean ± SEM Statistical analysis was performed by using Student's T-test***p<0.001 vs. WT mice. **(G-H)** Concentration-response curves of NaHS (**E**, 10 nM- 300 μM) and Erucin (**F**, 10 nM- 300 μM) on a stable tone of PE in aorta rings harvested from db/db and WT mice at 10 weeks of age. Values were expressed as mean ± SEM of n=5 for each group and expressed as % relaxation. Statistical analysis was performed by using two-way ANOVA followed by Bonferroni's for multiple comparisons. ***p<0.001 vs. WT.

4.3 Erucin and NaHS administration does not affect hyperglycemia and body weight in db/db mice

In *db/db* mice of 6 weeks of age glycemia levels and body weight were monitored weekly. As shown in figure 7, following 4 weeks of treatment, glycemia and body weight of *db/db* mice were significantly increased compared to WT mice. The administration of both H_2S donors did not affect neither glucose levels (fig. 14 A) nor body weight (fig. 14 B) compared to *db/db* mice trated with the vehicle (n=6 mice).

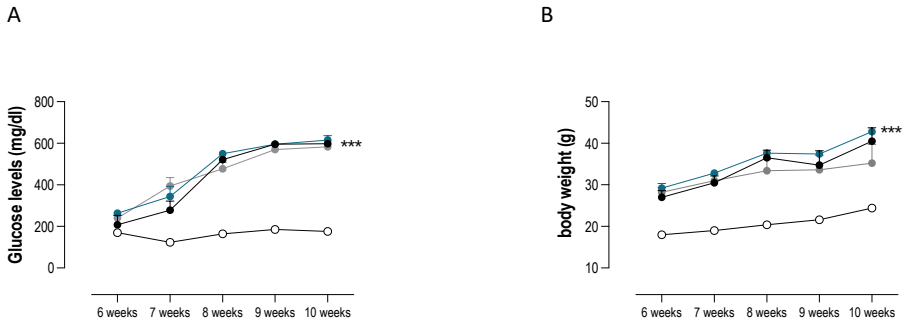

***Figure 14*. Measurements of glucose levels and body wight in *db/db* mice treated with NaHS or Erucin or vehicle.**
Glucose levels **(A)** and body weight **(B)** in *db/db* mice treated with vehicle or with H_2S donors related to WT BL6/J mice. Values were expressed as mean ± SEM of n=6 for each group. Statistical analysis was performed by using two-way ANOVA followed by Bonferroni's for multiple comparisons. ***$p<0.001$ vs. WT.

3.4 Erucin and NaHS ameliorate endothelial dysfunction in db/db mice independently from eNOS/NO signaling

Since L-cysteine/CSE/H_2S pathway is impaired in *db/db* mice, the next step was to evaluate if the chronic supplementation of H_2S could improve the vascular impairment observed. Therefore *db/db* mice were treated orally with Erucin, a slow natural H_2S donor or with NaHS, an inorganic salt, H_2S fast-donor, for 4 weeks (from 6 weeks of age up to 10 weeks of

age). In aorta rings harvested following both NaHS and Erucin treatments (3 mg/kg), acetylcholine-induced vasorelaxation was significantly improved (fig. 15 A). In contrast, H_2S donors' treatments slightly affected the relaxation induced by β_2 adrenergic agonist Isoprenaline (fig. 15 B). It is well known that the integrity of the endothelium is mandatory for Ach-induced vasodilatation, and it is mainly due to NO release [79]. Differently, Isoprenaline-induced vasorelaxation relies on a double mechanism that involves mainly the smooth muscle component, but also the endothelium through eNOS/NO signaling [144]. Our results suggest that both H_2S donors display a targeted action on eNOS/NO pathway, since it remarkably blocks Ach-induced vasorelaxation and only marginally affects Iso-induced vasorelaxation. To better dissect if the protective action of Erucin and NaHS was coupled with eNOS activation, experiments with L-NIO, a selective eNOS inhibitor, were performed. In particular, the increased tension induced by L-NIO administration over a stable tone of PE was evaluated [145]. As expected, such treatment resulted in a minor increase in tension in db/db mice compared to WT, indicating a reduced NO basal production in these mice (Figure 15 C) and confirming that a defective eNOS function occurs in MS, as already demonstrated [146]. To further investigate the involvement of eNOS/NO signaling in endothelial impairment observed in *db/db*, eNOS and caveolin-1 expression were measured. Caveolin-1 is a membrane resident protein that negatively regulates eNOS activity [147] . As shown in figure 15 D, eNOS expression was similar among the experimental groups, whilst Cav-1 was significantly augmented in the aorta of *db/db* mice (figure 15 E) confirming a reduced activity of eNOS in these mice, in agreement with a previous study [148], [149]. Interestingly, as shown in figures 15 C-E,

Erucin and NaHS treatment did not affect either the L-NIO-induced increase in tension or Cav-1 expression. Taken together, these data strongly suggest that the beneficial effect exerted by both Erucin and NaHS is not due to a direct action on eNOS/NO pathway, but rather downstream on the NO/sGC/cGMP axis.

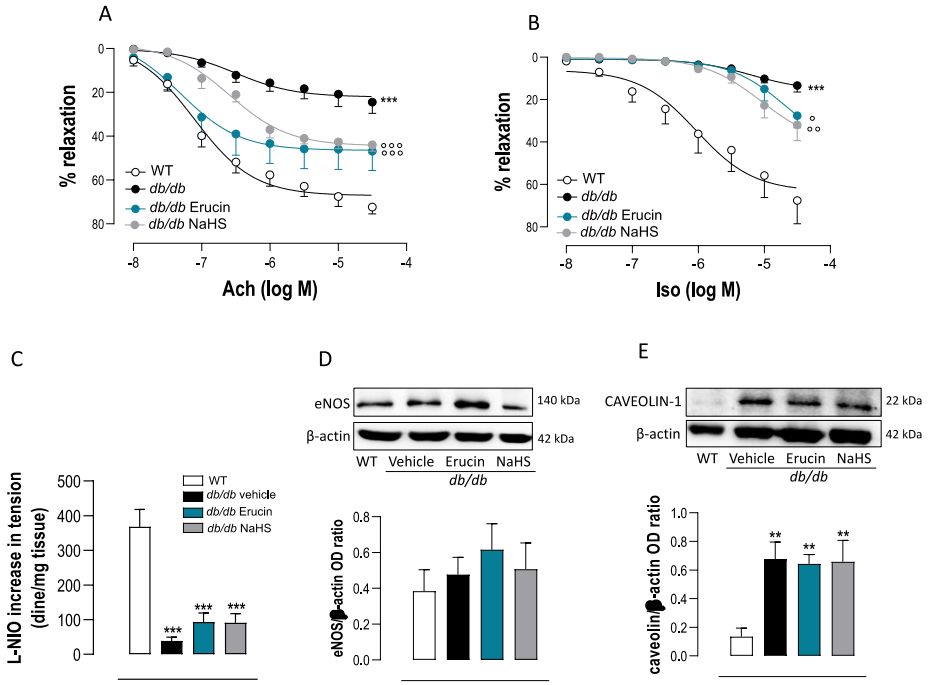

Figure 15. **Effect of Erucin on eNOS/NO pathway in isolated vessels harvested from db/db mice.**

(A-B) Concentration-response curves of Acetylcholine (A, 10nM-30µM) and Isoprenaline (B, 10nM-30µM) on a stable tone of PE (1 µM) in aorta rings harvested from db/db treated with Erucin, NaHS or vehicle and WT mice at 10 weeks of age. Values were expressed as mean ± SEM of n=5-6 for each group and expressed as % relaxation. Statistical analysis was performed by using two-way ANOVA followed by Bonferroni's for multiple comparisons. ***p<0.001 vs. WT mice, °p<0.05; °°°p<0.001 vs. db/db mice treated with vehicle. **(C)** Increase in tension induced by the exposure of PE-pre-contracted aortic rings (300 nM) to L-NIO (10 µM, 20 min) in aorta rings harvested from db/db treated with Erucin, NaHS or vehicle and WT mice at 10 weeks of age. Values were expressed as mean ± SEM of n=6 for each group and expressed as dine/mg of tissue. Statistical analysis was performed by using one-way ANOVA followed by Dunnett's for multiple comparisons. ***p<0.001vs. WT mice. **(D-E)** Representative western

blots of at least three separate experiments with similar results. Quantification of eNOS **(D)** and Cav-1 **(E)** protein levels in aorta lysates of db/db Erucin, NaHS or vehicle and WT mice at 10 weeks of age. Data were normalized to β-actin. Values were presented as mean ± SEM. Statistical analysis was performed by using one-way ANOVA followed by Dunnett's for multiple comparisons **p<0.01 vs. WT mice.

4.5 sGC/cGMP axis is dysregulated in db/db mice, NaHS and Erucin improve vascular impairment via sGC persulfidation.

It is well known that NO exerts its vasodilating properties enhancing cGMP synthesis through the activation of soluble guanylyl cyclase (sGC) [67]. As a second messenger, cGMP activates downstream signaling inducing vasorelaxation. The signaling is switched off by the action of phosphodiesterase-5 (PDE5), the main isoform expressed within the vasculature, which selectively hydrolyzes cGMP in the inactive metabolite 5'-GMP [79], [130]. To evaluate if the impaired vasorelaxation observed in *db/db* mice could involve sGC/cGMP signaling, and if H_2S donors treatment could act on it, the expression of sGC subunit α1 (sGCα1), the most abundant subunit within the vasculature, [144] and PDE5 were assessed. As shown in Fig. 16 A, sGCα1 expression was significantly reduced in the aorta of *db/db* mice in comparison to WT. Conversely, the PDE5 expression did not change among the strains (figure 16 B). The reduction of cGMP content, measured in the aorta of *db/db* mice, further corroborates our hypothesis of a reduced expression of sGC in the aorta of these mice (figure 16 C). These results indicate a defective sGC/cGMP signaling in *db/db* mice leading to a reduction of the vasorelaxation. As observed for eNOS expression, Erucin and NaHS treatments did not modify either sGCα1 or PDE5 expression (figure 16 A-B). However, the cGMP content was significantly enhanced by both Erucin and NaHS

treatments (figure 16 C). This finding strongly suggests that H_2S donor's beneficial action most likely relies on a post-translation modification on sGC, positively modulating its activity.

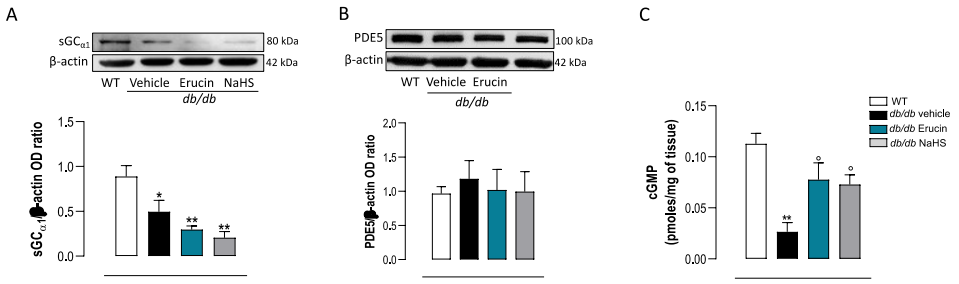

Figure 16. **Effect of Erucin on sGC/cGMP pathway in isolated vessels harvested from db/db mice. (A-B)**
Representative western blots of at least three separate experiments with similar results. Quantification of $sGC_{\alpha 1}$ **(A)** and PDE5 **(B)** protein levels in aorta lysates of db/db treated or not with Erucin and WT mice at 10 weeks of age. Data were normalized to β-actin. Values were presented as mean ± SEM. Statistical analysis was performed by using one-way ANOVA followed by Dunnett's for multiple comparisons **p<0.01 vs. WT mice. **(C)** cGMP levels in aorta harvested from db/db treated or not with Erucin and WT mice at 10 weeks of age. Values were expressed as mean ± SEM of n=3 for each group and expressed as pmoles/mg of proteins. Statistical analysis was performed by using one-way ANOVA followed by Dunnett's for multiple comparisons ***p<0.001 vs. WT mice, °p<0.05 vs. db/db treated with vehicle.

Current evidence, also from our research group, has demonstrated that persulfidation is a new H_2S molecular mechanism of action modifying their biological activity[102], [150], [151]. To test our hypothesis, by using the dimedone switch method, we explored whether Erucin and NaHS could persulfidate sGCα1 leading to changes in cGMP levels. To do so, we used sGC overexpressed CHO cells. As shown in figure 17 A, the persulfidation analysis clearly showed that sGCα1 was persulfidated in Erucin and NaHS-treated cells compared to cells exposed to vehicle. Notably, in the

presence of a reducing agent DTT, the band was reduced, confirming that the detected signal is specific to persulfidation. This data well fit with the cGMP content measured in these cells treated with both H_2S donors Indeed, as shown in figure 17 B, Erucin and NaHS treatments significantly increased the cGMP levels compared to the vehicle. Taken together, these results demonstrate that: i) in *db/db* mice associated vascular dysfunction, sGC/cGMP signalling is defective; ii) NaHS and Erucin, by persulfidating sGCα1, positively modulates sGC activity ameliorating vascular impairment.

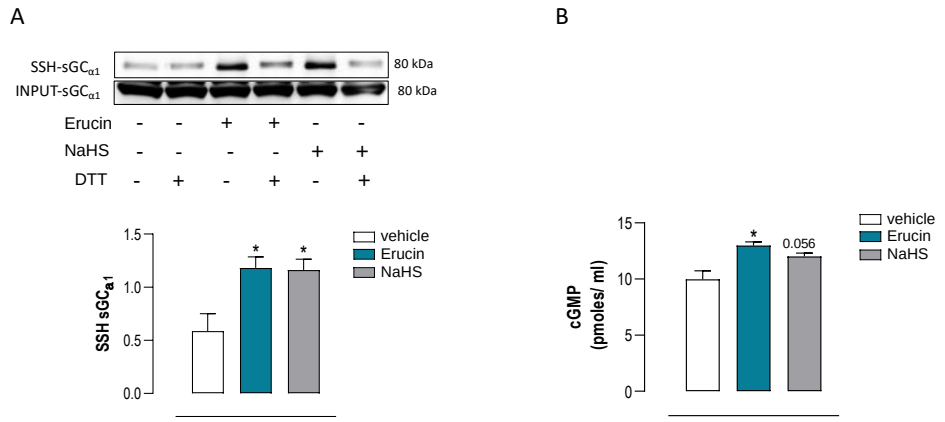

***Figure 17*. Persulfidation of $sGC_{\alpha 1}$ by Erucin increases cGMP production in sGC overexpressed cells.**

(A) Representative western blot of three separate experiments with similar results. Quantification of $sGC_{\alpha 1}$ persufidation levels in cell lysates of sGC overexpressed CHO cells treated with Erucin (1µM; 2 h) or NaHS (30 µM, 2h) or vehicle. DTT, a reducing agent, was used to eliminate the modification prior to detection. Data were expressed as mean values ± SEM. Statistical analysis was performed by using one-way ANOVA followed by Dunnett's for multiple comparisons *p<0.05 vs. vehicle. **(B)** cGMP content in sGC overexpressed CHO cells treated with Erucin or NaHS or vehicle. Data were expressed as mean ± SEM of n=4 for each group. Statistical analysis was performed by using one-way ANOVA followed by Dunnett's for multiple comparisons *p<0.05 vs. vehicle.

5. DISCUSSION

In this study, by using *in vitro* and *ex vivo* approaches, we have shown that in MS-associated vascular complications, an impairment of TSP takes place with a consequent reduction in H_2S biosynthesis. The reduction of H_2S production is counterbalanced *in vivo* by the supplementation of exogenous H_2S with Erucin, one of the major components of leaves of *Eruca sativa* a rocket plant belonging to the *Brassicaceae* family [152] and NaHS. The *in vitro* data were obtained by setting up a cellular model of MS. Exposure of BAEC to high concentrations of both sodium palmitate (SP) and glucose (HG), was used to mimic the hyperlipidemic and hyperglycemic conditions occurred in MS. In this experimental setting, a significant reduction of NOx, coupled with an increase in ROS generation, was found. Thus, this cellular model of MS, displays both hallmarks of endothelial dysfunction i.e., eNOS/NO signaling impairment, and ROS overproduction. Next, we assessed if the H_2S pathway could be affected in BAEC exposed to the SP+HG environment. The data obtained revealed a reduction of H_2S levels coupled with the downregulation of CSE expression. This result is in line with our previous reports in which, an impairment of CSE/H_2S pathway, has been demonstrated in vascular inflammation associated with glucocorticoid-induced hypertension, rat spontaneous hypertension (SHR), and in type one diabetes mice models [141], [142]. Conversely, CBS and 3MST protein expression levels were unchanged confirming the primary role of CSE within vasculature.

To better define the role played by the H_2S pathway in vascular dysfunction associated with MS, we switched from in vitro to ex vivo

approach by using a well-known genetic mouse model of MS, i.e., *db/db* mice. This strain, having a mutation in the gene encoding the leptin receptor (Leprdb), is characterized by a deficient leptin signaling which confers susceptibility to obesity, insulin resistance, and type 2 diabetes (T2DM) [153]. Aorta harvested from *db/db* mice displayed a significant decrease of L-cysteine-induced vasorelaxation associated with a downregulation of both CBS and CSE expression. This evidence showed similar data obtained from cells, confirming an essential role of H_2S signaling in MS-induced vascular dysfunction. The finding that the aorta of *db/db* mice displayed upregulation of the 3-MST expression could be most likely due to compensatory mechanisms for rebalancing the physiological H_2S levels. To evaluate if the impairment of H_2S pathway could also involve H_2S-degrading enzymes, the expression of sulfide quinone oxidoreductase (SQRLD) and persulfide dioxygenase (ETHE1) were assessed. The data showed that there was no difference in both enzymes' expression between wild-type and *db/db* mice. Taken together, these findings suggest that the impaired CSE-derived H_2S synthesis contributes, together with the augmented ROS generation and the dysregulation of eNOS/NO pathway, to vascular dysfunction observed in MS. To further dissect the molecular mechanisms of eNOS/NO signaling impairment, both pharmacological and molecular approaches were applied by using aortas harvested from *db/db* mice. In the organ bath studies, Ach- and Iso-induced vasorelaxation, as well as the increase in tension induced by the inhibition of eNOS with L-NIO, were evaluated and compared to WT mice. In aorta homogenates, eNOS and caveolin-1 expression was also measured. The data obtained show a remarkable reduction in both Ach- and Iso-induced relaxation, coupled with a diminished L-NIO-induced

contraction. Western blot analysis revealed that this effect involves an altered expression of eNOS/Cav-1 ratio in db/db mice. Indeed, a significant increase of Cav-1, but not of eNOS, expression was observed. Taken together, these findings indicate that in *db/db* mice a defective eNOS/NO signaling occurred. Specifically, the increased Cav-1 expression keeps eNOS in a less active state with consequent reduced NO production [147].

To further define the protective role of H_2S, we tested if the administration of Erucin and NaHS, a natural slow donor of H_2S and inorganic fast donor of H_2S, respectively, could ameliorate MS-induced vascular dysfunction. The treatment of *db/db* mice for 4 weeks with both Erucin and NaHS led to a significant improvement of the endothelium-dependent vasorelaxation in isolated aorta rings. In detail, Ach-induced vasorelaxation, that was severely impaired in *db/db* mice, was rescued by Erucin treatment, causing over 50% amelioration of the Emax, while the improvement in Ach-induced vasodilation mediated by NaHS administration was about 40 % in term of Emax compared to db/db mice treated with vehicle. Interestingly, H_2S donors treatmens did not modify L-NIO-induced tension suggesting that eNOS activation was not involved in the beneficial effect elicited by Erucin and NaHS. This hypothesis is further corroborated by the molecular data showing that Erucin and NaHS treatments did not affect either eNOS or Cav-1 expression. This evidence implies that H_2S donors' beneficial effect on vasculature does not involve eNOS function. The finding that Erucin and NaHS also failed to modulate the Isoprenaline-induced vasorelaxation confirms our hypothesis, further ruling out a role for endothelium in H_2S donors' beneficial effect. Indeed, Isoprenaline vasodilatory activity relies on β_2 adrenergic receptor activation, which is

expressed both on endothelium and smooth muscle cells [154]. Specifically, Iso-induced β_2 stimulation promotes vasorelaxation both via eNOS activation and adenylate cyclase/cAMP pathway [144], [155]. The weak effect of both H_2S donors treatment on Iso-induced vasorelaxation, detectable only up to 10 μM, confirms our data indicating both Erucin and NaHS ameliorated MS-associated vascular dysfunction by acting through a mechanism that involves the signaling downstream NO biosynthesis, on smooth muscle component rather than endothelium.

The NO signaling starts from the endothelium leading to activation of sGC in smooth muscle cells. endothelium-derived NO permeates through the vascular smooth muscle cells where binds sGC, promoting cGMP production that, in turn activates a downstream signaling which culminates in vasodilatation [67] . The cGMP signaling is turned off by the action of phosphodiesterase-5 (PDE)-5, the main isoform expressed within the vasculature, which selectively hydrolyses cGMP in its inactive metabolite 5'-GMP [130]. Moreover, it is well established that H_2S is an endogenous inhibitor of PDEs activity, preserving cGMP catabolism [Bucci et al;2012]. In *db/db* mice aorta cGMP levels were almost 4-fold reduced as compared to WT and this effect could be attributable to i) an increased cGMP degradation due to an enhanced expression/activity of PDE-5; ii) a diminished cGMP production caused by a reduced expression/activity of sGC. Therefore, we determined the expression of PDE5 and sGC subunit α1 (the most abundant subunit within the vasculature, [144], [156] in aorta harvested from both strains. The data obtained showed a significant reduced expression of sGCα1 in *db/db* mice vessels only. Conversely, PDE5 expression was unchanged, implying that in MS-associated vascular complications, the reduced levels of cGMP were mainly due to a defective

sGC/cGMP signalling. It is important to underline those low levels of cGMP are even worsted by the increased activity of PDE5, due to the reduced endogenous levels of H_2S . Thus, in *db/db* mice L-cys/CSE pathway disruption leads to a reduced level of cGMP levels that are not only due to a diminished sGC expression, but also to an enhanced cGMP degradation operated by PDE5, in absence of H_2S negative regulation. The involvement of this molecular mechanism in vascular dysfunction is further supported by the *in vitro* data obtained from *db/db* mice aorta. Vasorelaxation induced by H_2S donors in PE-precontracted aortic rings shows a significant reduction of vasodilating concentration-response curves to NaHS and/or Erucin, compared to WT. This finding demonstrates that despite the acute inhibition of PDE operated by the administration of H_2S donors, we still observed an impaired vasorelaxation, most likely due to a low cGMP- derived sGC content. For this reason, we determined the effect exerted by chronic administration of Erucin and NaHS on sGC/cGMP axis.

Interestingly, in aorta of *db/db* mice the treatments wih Erucin and NaHS did not modify the PDE5 and sGCα1 expressions, nevertheless it fully recovered the cGMP content. Most likely, chronic administration of both H_2S donors, by releasing H_2S, put PDE5 in a reduced activity state, enhancing cGMP content. An additive explanation for the full recovery of cGMP levels could be due to a direct action of H_2S on sGC activity. Indeed, it has been shown that H_2S can influence the redox state of sGC and thus its activity [157], [158]. However, the molecular mechanism through which H_2S can modulate sGC activity is not yet clarified. Persulfidation is a recent discovered biological effect elicited by H_2S. Specifically, it is a post-translational modification (PTM) of proteins on L-cysteine residue

that modifies protein biological activity [151], [159], [160] . By using overexpressed sGC cells, we demonstrated that Erucin and NaHS persulfidated sGCα1 and this event was coupled with an increase in cGMP levels. This evidence suggests that exogenous H_2S can modify sGC activity, through the PTM persulfidation, leading to an enhanced enzymatic activity, detectable as an increase of cGMP content.

In summary, we showed that in *db/db* mice the vascular dysfunction coupled with MS is characterized by an impairment of L-cys/CSE/H_2S/PDE/cGMP and eNOS/NO/sGC/cGMP pathways, both converging on a reduced level of cGMP. Erucin and NaHS treatments, by releasing H_2S, improve vascular dysfunction through two complementary actions: i) the direct interaction with sGC via persulfidation; ii) the inhibitory effect on PDE activity, both mechanisms leading to an enhancement of cGMP levels. Our study demonstrated that in *db/db* mice, the reduced level of cGMP is the main hallmark of impaired vasorelaxation. This feature is due to the damaging of both H_2S and NO signaling. The exogenous H_2S supplementation, through the H_2S donor Erucin and NaHS, by acting on smooth muscle component of the vessels, i.e. upstream on sGC and downstream on PDE5, fosters cGMP content, ameliorating vascular function (fig. 18).

Hence, by taking advantage from Erucin and NaHS, our study suggests a potential use H_2S donors, as a promising alternative/additive approach, in the complex management of MS therapy and support the importance of a correct lifestyle and nutrition in MS patients.

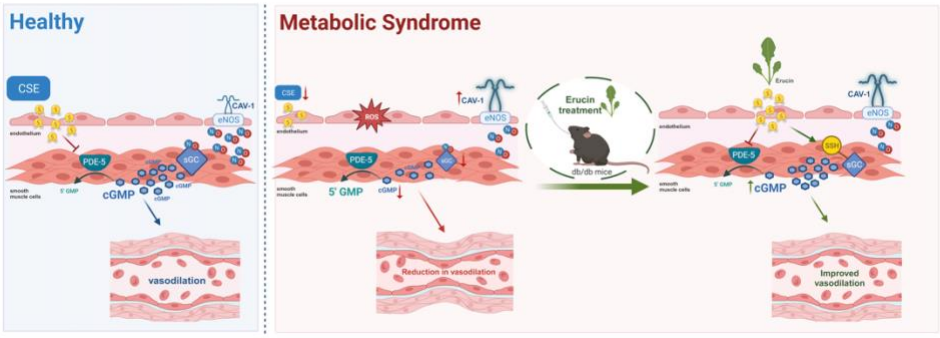

Figure 18. **Graphical abstract** summarizing the results of the study.

Chapter 2

"ROLE OF H_2S DONORS IN ENDOTHELIAL DYSFUNCTION ASSOCIATED WITH TYPE 1 DIABETES"

6. AIM OF THE STUDY II

Type I Diabetes is one of the most important public health problems worldwide, and associated cardiovascular complications are the leading cause of morbidity and mortality in the diabetic population. Untreated T1D causes profound metabolic derangements (e.g. hyperglycemia, cachexia, and ketoacidosis) and is deadly. While a cure is lacking, insulin therapy is the cornerstone of T1D management as it prevents T1D-induced lethality. Yet, this approach does not restore metabolic homeostasis and may even bring about some serious complications such us overweight/obesity. Increasing the incidence of cardiovascular complications. Therefore, the identification of new molecules and/or new therapeutic targets is necessary to enable the development of new adjuvant therapies in order to achieve better control of glycemia, and associated vascular complications, and, thus, improved quality of life for diabetic patients. In light of the data offered by the literature demonstrating a beneficial/protective effect of H_2S at the vascular level and, considering that an alteration of the H_2S pathway, has been found in several inflammatory-based vascular diseases [141], [142], the second part of my PhD project aims to evaluate a potential beneficial effect of different H_2S donors, characterized by different release kinetics, in vascular disease associated to type I diabetes, by using Non Obese Diabetic mice, a murine model of type I diabetes.

7. MATERIALS AND METODHS II

7.1 Animal model- NOD/ShiLtJ mice

Animal care and experimental procedures in this study follow specific guidelines of the Italian and European Council law for experiments involving animals. All procedures were approved by the local animal care office (Centro Servizi Veterinari, University of Naples, Federico II) and carried out following ARRIVE guidelines and EU recommendations (Directive 2010/63/EU) for experimental design and analysis in pharmacology care. The procedure was authorized by Ministero della Salute (prot. n. 97/2020). For this study, female NOD/ShiLtJ mice or CD-1 control mice of 5 weeks of age were purchased from Charles River Laboratories (MI, Italy). All mice were housed in pathogen-free cages (three mice per cage) with a 12 h light-dark cycle (temperature 23 ± 2 °C, humidity 60%) and free access to dry feed and water. NOD/ShiLtJ mice strain is a polygenic model for autoimmune type 1 diabetes (IDDM) [161]. These mice show changes with evolution of pathology, in particular there is an early phase characterized by a localization of inflammatory cells, such as T cells and activated macrophages, around pancreatic islet, inducing peri-insulitis (4–10 weeks of age); consequently, these cells infiltrate islets and initiate a progressive destruction of pancreatic β cells, resulting in a drastic reduction in insulin plasma levels (12–30 weeks of age). The progression of diabetic pathology and its clinical outcomes in these animals are similar to those in humans and associated with vascular disorders Female NOD mice develop spontaneously and progressively type 1 diabetes disease starting from the 8 to 27 weeks of age. As previously shown, in these a progressive endothelium impairment related

to hyperglycemia levels takes place (Bucci, 2004). For our purposes, NOD mice, starting from 8 weeks of age, glycemia values have been monitored every two weeks to establish the disease progression, classified as follows according to the glycemic levels:

- NODI glycemia< 150 mg/dL = healthy normoglycemic mice
- NOD II glycemia >250 mg/dL
- NODIII: glycemia> 400 mg/dL = diabetic mice
-

7.2 Glycemia measurement

Animals were deprived of food for 2h to normalize glucose plasma levels. Then, glycemia was measured on the blood drop from tail vein following a superficial incision.

7.3 H_2S donors' treatments.

Once glycemia reached values over 250 mg/dL, NOD mice were treated daily with NaHS or Erucin (3mg/Kg) or vehicle (PPB) by oral gavage administration until the mice reached to NOD III pathological state.

7.4 RNA extraction and quantity Real-Time PCR

Mouse aortas tissues from each experimental group mice were immediately stored at -80°C until RT-PCR analysis. Total RNA has been isolated from tissues using QIAzol lysis reagent (Qiagen,) following the manufacturer's instructions. Total RNA was purified, quantified, characterized and retrotranscribed using iScript Reverse Transcription Supermix (Biorad) for quantitative real-time PCR. Quantitative real-time

PCR was carried out in Biorad CFX384 real-time PCR detection system by use of SYBER Green Mix (Biorad,) and genes specific primers. Each sample was amplified simultaneously and GAPDH (glyceraldehyde-3-phosphate dehydrogenase, constitutively expressed proteins) expression was used as the housekeeping gene for PCR efficiency determination. Data were calculated using the 2^-ΔΔCt formula.

Gene	FORWARD Sequence (5'->3')	REVERSE Sequence (5'->3')
Mouse		
CBS	CCAGGCACCTGTGGTCAAC	GGTCTCGTGATTGGATCTGCT
CSE	TTCCTGCCTAGTTTCCAGCAT	GGAAGTCCTGCTTAAATGTGGTG
3-MST	GAACCTGCCAATCAGCTCC	CCGGGCATCCAAGTTCTCC

Table 2. Primers used in qPCR analysis

7.5 Vascular reactivity on aortas rings

Aortas were rapidly harvested from NOD, and WT CD-1 mice and adherent connective and fat tissue were removed. Rings of 1–1.5 mm length were cut and placed in organ baths (3.0 mL) filled with oxygenated (95% O2–5% CO2) Krebs' solution. The rings were connected to an isometric transducer (7006, Ugo Basile, Comerio, Italy) and changes in tension were continuously recorded with a computerized system (PowerLAb, ADInstrument). The rings were initially stretched until a resting tension of 1.5 g was reached and then were allowed to equilibrate for at least 45 min; during this period the tension was adjusted, when necessary, to 1.5 g and the bath solution was periodically changed. In each set of experiments, rings were firstly challenged with phenylephrine (PE, 1μM, Sigma-Aldrich) until the responses were reproducible. To verify the integrity of the endothelium, cumulative concentration-response curves to

ACh (10 nM–30 μM) were performed with PE pre-contracted rings. Then, Isoprenaline (Iso) cumulative concentration-response curve (10nM-30 μM) was performed. In a separate set of experiments, once rings have been standardized, PE and 5-HT cumulative response curves were performed. In interest of evaluating the NO pathway contribution, a concentration-response curve of DEA NONOATE (DEA 10 nM – 3 μM) was performed on precontracted rings. In a further set of experiments. The ring was pre-contracted with a submaximal dose of PE (300 nM) and once stable tone was reached L-Nio (10 μM) was administrated and rings incubated for 20 minutes. In these experiments we also used L-cysteine to investigate the H_2S contribution. H_2S release from L-cysteine is correlated to enzymatic activity of both CBS ans CSE. L-cysteine cumulative concentration-response curves (10 nM-3 μM) were performed on PE- precontracted rings. The composition of Krebs solution was as follows (in mM): NaCl 118, KCl 4.7, MgSO4 1.2, KH2PO4 1.2, CaCl2 2.5, NaHCO3 25 and glucose 11.

7.6 FACS Analysis

Lymphocytes isolated from spleen were resuspended in FACS buffer (PBS containing 1% BSA and 0.02% NaN2) and directly stained with the following conjugated antibodies (all from BioLegend, London, UK): CD4 (1:200; clone GK1.5), CD25 (1:200; clone 3C7) for 60 minutes at 4°C. After washing, cells were fixated, permeabilized, and stained intracellularly with IL-17A (1:200; clone TC11-18H10.1), IL-4 and Foxp3 antibody (1:200: clone MF-14). Th1, Th2, Th17 and Treg populations were defined as CD4+/IFN-γ, CD4+/IL-4, CD4+/IL-17, CD4+/CD25+/FOXP-3+respectively. At least 1×104 cells were analysed per sample, and

determination of positive and negative populations was performed based on the staining obtained with related IgG isotypes. Flow cytometry was performed on BriCyte E6 flow cytometer (Mindray Bio-Medical Electronics, Nanshan, China) using MRFlow and FlowJo software operation.

7.7 Data Analysis

All data were reported as mean ± SEM and the number of the replicated experiments for all data sets is at least n=5. The relaxation data have been reported as % of relaxation calculated against the maximal contraction to phenylephrine-induced tone. Statistical analysis has been performed by using one-way or two-way analysis of variance (ANOVA) where appropriate, followed by the Bonferroni or Dunnett posthoc test, where applicable. Data were analyzed by using Prism Graphpad 8.0. Data sets were considered statistically significant when a value of $p < 0.05$ was reached.

8. RESULTS II

8.1 L-cys/H_2S pathway is defective in NOD III mice contributing to vascular dysfunction coupled to type I diabetes.

To verify if the type I diabetes-associated vascular dysfunction could involve a defective H_2S pathway, we carried out *ex vivo* and molecular experiments on aorta harvested from NOD mice. Firstly, a concentration–response curve to L-cys on PE-stable tone was performed. As shown in Figure 19, the vasorelaxation induced by L-Cys was strongly impaired in NOD III isolated aorta rings in comparison with NOD I. Despite the L-Cys reduced vasodilation, and the reduced circulating H_2S levels measured in NOD III mice, already showed by Brancaleone and collaborators [141]Real-Time PCR Real-Time PCR showed a significant upregulation of either CSE, CBS and 3-MST in vessels harvested from NOD III mice. This finding could be ascribed to an attempt to restore physiological H_2S production. Taken together these results indicate that in NODIII-associated vascular dysfunction, a significant impairment of L-cys/H_2S pathway.

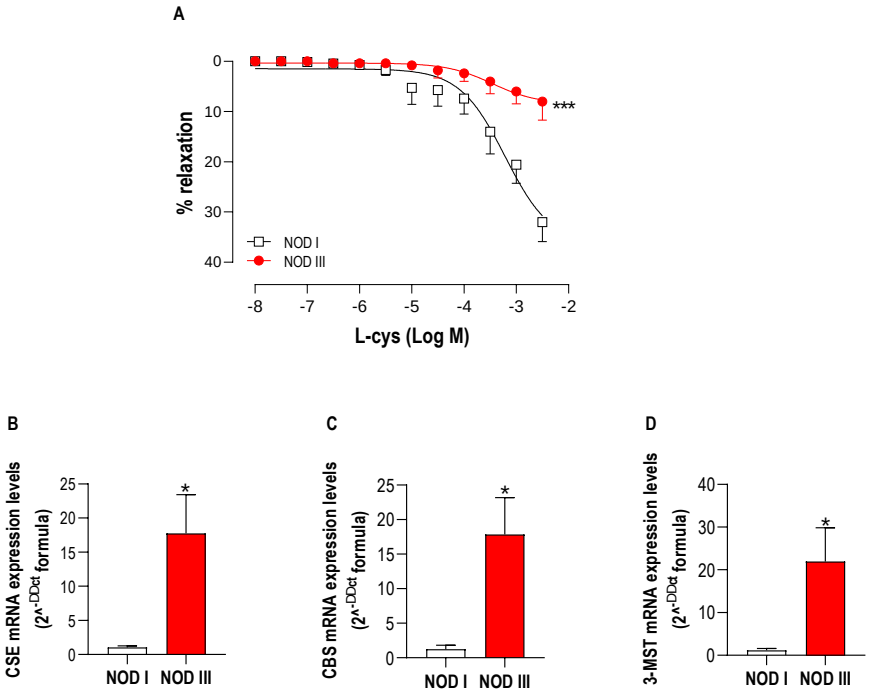

Figure 19. **Evaluation of H_2S signaling in isolated aortic rings of NOD mice.**

(A) Concentration-response curve of L-cysteine (10 nM-3 mM)- on a stable tone of phenylephrine (PE 1 μM) in aorta rings harvested from NOD III and NOD I mice. Values were expressed as mean values ± SEM of n=6 for each group and expressed as % relaxation. Statistical analysis was performed by using two-way ANOVA followed by Bonferroni's for multiple comparisons. ***p<0.001 vs. NOD I. Bar graphs showing the quantification of transcripts levels of CSE **(B)**, CBS **(C)**, 3MST **(D)** evaluated by qPCR in aortas of NOD mice (n=3). Data are expressed as $2^{-\Delta\Delta ct}$ relative to β-actin. Values were presented as mean ± SEM Statistical analysis was performed by using Student's T-test*p<0.05 vs. NOD I mice.

8.2 NaHS and Erucin treatment does not affect hyperglycemia in T1D.

At 8 weeks of age, the levels of glycemia of NOD mice were monitored every two weeks. After 2h of starvation, glucose levels were measured in the blood sample harvested from tail vein, following a superficial incision. When glycemic values were < 150 mg/dL NOD mice were considered healthy normoglycemic (NOD I). In a view of a therapeutic approach, treatments with NaHS and Erucin (3mg/Kg daily) or vehicle started when glycemia increased to levels of 250-300 mg/dL. As shown in figure, two weeks of treatment with both H_2S-donors did not affect glycemia increase in NOD mice. Indeed, in NOD III treated with vehicle, the plasmatic levels of glucose increased up to 498.0 ± 2,3 mg/dL (n=6). Similar results, in mice treated with both NaHS and Erucin (n= 6 mice) (fig.20).

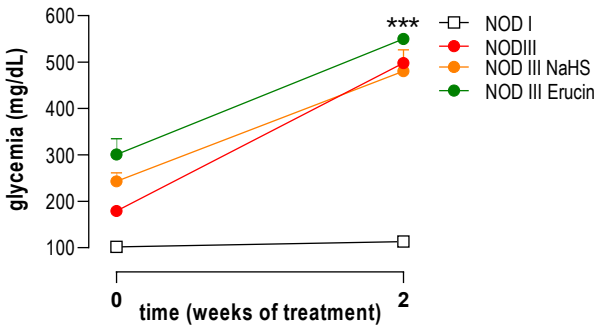

Figure 20. **NaHS and Erucin treatment does not affect glycemic levels in NOD III mice**

Mice presenting glycemic levels <150 mg/dL were considered non-diabetic (NODI), the dashed line indicates average glucose blood value in normoglycemic mice. When glucose levels reached values between 250-300 mg/dL, NOD mice were treated with NaHS or Erucin (3mg/kg daily by oral gavage) or vehicle (PPB) (n=6 mice; ***= $p<0.001$ vs normoglycemic mice).

8.3 NaHS and Erucin treatment significantly ameliorates the impairment of Ach-induced vasodilation, however the treatment does not affect Iso-induced vasodilation in NOD III mice.

Since L-cysteine/CSE/H_2S pathway is impaired in NOD mice, the next step has been to evaluate if exogenous supplementation of H_2S could improve the vascular impairment observed. Therefore, mice were treated orally with Erucin, a slow natural H_2S donor or with NaHS, an inorganic salt, H_2S fast-donor. In the therapeutic approach, treatments with NaHS and Erucin (3mg/Kg daily) or vehicle started when glycemia increased to levels of 250-300 mg/dL. In order to assess a possible beneficial effect of H_2S donors on endothelial disfunction associated with T1D we evaluated the Ach-induced and Iso-induced vasorelaxation. As expected, aortas of NOD III mice displayed a significant impairment of both Ach-induced relaxation (fig 21 A) and Iso-induced relaxation (fig 21 B) compared to NOD I mice. Treatment of NODIII mice with both NaHS and Erucin partially recovered the Ach- induced vasorelaxation compared to NOD III mice treated with vehicle. Conversely, the impaired vasodilation induced by Isoprenaline was not influenced by both H_2S donors (fig. 21 B). It is widely acknowledged that endothelial integrity of is crucial for Ach-induced vasodilatation, primarily mediated by the release of NO [79]. Differently, Isoprenaline-induced vasorelaxation operates through two different mechanisms double mechanism that involves mainly the smooth muscle component, but also the endothelium through eNOS/NO signaling [144]. Our findings indicate that both H_2S donors display a targeted action on eNOS/NO pathway.

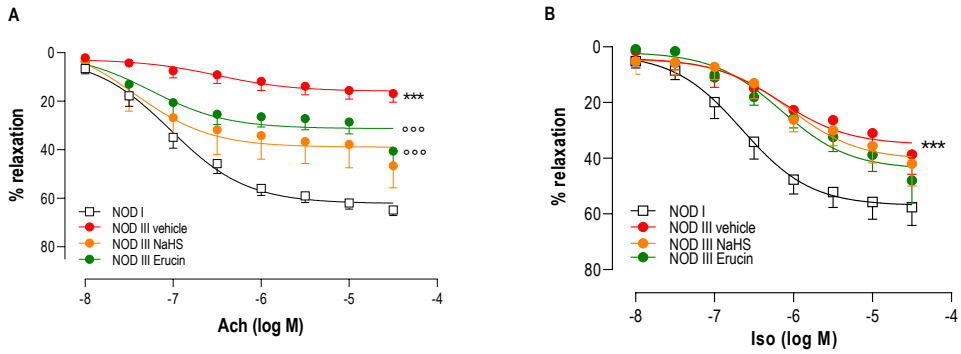

Figure 21. **NaHS and Erucin significantly ameliorates the impairment of Ach-induced vasodilation however the treatments do not affect Iso-induced vasodilation.**

Ach- (**A**) and Iso- cumulative concentration response curve (**B**) performed on sta ble tone of PE (1 µM) of mice NOD I. Values were expressed as mean values ± SEM of n=6 for each group and expressed as % of relaxation. Statistical analysis was performed by using two-way ANOVA followed by Bonferroni's for multipl e comparisons. (n=6 mice; *** = p<0.001 NODIII vs NODI; °°°=p NODIII+Na HS and NODIII+Erucin vs NODIII vehicle).

8.4 NaHS and Erucin treatment does not modify PE- and 5HT-induced vasoconstriction in NOD III mice

Aortas of diabetic mice NOD III displayed a significant impaired contraction when challenged with both PE and 5HT (n=6) compared to NOD I mice, confirming the vascular dysfunction associated to hyperglycemia characteristic of this disease (Bucci et al;2004). Conversely to what observed for vasodilation, the treatments of NODIII mice with both NaHS or Erucin did not improve neither PE- (fig.22 A) nor 5HT (fig. 22 B)-induced contraction (n=6).

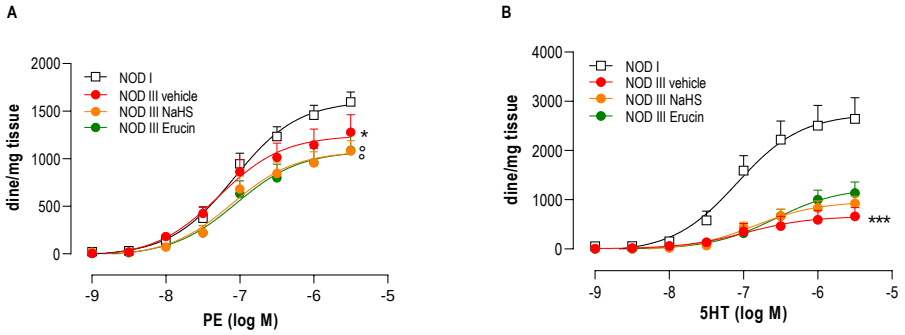

***Figure 22*. NaHS and Erucin treatement has no effect on PE- and 5HT-induced vasoconstriction in NOD III mice**

PE- **(A)** and 5HTinduced cumulative concentration response curve **(B)** performed on aorta rings of NOD I, NODIII vehicle and NODIII treated with NaHS or Erucin (3mg/Kg). Statistical analysis was performed by using two-way ANOVA followed by Bonferroni's for multiple comparisons (*** = $p<0.001$ NODIII vs NODI; °=$p<0.05$ NODIII+NaHS and NODIII+Erucin vs NODIII vehicle; n=6).

8.5 NaHS and Erucin improves endothelial function via eNOS-NO signaling pathway in NOD III mice

In order to assess whether the beneficial effect of H_2S donors could be associated to the activation of the eNOS/NO pathway, we incubated aortas rings with L-NIO, a selective eNOS inhibitor, in order to evaluate the basal, unstimulated NO release. L-NIO addition on a PE-induced stable tone was significantly reduced in NOD III mice compared to NODI mice. Treatment of NODIII mice with NaHS and Erucin recovered the L-NIO induced contraction, over PE-induced stable tone, to the same extend observed in normoglycemic mice (NOD I) (fig. 23 A). To verify the integrity of smooth muscle component, a concentration response curve of the NO-donor DEA NONOATO was performed. As shown in figure 23 B, no significant difference between the groups was observed, suggesting that the vascular damage was confined to the endothelium and not the smooth muscle cells.

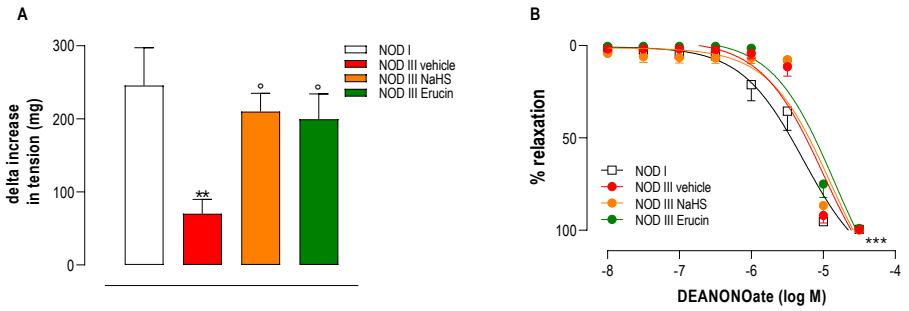

***Figure 23*. NaHS and Erucin improves endothelial function via eNOS-NO signaling pathway**

(**A**)L-NIO induced contraction over PE-induced stable tone. (**B**) DEA NONOATE cumulative concentration response curve performed on stable tone of PE (1 µM) of mice NOD I, NODIII and NODIII treated with NaHS or Erucin (3mg/Kg) ; Statistical analysis was performed by using two-way ANOVA followed by Bonferroni's for multiple comparisons (** = $p<0.001$ NODIII vs NODI; °=$p<0.05$ NODIII+NaHS and NODIII+Erucin vs NODIII vehicle; n=6).

8.6 NaHS and Erucin blunt Th17 and Th1 cells in NOD III mice

It is well known that T1D is an autoimmune disease characterized by a localization of inflammatory cells, such as T cells and activated macrophages, around pancreatic islet, inducing peri-insulitis. These cells infiltrate initiates a progressive destruction of pancreatic β cells, resulting ina drastic reduction in insulin plasma level. Taking into account this aspect, we next assessed if the treatment with H_2S improved not only the vascular reactivity but also the immune profile of NOD mice, evaluating the Th1-Th2-Th17 and Treg balance. As shown in figure 24 in NOD III mice there was an increase in Th1 and Th17 pro-inflammatory T cells compared to NOD I (### $p<0.001$ NOD III vs NOD I) while there were no differences in Th2 and Treg profile. Interestingly both treatment with NaHS and Erucin reduced Th1 and Th17 cell infiltrate compared to NOD III mice (*$p<0.05$ NODIII+NaHS and NODIII+Erucin vs. NODIII vehicle).

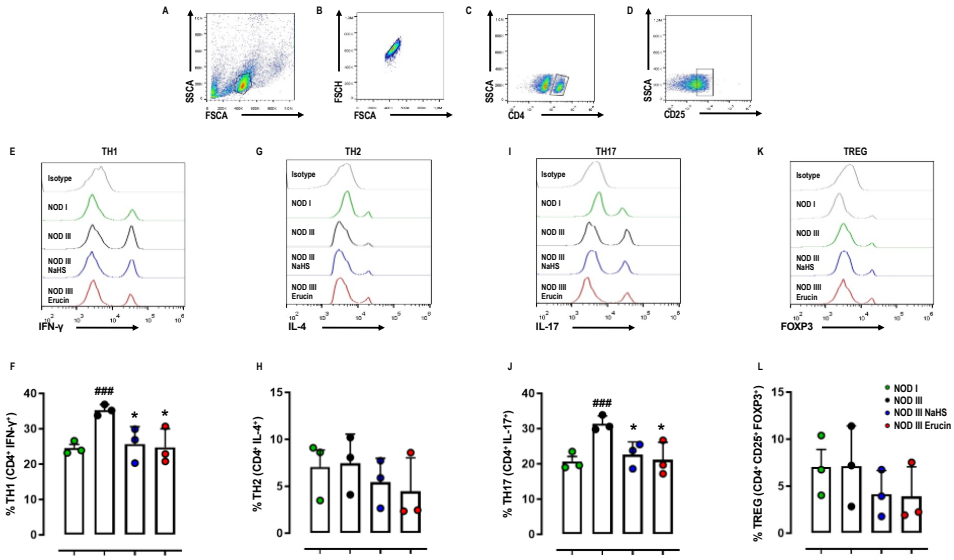

***Figure 24*. NaHS and Erucin blunt Th17 and Th1 cells in NOD III**
Flow cytometry analysis was employed to determine *in situ* levels of $CD4^+$T cell s, Th1, Th2, Th17 and Tregs subsets. Flow cytometry gating strategy applied (**A, B, C, D**). Th1, Th2, Th17 and Treg populations were defined as $CD4^+$/IFN-γ **(C, E, F)**, $CD4^+$/IL-4 (**C, G, H**), $CD4^+$/IL-17 (**C, I, J**) $CD4^+/CD25^+/FOXP\text{-}3^{+.}$ **(C, D, K, L)** respectively. Representative FACS plots of three independent experiments with similar results are shown (n=3 mice; ### = $p<0.001$ NODIII v s NODI; *$p<0.05$ NODIII+NaHS and NODIII+Erucin vs NODIII vehicle).

9. DISCUSSION II

Diabetes stands as one of the most critical public health issues globally, with cardiovascular complications being the leading cause of morbidity and mortality in the diabetic population. Despite a lot of drugs targeting glycemic control, the incidence of cardiovascular complications keeps rising. Therefore, the identification of new molecules and/or therapeutic targets is imperative to facilitate the development of novel adjunct therapies for better glycemic control, management of associated vascular complications, and ultimately, an enhancement in the quality of life for diabetic patients. Recent evidence demonstrates a reduction in hydrogen sulfide (H_2S) levels in diabetes, whether of type 1 or type 2, a gasotransmitter known for its vasodilatory properties [141]. In light of this, the propose of the second part of my PhD project has been to assess a potential beneficial effect of H_2S donors in diabetes and its associated cardiovascular complications focusing our attention on Erucin, a diet-derived H_2S slow-donor, present in *Eruca sativa*, commonly known as rocket salads, and NaHS, an inorganic salt, a H_2S fast-donor. To achieve this goal, we used Non-Obese Diabetic mice (NOD), a spontaneous type 1 diabetes model. This strain develops an autoimmune disease leading to the destruction of pancreatic β-cells, resulting in insulin deficiency over time. Aorta harvested from NOD III mice displayed a significant decrease of L-cysteine-induced vasorelaxation compared to NOD I healthy mice . Despite the L-Cys reduced vasodilation, mRNA expression analysis showed a significant upregulation of either CSE, CBS and 3-MST in the vessels harvested from NOD III mice. This apparently unexpected findings, is, however, consistent with previous studies demonstrating that in diabetic mice, characterized by reduced plasma levels of H_2S there is an

increase in the expression of the enzymes involved in H_2S production [141]. This result could be attributed to a compensatory response of the organism to restore physiological levels of H_2S. In order to evaluate a potential beneficial effect of H_2S donors on diabetes-associated endothelial dysfunction, the action of vasodilatory substances such as Acetylcholine (Ach) and Isoprenaline (Iso) was assessed. The first set of experiments allowed us to evaluate the level of vasodilation in the aortas of NOD III subjected to chronic treatment with H_2S donors following the administration in the organ bath of Ach, a neurotransmitter directed towards muscarinic receptors. Vascular function in NOD III under pathological conditions was strongly reduced compared to NOD I mice and significantly restored in animals treated with NaHS and Erucin. This led us to propose a positive action of H_2S on the pathway regulating endothelial-dependent vasodilation. Considering the use of Isoprenaline, a vasodilating agent that interacts with β-adrenergic receptors, especially in smooth muscle, no differences in the vasodilation pattern was observed in treated and untreated NOD III. This suggests that the positive effect of H_2S specifically targets the eNOS/NO pathway, directly at the endothelial level. It worthy to underline that *in-vivo* treatment with both H_2S donors increased NO-dependent vasodilatation, independently from the development of diabetes, indeed, the spontaneous increase of glycemia levels in NOD mice are not affected during all treatment. To assess a possible improvement in vascular contractility in diabetic mice, aortas of each experimental groups were exposed in the organ bath to Phenylephrine (PE) and Serotonin (5HT). The results revealed that the administration of both substances in NOD III display a significant reduction in aorta contractility compared to NOD I mice confirming vascular damage.

Moreover, therapeutic treatment with H_2S donors did not significantly improve vascular contractility following stimulation with PE and 5HT. These results once again support the hypothesis that the restoration of vascular function, i.e., the eNOS/NO pathway postulated after treatment with H_2S donors, is targeted at the endothelial level. To further confirm the discussed results, additional experiments allowed us to assess the beneficial effect of H_2S on the eNOS/NO pathway. Using an eNOS inhibitor, L-NIO, we found that in pathological NOD III, vascular tension is minimal, indicating a clear endothelial dysfunction. in NOD III treated with both H_2S donors NaHS and Erucin, vascular tension following L-NIO administration were restored back to the healthy levels. These results together with no changes observed in DEA-nonoate (NO donor) vasodilation, confirm that the effect of H_2S donors is specific on eNOS/NO pathway and therefore at the endothelial level. Type 1 Diabetes (T1D) is characterized by an autoimmune response leading to the destruction of pancreatic beta cells. The involvement of distinct T-helper (Th) cell subsets, namely Th1, Th2, Th17, and regulatory T (Treg) cells, plays a crucial role in the pathogenesis of T1D. Th1 cells, known for promoting cell-mediated immunity, contribute to T1D progression through the release of pro-inflammatory cytokines such as interferon-gamma (IFN-γ) and tumor necrosis factor-alpha (TNF-α) [162]. This pro-inflammatory event contributes to the autoimmune attack on pancreatic beta cells. Conversely, Th2 cells, responsible for humoral immunity, generally produce anti-inflammatory cytokines. While less emphasized in T1D, an imbalance in Th1/Th2 responses may influence disease progression. Th17 cells, a subset linked to autoimmunity, have been implicated in various autoimmune diseases, including T1D. Their presence in pancreatic islets contributes to

local inflammation through the secretion of interleukin-17 (IL-17) [163]. Treg cells, on the other hand, are pivotal in maintaining immune tolerance and preventing autoimmunity. In T1D, a deficiency in Treg cells or impaired function may contribute to the failure in controlling the autoimmune response [164]A comprehensive understanding of the dynamic interplay among Th1, Th2, Th17, and Treg cells is essential for unraveling the complex immunopathogenesis of T1D. Considering this aspect, our subsequent investigation aimed to determine whether H_2S treatment not only improved vascular reactivity but also influenced the immune profile of NOD mice. This evaluation included an assessment of the Th1-Th2-Th17 and Treg balance. Our results suggested that in NOD III mice there was an increase in Th1 and Th17 pro-inflammatory T cells compared to NOD I while there were no differences in Th2 and Treg profile. Interestingly both treatment with NaHS and Erucin reduced Th1 and Th17 cell infiltrate compared to NOD III mice

In conclusion, the results obtained suggest that in NOD mice, treatments with NaHS and Erucin ameliorate vascular disfunction by acting on the endothelium on eNOS/NO and CSE/H_2S pathways. Furthermore, treatment with both donors improves NOD III systemic immune profile by reducing the production of pro-inflammatory T cells: Th1 and Th17.
The interesting aspect of these two studies conducted during my PhD project is that the same donors, in two different metabolic pathologies such as Metabolic Syndrome and Type 1 diabetes, improve the pathological condition through two different but complementary mechanisms, highlighting the versatility of H_2S as a gastrasmitter.

Chapter 3

"HOW THE LOSS OF NOGO-B IMPACTS MACROPHAGE FUNCTIONS IN A NOVEL MOUSE MODEL OF CORONARY ATHEROSCLEROSIS".

In the third chapter of my Ph.D., I had the opportunity to work for 1 year (from July 2022 to July 2023) with Dr. Di Lorenzo, esteemed worldwide expert in metabolic disease, and her team at Weill Cornell University in New York (U.S.A.). Here, I explored the primary cause of mortality in individuals with metabolic disease: coronary atherosclerosis. My research specifically delved into the intricate realm of sphingolipids and their crucial role in this pathology.

10. BACKGROUND AND AIM OF THE STUDY

Cardiovascular diseases (CVD) account for most of the death worldwide, with coronary artery disease (CAD) being the leading cause [165]. Coronary artery disease (CAD) is a pathological condition affecting the arteries that supply the heart with blood. It is usually caused by atherosclerosis which is a buildup of plaques inside the arterial walls, causing the arteries to become narrower and slowing the passage of blood. In atherosclerosis, monocytes are recruited into the arterial wall, following the accumulation of lipoproteins in the intima. Monocytes differentiate in macrophage foam cells leading to a maladaptive inflammatory response resulting in subendothelial expansion with neointimal proliferation, inflammatory cell recruitment, lipids, and matrix accumulation. The lesion can progress and manifest a necrotic core covered by a thin layer of matric and smooth muscle cells called fibrous cap. These lesions are defined "vulnerable" because they can disrupt triggering an acute thrombotic vascular event, manifesting in myocardial infarction in the heart, or stroke when affect the brain, and sudden death [65]

Sphingolipids (SL) are both fundamental structural components of the eukaryotic membranes and signaling molecules regulating a variety of biological functions, including proliferation, migration, and apoptosis. Ceramide and sphingosine-1-phosphate are highly bioactive lipids with important regulatory functions in the cardiovascular health and diseases [166]. Altered sphingolipid levels correlates with atherosclerosis. However, whether the dysregulation of this pathway is causal or consequential and specific molecular mechanisms remain poorly understood. SL are synthetized *de novo* in the membrane of the smooth endoplasmic reticulum (ER), where serine palmitoyltransferase (SPT) catalyzes the first and rate-limiting step. The activity of SPT enzyme is negatively regulated by the protein ORMDL [167]. Recently, Di Lorenzo group discovered that Nogo-B, a membrane protein of the ER, binds to and inhibits the activity of SPT, hence downregulates sphingolipid *de novo* biosynthesis, particularly S1P and ceramides, to impact vascular inflammation, blood pressure and heart failure [168]. Nogo-B is highly expressed in macrophages (MΦ) but its role in atherosclerosis is unknown. Thus, in the last part of my PhD program in Professor Di Lorenzo's Lab I have been interested into investigate how the loss of Nogo-B impacts macrophage functions in a novel mouse model of coronary atherosclerosis [169].

11. MATERIALS AND METHODS III

11.1 Animals and transverse aortic constriction (TAC) surgery

To delete Nogo-B specifically in monocytes/macrophages, floxed-Nogo-A/B mice (Nogo-A/B$^{f/f}$), were crossed with transgenic mice Lyz2 (lysozyme 2 gene) in which the Lyz2 promoter drives constitutively the expression of Cre (LysM-Cre). These mice were further crossed with ApoE$^{-/-}$ mice (Jackson Laboratory) to generate mice lacking Nogo-B specifically in myeloid line on ApoE$^{-/-}$ background (MΦ Nogo-B KO ApoE-/-). Nogo-B$^{f/f}$ ApoE-/- mice were used as control mice.

Cardiovascular disease, including coronary artery disease (CAD), is the number one cause of death worldwide and hypercholesterolemia and hypertension are two major risk factors for coronary artery disease. ApoE-/- as well LDL -/- (receptor-knockout) mice have been extensively utilized to study atherosclerosis pathogenesis, but they develop these pathological conditions only when they fed with Western-type diet, resulting in high cholesterol levels >1400mg/dl compared to humans [Nakashima et al; 1994]. In addition, the principal limitation for these experimental animal models is that mice develop atherosclerosis only in the aorta and aortic root but not in coronary artery vessels, the principal site where atherosclerosis plaque is built up in human [170]. To overcome this inconvenient we decided to use a novel mouse model of coronary lesion this is possible by combining two major risk factors: high cholesterol given by the ApoE-/- background and pressure-overload given by transverse aortic constriction (TAC) surgery [169]. This surgery consists of the constriction of the aortic arch between the innominate artery and the left common carotid artery with a surgical suture, with consequent high pressure in the right carotid and in

the coronary arteries. Briefly, mice (8–10 weeks of age: 25-27 g) were anesthetized with a single intraperitoneal injection of a cocktail of ketamine (100 mg/kg) and xylazine (5 mg/kg). After fur removal, a horizontal incision was made at the second intercostal space. After retracting the thymus, the aortic arch was visualized with a dissecting scope (Zeiss Axio Observer.Z1). A 7-0 nylon ligature was tied between the innominate and left common carotid arteries with an overlapping 28-gauge needle, which was then rapidly removed (fig.25).

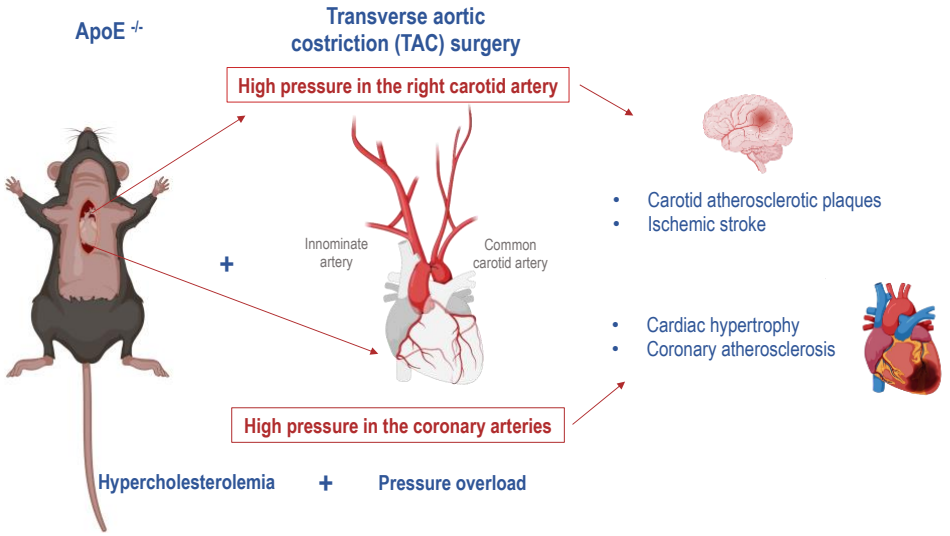

***Figure 25*. Schematic representation of transverse aortic constriction (TAC) surgery on ApoE -/- mice.**

11.2 Histology and Immunofluorescent staining of myocardial sections

MΦ Nogo-B KO ApoE-/- and Nogo-B$^{f/f}$ ApoE-/- were subjected to TAC. 8 weeks later the heart was sectioned from the base to the apex to measure coronary stenosis, fibrous cap thickness and necrotic core. For immunofluorescent analysis of coronary arteries in mice, hearts were perfused with PBS, followed vt 4% paraformaldehyde (PFA) solution, collected, and incubated overnight in 4% PFA solution at 4°C. The following day, 4% PFA solution was replaced by 30% sucrose and left overnight at 4°C on rotation. The hearts were divided into 3 parts (base, middle, and apex), submerged overnight in OCT/sucrose 30% (1:1 ratio), and consequently embedded in OCT. The whole heart was sectioned from the base to the apex. Heart sections every 200 μm were stained with Oil-Red O and H&E and coverslipped with aqueous mounting medium. For immunofluorescence analysis, the heart sections were permeabilized with 0.5% Triton X-100 in a solution of 5% BSA, followed by blocking in BSA 5%, and overnight incubation at 4°C with antibodies against α-SMA (1:200; ThermoFisher) and collagen I antibody (1:200; Abcam) in 5% BSA solution. After washing with PBS, heart sections were incubated with secondary antibodies: Alexa Fluor 568–conjugated donkey anti-mouse IgG (1:200; Abcam), and Cy5-labeled donkey anti-rabbit IgG (1:500; Jackson ImmunoResearch) were added for 1 hour at room temperature. Nuclei were counterstained with DAPI (1:10,000; Calbiochem). Immunofluorescence images of coronary sections were acquired by using Zeiss Axio Observer. To quantify LAD, diagonal and marginal stenosis throughout the heart, myocardial sections from the base to the apex, stained with oil-red-O and hematoxylin, were measured for the area of the lumen

(L) and area defined by the internal elastic lamina (IEL). The percentage of stenosis was calculated as (IEL–L)/IEL×100. Lipid content was expressed as a percentage of Oil-red-O positive staining versus the area of the LAD plaque. For fibrous cap thickness, collagen-I and α-SMA-positive staining of the cap overlaying the plaque core was measured and expressed as average per plaque. H&E-stained sections were quantified for necrotic core and expressed as percentage of the acellular area versus to the area of the plaque. All images were acquired by using a Zeiss Axio Observer.Z1 microscope and analyzed by using ImagePro analyzer 7.0 software (Media Cybernetics).

11.3 Peritoneal macrophages isolation

MΦ Nogo-B KO ApoE-/- and Nogo-B$^{f/f}$ ApoE-/- mice received TAC surgery and 3 days later were intraperitoneally injected with 1 ml of 3.9% thioglycolate solution, which induced the recruitment of inflammatory cells, particularly monocytes. 3 days later mice were sacrificed in a CO_2 chamber (70%) and a little bit of belly skin was removed (around 5-8 mm) being careful to not break the peritoneum, the peritoneal leukocytes were collected by injecting into the skinless area 5 mL of Ca^{++}/Mg^{++}-free PBS. Cells were than plated for 2 h in DMEM supplemented by 10 % FBS, 1% glutamine and 1% penicillin/streptomycin in order to isolate macrophages by adhesion. After 2h, all the non-adherent cells were removed, while the adherent monocyte were harvested by using PBS+10mM of EDTA solution and seeded in 6 multiwells ($1.8x10^6$ cells/ well).

11.4 Experimental protocol-peritoneal macrophages stimulation

To best mimic the atherosclerotic plaque environment in vitro, macrophages were stimulated with Ac-LDL (120 μM, 12h), LPS (10 ng/mL, the last 3 of 12h), TNFα (10 ng/mL, 12h) and ATP (5mM, the last 45 minutes) in DMEM supplemented by 1% charcoal-stripped FBS + 1% Glutamine + 1% Pen/Strep. In another set of experiments cells were pretreated with myriocin 30 nM for 30 minutes before the stimulation as described above. In a further set of experiments macrophages were stimulated with LPS (10ng/ml,12h) and ATP (5mM, the last 45 minutes) in DMEM supplemented by 1% charcoal-stripped FBS + 1% Glutamine + 1% Pen/Strep and treated with Ceramide 16 (0.3-1-3 uM) the last 3h.

11.5 Western Blot Analysis

Cellular pellets of macrophages isolated from MΦ Nogo-B KO ApoE-/- and Nogo-B$^{f/f}$ ApoE-/- mice were lysate in RIPA buffer (50 mM TRIS-HCl pH 7.4, 150 mM NaCl, 0.5% sodium deoxycholate, 1% NP-40, 0.1% SDS) supplemented with 2 mM sodium orthovanadate, and inhibitors of proteases (ThermoFisher Scientific #88665) and phosphatases (Roche, #04906845001). WB analysis was performed by using 40 μg of cell lysates, and proteins were analyzed with sodium dodecyl sulfate polyacrylamide gel electrophoresis (SDS-PAGE) and immunoblotting. Nitrocellulose membranes were probed with the following primary antibodies: anti-NOGO-B (R&D cat# AF6034), SPTLC1 (BD Biosciences #611305) SPTLC2 (ABclonal #A12935), ORMDL3 (Millipore cat# ABN417), Caspase-1 (Adipogen cat#AG-20B-0042-C100), Gasdermin-D (Cell-signaling cat#E9S1X) and HSP90 (Millipore cat#5392). SPTLC1

and SPTLC2 were detected with secondary antibodies, IRDye 800 anti-mouse (Li-Cor #92632210) and IRDye 680 anti-rabbit (Li-Cor #92668071) and images acquired using the Odyssey Infrared Imaging System (Li-Cor). Nogo-B, ORMDL3, Caspase-1, Gasdermin D and HSP90 were detected using horseradish peroxidase-conjugated secondary antibody, respectively. Enhanced Chemiluminescence Substrate (Clarity TM Western ECL Substrate, Bio-Rad Laboratories #1705061) was used for the development of the WB. The intensity of the protein bands was quantified using ImageJ Software (version 1.52a, U.S. NIH).

11.6 Lipidomic analysis by LC/MS/MS

Lipids levels were measured in MΦ Nogo-B KO ApoE-/- and Nogo-$B^{f/f}$ ApoE-/- mice peritoneal macrophages in basal condition on stimulated with LPS/TNFα/Ac-LDL by LC/MS/MS. Levels of cholesteryl ester and ceramide species were analyzed by LC/MS/MS at the WCM Lipidomic facility.

11.7 RNA Sequencing

RNA was extracted from peritoneal macrophages of mice MΦ Nogo-B KO ApoE-/- and Nogo-$B^{f/f}$ ApoE-/- in basal condition or stimulated with LPS/TNFα/Ac-LDL using Qiagen RNeasy Mini Kit, following the manufacture instruction (Qiagen cat#74104). RNA-seq was performed by RNA core facility of Weill Cornell Medicine. Total RNA integrity was evaluated with the Agilent Bioanalyzer 2100 (Agilent Biotechnologies, Santa Clara, CA), and only samples with an RNA integrity number (RIN) >9.0 were further processed for RNA-seq. All RNA-seq libraries were prepared using 100 ng of total RNA with the TruSeq Stranded Total RNA

sample preparation kit (ribosomal RNA depletion and stranded RNA-Seq) with Ribo-Zero according to the manufacturer's specified protocol (Illumina, San Diego, CA). Samples were multiplexed and sequenced across multiple lanes of a HiSeq 4000 Sequencing System (Illumina) using 50-base paired-end reads to achieve a minimum depth of 30 million aligned read-pairs. Data were analyzed by the Englander Institute for Precision Medicine of Weill Cornell Medicine (New York, NY).

12. RESULTS III

12.1 Depletion of Nogo-B in macrophages enhances atherosclerotic lesion in the marginal and diagonal arteries

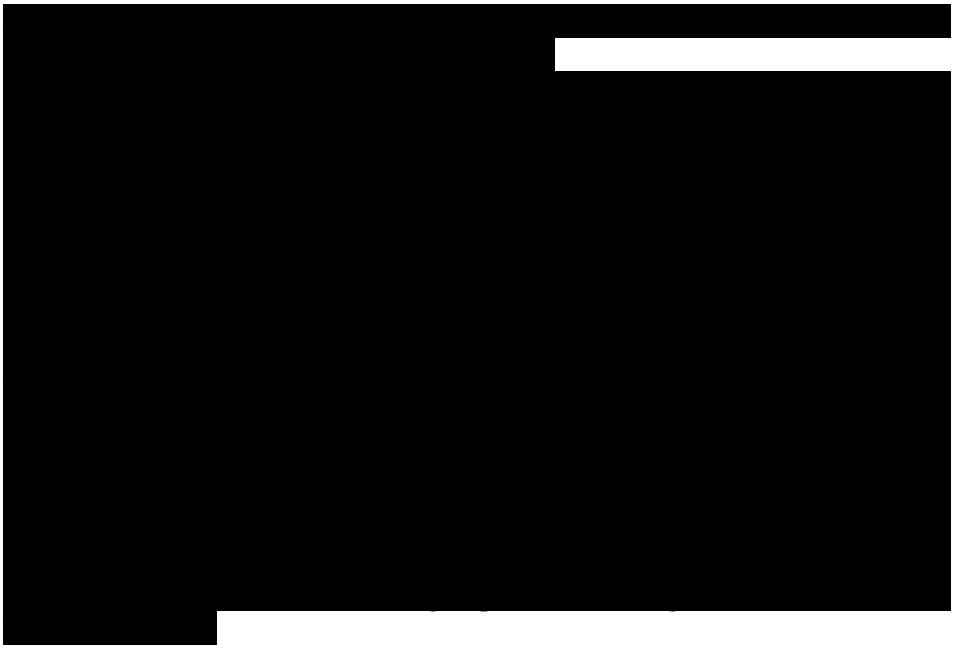

[redacted]

12.2 Depletion of Nogo-B in macrophages reduces coronary plaque stability

[redacted]

12.3 Lack of Nogo-B increases ceramides content in macrophages under atherogenic conditions in vitro

[redacted]

12.4 Lack of Nogo-B enhances cholesterol biosynthesis and storage in macrophages under atherogenic conditions in vitro.

[redacted]

[redacted]

12.5 Lack of Nogo-B enhances inflammasome activation in macrophages under atherogenic conditions in vitro.

[redacted]

[redacted]

12.6 Macrophagic inflammasome activation due to Nogo-B depletion is independent of its physiological negative regulation on SPT.

[redacted]

[redacted]

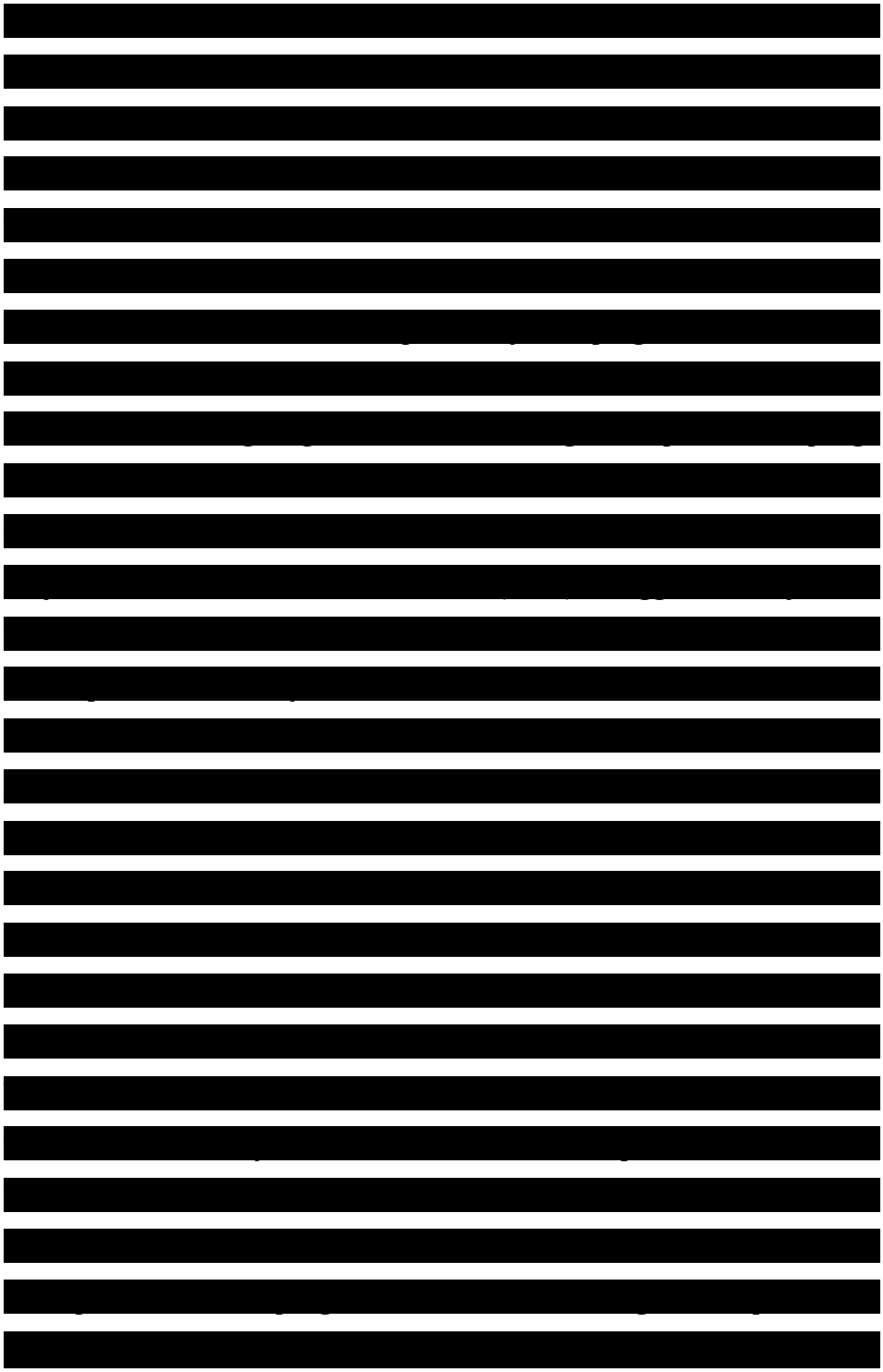

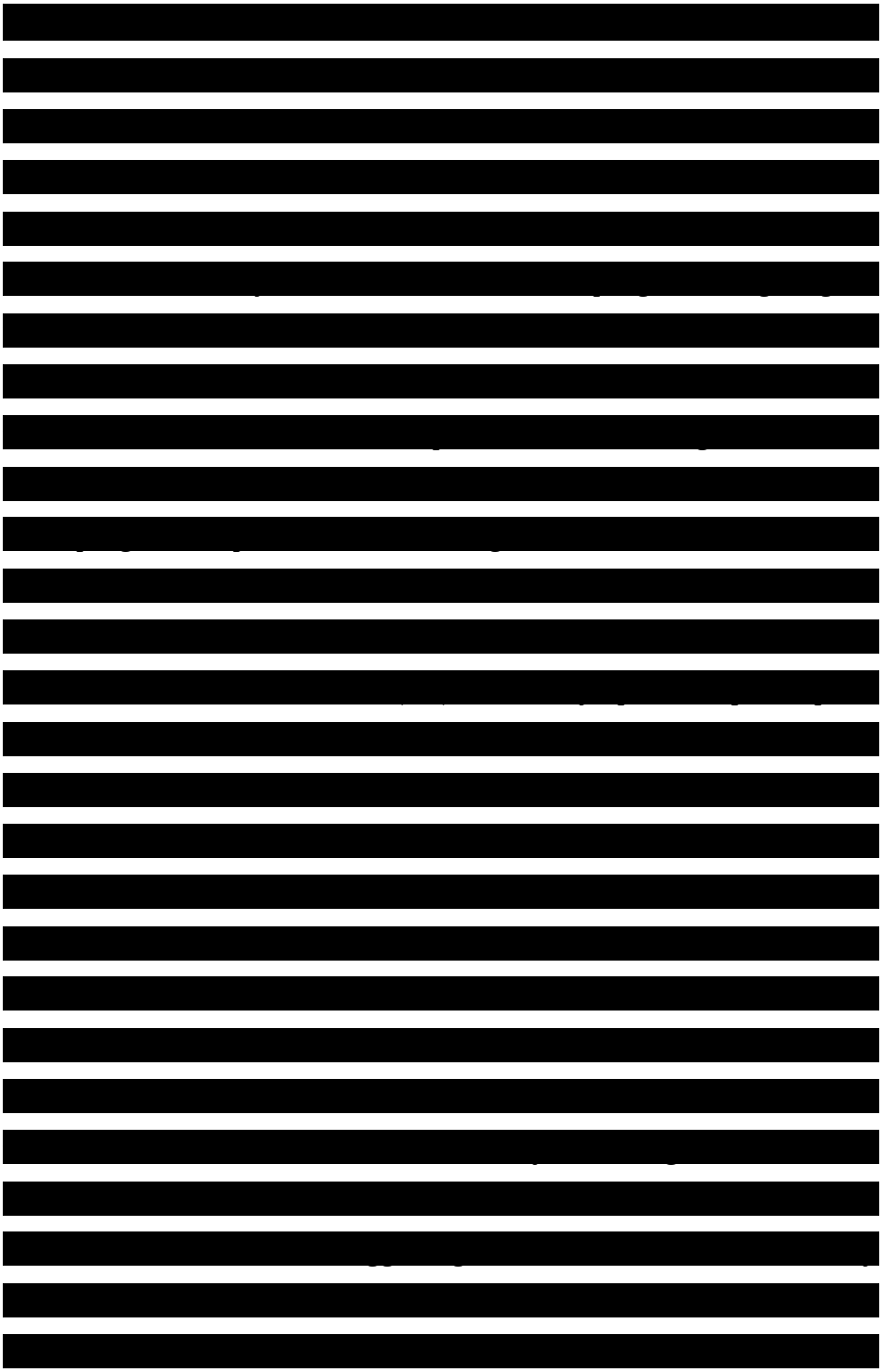

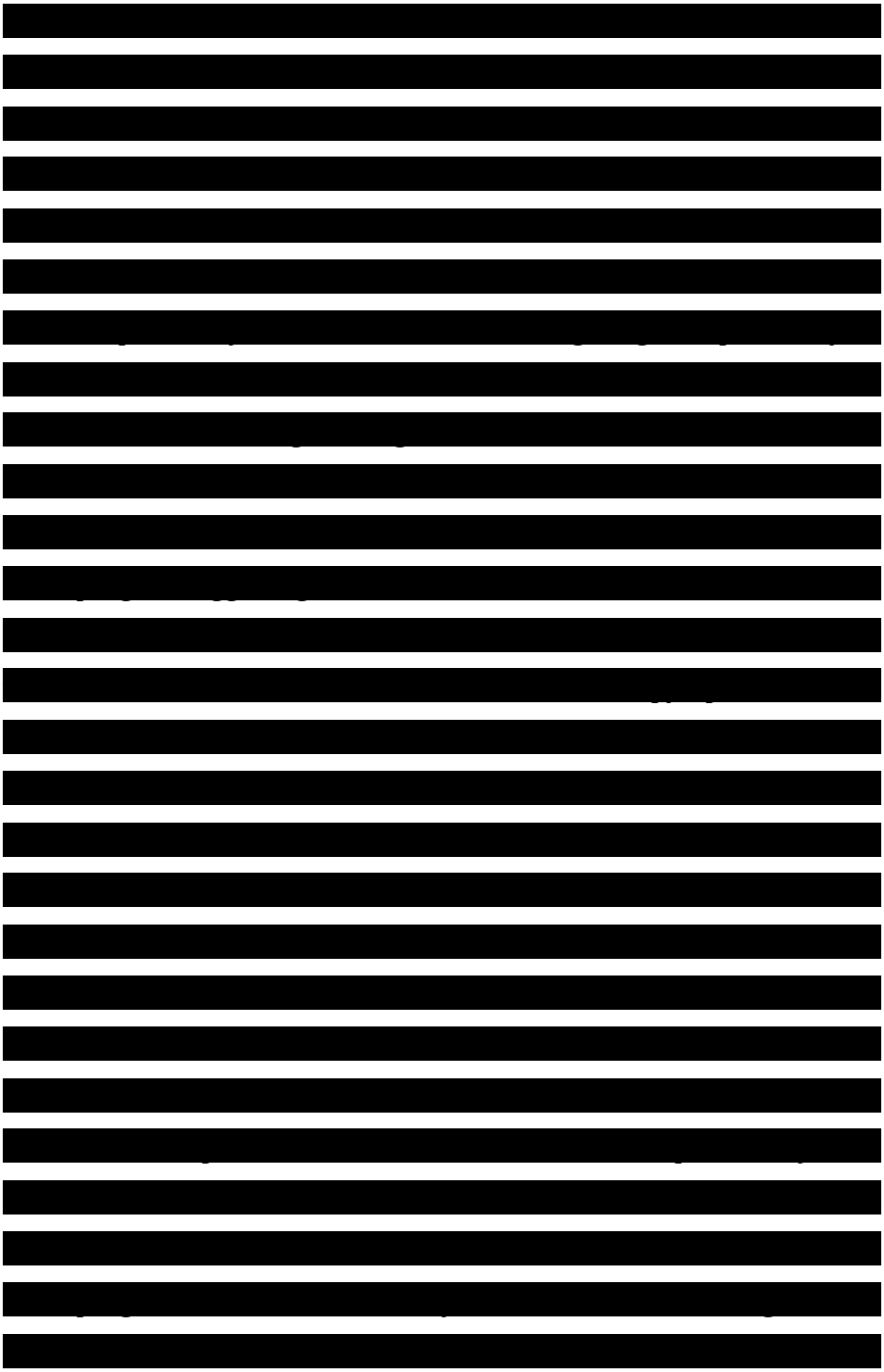

[redacted]

Chapter 4

14. Nutraceutical formulation containing Eruca sativa Mill. as a new potential additive approach to face cardiovascular disorders related to MS.

In compliance with "Programma Operativo Nazionale 2014-2020 Dottorati Innovativi con caratterizzazione industriale a.a. 2020/2021-ciclo XXXVI" I spent 6 months of my PhD program at Neilos S.r.l Company. Here I approached the nutraceutical sector to find a possible placing on market for a novel formulation containing Eruca sativa Mill. as a supporting treatment for MS-related disorders.

Nowadays, the hectic lifestyle, where work and stress often force people to consume quick meals outside home, increases the incidence of metabolic diseases. In this context, nutritional balance can be regained through the intake of specific dietary supplements, which compensate for nutritional deficiencies. For this reason, based on our experimental study, the next step in my doctoral research project was to analyze the nutraceutical market specializing in Metabolic Syndrome. To achieve this, at Neilos S.r.l company, I have been interested in a strategic positioning analysis of a hypothetical nutraceutical formulation containing *Eruca sativa* Mill., taking into consideration the main regulations related to the field of botanicals. The regulatory landscape for nutraceuticals is dynamic, with stringent requirements to ensure consumer safety and prevent misleading claims. Therefore, the first step of our study involved confirming the approval status of the *Eruca sativa* Mill. extract by the Italian Ministry of Health. This critical inquiry was conducted with

meticulous reference to the regulatory framework stipulated in 'Allegato 1 al DM 10 agosto 2018' focusing on regulations pertaining to botanicals. As shown in *Table 1*, *Eruca sativa* Mill. is included in the document, ensuring that it complies with applicable regulations and standards. This botanical already boasts several claims, including fluid drainage and improvement of urinary tract functionality. However, to date, there is no reference to its potential use in cardiovascular pathologies associated with MS.

ALLEGATO 1- BOTANICALS						
NOME BOTANICO	FAMIGLIA	SINONIMO	PARTE IMPIEGATA TRADIZIONALMENTE	PRESCRIZIONI ETICHETTA	ALTRE PRESCRIZIONI	LG MINISTERIALI DI RIFERIMENTO PER GLI EFFETTI FISIOLOGICI
Eruca vesicaria L. Cav.	*Brassicaceae*	*Eruca sativa Mill*	*Folium, flors herba*			*Folium, herba:* Funzione digestiva, Drenaggio dei liquidi corporei, Funzionalità delle vie urinarie.

***Table 3*. Guidelines "botanicals" established by 'Allegato 1 al DM 10 agosto 2018'.** Highlighted in red *Eruca sativa* Mill. with the main claims attributed to it.

Once it has been established that the use of *Eruca sativa* Mill. is authorized, the next step was to study the current market of nutraceuticals used in the treatment of metabolic diseases. This study aims to gain insights into the existing landscape, trends, and demands within this market segment, trying to understand how our product can best fit into the market, cater to consumer needs, and differentiate itself from other offerings. To do so, a "Funnel" approach was used: the methodology involves applying a funnel-like logic that unfolds in various phases. It starts from a general perspective to subsequently delve into more detail, following a progressive narrowing of the analysis perspective. First, we evaluated the market of nutraceuticals used for general metabolic disorders, then we focused on the existing nutraceutical formulation specifically used in MS. Through this analysis we identified six formulations used solely for the treatment of Metabolic Syndrome:

- Profemet (Profenix)
- Metarecod (Aboca)
- Metasyd (Longevo s.r.l.)
- Gdue (Aesculapius farmaceutici)
- Sindromet (Princeps)
- Desimet (Go Farma)

Eventually, we examined the identified formulations, studying their ingredient's functions and usage as summarized in *Table 4.*

Neilos Science, Research & Innovation

RICERCA DI MERCATO

MNLS005 rev.1 del 06/12/2019

VALORI INDICATI PER SINGOLA DOSE IN mg

INGREDIENTI	Profemet (Profenix)	Metarecod (Aboca) MD	Metasyd (Longevo SRL)	Gdue (Aesculapius farmaceutici)	Sindromet (Princeps)	Desimet (Go Farma)
Gymnema sylvestre	125					
Riso fermentato	100					99.6
Monacolina k,Coleus Forskolii Radice	75					
Lagerstroemia speciosa	75					
Goji	65					
Guggul resina	35					
Vitamina B3	7					
Coenzima Q10	5					
NeoPolicaptil Gel Retard 86%		X				
aroma naturale di arancia e pesca		X				
gomma arabica		X				
stevia foglie polvere		X				
fieno greco e.s						
rosmarino e.s						
melograno e.s						
Cannella e.s.						
zenzero e.s						
BPF (Bergamot polyphenolic fraction)					500	
VEZGUARD (estratto di bergamotto)			500			
neoericitrina					23	
neoesperidina					29	
melitidina					3.65	
bruteridina					9	
vitamina c					50	
acido folico						0.2
vitamina E			5			
Vitamina B12						
centella						24
inositolo						1000
caigua						200
orthosiphon						100
›				237.5		
Fucus Vesiculosus				12.5		
Cromo				0.0075		
Note						
Forma Farmaceutica	30 compresse da 0,9 g	40 bustine granulari	60 capsule	60 capsule	30 compresse	20 bustine
Prezzo	€ 27.00	€ 31.50	€ 16.90	€ 29.90	€ 20.90	€ 18.00
Modalità d'uso/Posologia	2 compresse/die 1 prima di pranzo e 1 prima di cena	2 bustine/die 1 prima di pranzo e 1 prima di cena	2 capsule/die	1 capsula mezz ora prima dei pasti principali, fino a 3 volte al giorno	2 compresse/die 1 prima di pranzo e 1 prima di cena	1 bustina/die

Table 4. **Main products on the nutraceutical market specifically used in MS and relative formulations.**

For each main ingredient we performed a bibliographic research in order discover the scientific approved affect and where possible, the related molecular mechanism.

As can be observed in the table representing the selected nutraceuticals currently on the market for Metabolic Syndrome (MS), the primary effective ingredients for the treatment of this condition are:

- *Gymnema sylvestre* is a plant included in Apocynaceae family and is located in many regions of Asia, Africa and Australia. This plant is widely used as a traditional therapy for different purposes. It reduces blood glucose levels through different mechanisms of action, including the reversible blocking of glucose receptors at the intestinal level, modulation of incretin activity triggering insulin secretion and release, and the enhancement of beta cell regeneration in the islets of Langerhans [172].

- Fermented red yeast rice extract is a nutraceutical derived from the fermentation of rice (*Oryza sativa*) by some yeasts (*Monascus purpureus, M. pilosus, M. floridanus, or M. ruber)*. During fermentation, the yeast enriches the rice with a complex of substances having significant hypocholesterolemic activity, including polyketides such as monacolins. Depending on the fermentation conditions and the type of yeast, various types of monacolins (compactin, monacolin M, L, J, X) and the subtype monacolin K, structurally identical to lovastatin, can be released. The hypocholesterolemic mechanism of fermented red yeast rice is attributed to the reversible inhibition of the enzyme 3-hydroxy-3-

methyl-glutaryl-CoA (HMG-CoA) reductase (a key enzyme in endogenous cholesterol synthesis) [173]

- *Lagerstroemia speciosa*, commonly referred to as Queen's Crape Myrtle or Banaba, originates from Southeast Asia, particularly the Philippines and India, this tree has found its way into gardens worldwide due to its aesthetic appeal. Beyond its ornamental value, L. speciosa has garnered attention for its hypoglycemic properties. The active ingredient attributed to these hypoglycemic properties is the corosolic acid, which reveals an insulin-like mechanism of action, active even through oral administration, promoting the up-take of the glucose by cells. It seems so powerful that corosolic acid has been named phyto-insulin. Simultaneously with the reduction of blood glucose, corosolic acid inhibits the differentiation of adipocytes (cells in whose cytoplasm fat is deposited, forming adipose tissue), providing additional assistance in facing overweight [174]

- Goji Berries, scientifically known as *Lycium barbarum*, have gained widespread popularity as a nutritional superfood. Originating from the Himalayan regions of China, Mongolia, and Tibet, these small, red berries have been consumed for centuries for their purported health benefits, specifically Goji berries reduce abdominal fat and oxidative stress in patients with MS [175]

- Guggul, the resin obtained from the Commiphora wightii tree, is renowned for its therapeutic properties, one of the well-researched

aspects of guggul resin is its impact on cholesterol level due to guggulipid, a lipid able of significantly reduce total cholesterol, LDL cholesterol, and triglycerides. This action is partly attributed to an increase in the number of LDL cholesterol receptors on the surface of liver cells and an improvement in cholesterol-receptor binding. In this way, lipids are eliminated in the bloodstream and then degraded through bile [176].

- *Bergamot extract,* fragrant citrus fruit predominantly grown in the Calabria region of Southern Italy, has long been admired for its distinctive aroma and unique flavor. Beyond its culinary uses, bergamot extract has emerged as a potent source of health benefits, drawing attention for its potential positive effects on various aspects of well-being. Recent studies suggested that compounds found in bergamot, such as flavonoids and polyphenols, may contribute to lowering cholesterol levels. The hypocholesterolemic effect associated with the modulation of the activity of enzymes involved in cholesterol esterification and trafficking reactions. In pathologic fatty liver, the BPF-induced modulation of the MAPK JNK/p38 represents the protective mechanism responsible for improving insulin sensitivity. Furthermore, the reduction in hepatic inflammation and fibrosis is correlated with the direct inhibition by BPF of poly [ADP-ribose] polymerase 1 (PARP1), considered a direct suppressor of mitogen-activated protein kinase inhibitor protein-1 (MPK-1). It has also been hypothesized that the reduction in serum and tissue cholesterol levels is due to the statin-like activity exerted by BPF. The structural similarity of bergamot

polyphenols to the substrate of HMG-CoA reductase allows them to mimic the natural substrates of HMG-CoA and blocking the rate-limiting step in cholesterol synthesis. The potent antioxidant effects of BPF play a significant role in all observed protective effects. BPF directly reduces biomarkers of lipid peroxidation (TBARS and MD). BPF also enhances the activity of endogenous antioxidant enzymes such as SOD, GPx, and GSTP1 [177]

- *Ascophyllum Nodosum and Fucus vesiculosus* are two algas traditionally used for the treatment of obesity and several gastrointestinal diseases. A recent study demonstrated that the phytocomplex obtained from these algae (Gdue™) controls postprandial glucose levels in a mouse model of steatohepatitis, a condition often associated with obesity and type 2 diabetes mellitus by inhibiting the two intestinal enzymes α-amylase and α-glucosidase, which are both involved in carbohydrate digestion. This mechanism can significantly lower the increase of blood glucose levels, after a mixed carbohydrate meal, by delaying glucose absorption.

From our analysis, all the main extracts currently used in nutraceutical formulations intended for the treatment of Metabolic Syndrome, are focused on improving blood glucose and/or cholesterol parameters. However, none of this, aims to act on the leading cause of morbidity and mortality in individuals with MS: cardiovascular complication. *Eruca sativa* Mill. (rocket salad) is an edible cruciferous plant belonging to the family of Brassicaceae [178]. These plants represent not only a great source of macro- and micronutrients necessary for sustenance, but also one

of the most valuable sources of phytochemicals such as glucosinolates (GLs), phenols and isothiocyanates (ITCs) [179]. Isothiocyanates, among which Erucin, have elicited interest of the scientific research due to fact that they exert beneficial effects on human health. ITCs bioactivity is attributed to the property of these molecules, to release hydrogen sulfide (H_2S) slowly and steadily, mimicking the physiological concentration of the endogenous gaseous transmitter [180] Regarding Erucin, the ability of this isothiocyanate to release H_2S is dependent on the presence of thiols (R-SH) and, indeed, it occurs preferentially in the cellular cytoplasm, a microenvironment characterized by high concentrations of organic thiols, cysteine (30-200 μM), and glutathione (1-10 mM) [152]. Several studies already demonstrated that Erucin has anti-inflammatory and antioxidant activity [181]; by our side, in this study we showed that Erucin has a protective effect against endothelial dysfunction, the first event that occurs in vascular wall during the onset of vascular inflammation related to MS. Therefore, we consider that *Eruca sativa* Mill. extract could add value to a new nutraceutical formulation for MS treatment, as it improves vascular dysfunctions associated to MS, underestimated (not considered) by the other nutraceuticals currently on the market. This new approach could improve the effectiveness of the nutraceutical formulation by managing the complex pathology of MS from different perspectives.

15. REFERENCES

[1] A. P. Fishman, “Endothelium: a distributed organ of diverse capabilities,” *Ann N Y Acad Sci*, vol. 401, no. 1, pp. 1–8, 1982, doi: 10.1111/J.1749-6632.1982.TB25702.X.

[2] J. E. Wagenseil and R. P. Mecham, “Vascular extracellular matrix and arterial mechanics,” *Physiol Rev*, vol. 89, no. 3, pp. 957–989, Jul. 2009, doi: 10.1152/PHYSREV.00041.2008.

[3] R. Ross, “The pathogenesis of atherosclerosis: a perspective for the 1990s,” *Nature*, vol. 362, no. 6423, pp. 801–809, 1993, doi: 10.1038/362801A0.

[4] M. Aikawa *et al.*, “Redifferentiation of smooth muscle cells after coronary angioplasty determined via myosin heavy chain expression,” *Circulation*, vol. 96, no. 1, pp. 82–90, Jul. 1997, doi: 10.1161/01.CIR.96.1.82.

[5] S. A. Fisher, “Vascular smooth muscle phenotypic diversity and function,” *Physiol Genomics*, vol. 42A, no. 3, pp. 169–187, Nov. 2010, doi: 10.1152/PHYSIOLGENOMICS.00111.2010.

[6] L. A. Martinez-Lemus, M. A. Hill, and G. A. Meininger, “The plastic nature of the vascular wall: a continuum of remodeling events contributing to control of arteriolar diameter and structure,” *Physiology (Bethesda)*, vol. 24, no. 1, pp. 45–57, Feb. 2009, doi: 10.1152/PHYSIOL.00029.2008.

[7] C. A. Lemarié, P. L. Tharaux, and S. Lehoux, “Extracellular matrix alterations in hypertensive vascular remodeling,” *J Mol Cell Cardiol*, vol. 48, no. 3, pp. 433–439, Mar. 2010, doi: 10.1016/J.YJMCC.2009.09.018.

[8] B. M. Wynne, C. W. Chiao, and R. C. Webb, “Vascular Smooth Muscle Cell Signaling Mechanisms for Contraction to Angiotensin II and Endothelin-1,” *J Am Soc Hypertens*, vol. 3, no. 2, pp. 84–95, Mar. 2009, doi: 10.1016/J.JASH.2008.09.002.

[9] L. J. Ignarro, G. Cirino, A. Casini, and C. Napoli, “Nitric oxide as a signaling molecule in the vascular system: an overview,” *J Cardiovasc Pharmacol*, vol. 34, no. 6, pp. 879–886, Dec. 1999, doi: 10.1097/00005344-199912000-00016.

[10] I. Fleming and R. Busse, “Molecular mechanisms involved in the regulation of the endothelial nitric oxide synthase,” *Am*

J Physiol Regul Integr Comp Physiol, vol. 284, no. 1, Jan. 2003, doi: 10.1152/AJPREGU.00323.2002.

[11] M. Oelze *et al.*, "Vasodilator-stimulated phosphoprotein serine 239 phosphorylation as a sensitive monitor of defective nitric oxide/cGMP signaling and endothelial dysfunction," *Circ Res*, vol. 87, no. 11, pp. 999–1005, Nov. 2000, doi: 10.1161/01.RES.87.11.999.

[12] P. Ruth, A. Pfeifer, S. Kamm, P. Klatt, W. R. G. Dostmann, and F. Hofmann, "Identification of the amino acid sequences responsible for high affinity activation of cGMP kinase Ialpha," *J Biol Chem*, vol. 272, no. 16, pp. 10522–10528, Apr. 1997, doi: 10.1074/JBC.272.16.10522.

[13] S. H. Francis and J. D. Corbin, "Cyclic nucleotide-dependent protein kinases: intracellular receptors for cAMP and cGMP action," *Crit Rev Clin Lab Sci*, vol. 36, no. 4, pp. 275–328, 1999, doi: 10.1080/10408369991239213.

[14] D. M. Gamm, S. H. Francis, T. P. Angelotti, J. D. Corbin, and M. D. Uhler, "The type II isoform of cGMP-dependent protein kinase is dimeric and possesses regulatory and catalytic properties distinct from the type I isoforms," *J Biol Chem*, vol. 270, no. 45, pp. 27380–27388, Nov. 1995, doi: 10.1074/JBC.270.45.27380.

[15] W. Landgraf, F. Hofmann, J. T. Pelton, and J. P. Huggins, "Effects of cyclic GMP on the secondary structure of cyclic GMP dependent protein kinase and analysis of the enzyme's amino-terminal domain by far-ultraviolet circular dichroism," *Biochemistry*, vol. 29, no. 42, pp. 9921–9928, Oct. 1990, doi: 10.1021/BI00494A024.

[16] J. A. Smith, S. H. Francis, K. A. Walsh, S. Kumar, and J. D. Corbin, "Autophosphorylation of type Ibeta cGMP-dependent protein kinase increases basal catalytic activity and enhances allosteric activation by cGMP or cAMP," *J Biol Chem*, vol. 271, no. 34, pp. 20756–20762, 1996, doi: 10.1074/JBC.271.34.20756.

[17] S. H. Francis, C. Poteet-Smith, J. L. Busch, R. Richie-Jannetta, and J. D. Corbin, "Mechanisms of autoinhibition in cyclic nucleotide-dependent protein kinases," *Front Biosci*, vol. 7, 2002, doi: 10.2741/A796.

[18] F. HOFMANN, H. -P GENSHEIMER, and C. GÖBEL, "cGMP-dependent protein kinase. Autophosphorylation

changes the characteristics of binding site 1," *Eur J Biochem*, vol. 147, no. 2, pp. 361–365, 1985, doi: 10.1111/J.1432-1033.1985.TB08758.X.

[19] A. Geiselhöringer, M. Gaisa, F. Hofmann, and J. Schlossmann, "Distribution of IRAG and cGKI-isoforms in murine tissues," *FEBS Lett*, vol. 575, no. 1–3, pp. 19–22, Sep. 2004, doi: 10.1016/j.febslet.2004.08.030.

[20] S. Moosmang *et al.*, "Dominant role of smooth muscle L-type calcium channel Cav1.2 for blood pressure regulation," *EMBO J*, vol. 22, no. 22, pp. 6027–6034, Nov. 2003, doi: 10.1093/EMBOJ/CDG583.

[21] A. P. Somlyo and A. V. Somlyo, "Ca2+ sensitivity of smooth muscle and nonmuscle myosin II: modulated by G proteins, kinases, and myosin phosphatase," *Physiol Rev*, vol. 83, no. 4, pp. 1325–1358, 2003, doi: 10.1152/PHYSREV.00023.2003.

[22] P. F. Chen, A. L. Tsai, V. Berka, and K. K. Wu, "Mutation of Glu-361 in human endothelial nitric-oxide synthase selectively abolishes L-arginine binding without perturbing the behavior of heme and other redox centers," *J Biol Chem*, vol. 272, no. 10, pp. 6114–6118, Mar. 1997, doi: 10.1074/JBC.272.10.6114.

[23] W. C. Sessa, J. K. Harrison, D. R. Luthin, J. S. Pollock, and K. R. Luthin, "Genomic analysis and expression patterns reveal distinct genes for endothelial and brain nitric oxide synthase," *Hypertension*, vol. 21, no. 6, pp. 934–938, 1993, doi: 10.1161/01.HYP.21.6.934.

[24] J. Hoyer, R. KÖhler, and A. Distler, "Mechanosensitive Ca2+ oscillations and STOC activation in endothelial cells," *FASEB J*, vol. 12, no. 3, pp. 359–366, Mar. 1998, doi: 10.1096/FASEBJ.12.3.359.

[25] S. Dimmeler, I. Fleming, B. Fisslthaler, C. Hermann, R. Busse, and A. M. Zeiher, "Activation of nitric oxide synthase in endothelial cells by Akt-dependent phosphorylation," *Nature*, vol. 399, no. 6736, pp. 601–605, Jun. 1999, doi: 10.1038/21224.

[26] G. García-Cardeña *et al.*, "Dynamic activation of endothelial nitric oxide synthase by Hsp90," *Nature*, vol. 392, no. 6678, pp. 821–824, Apr. 1998, doi: 10.1038/33934.

[27] M. E. Davis, H. Cai, G. R. Drummond, and D. G. Harrison, “Shear stress regulates endothelial nitric oxide synthase expression through c-Src by divergent signaling pathways,” *Circ Res*, vol. 89, no. 11, pp. 1073–1080, Nov. 2001, doi: 10.1161/HH2301.100806.

[28] T. Ziegler, P. Silacci, V. J. Harrison, and D. Hayoz, “Nitric oxide synthase expression in endothelial cells exposed to mechanical forces,” *Hypertension*, vol. 32, no. 2, pp. 351–355, 1998, doi: 10.1161/01.HYP.32.2.351.

[29] A. M. Malek, S. L. Alper, and S. Izumo, “Hemodynamic shear stress and its role in atherosclerosis,” *JAMA*, vol. 282, no. 21, pp. 2035–2042, Dec. 1999, doi: 10.1001/JAMA.282.21.2035.

[30] K. G. M. M. Alberti *et al.*, “Harmonizing the metabolic syndrome: a joint interim statement of the International Diabetes Federation Task Force on Epidemiology and Prevention; National Heart, Lung, and Blood Institute; American Heart Association; World Heart Federation; International Atherosclerosis Society; and International Association for the Study of Obesity,” *Circulation*, vol. 120, no. 16, pp. 1640–1645, Oct. 2009, doi: 10.1161/CIRCULATIONAHA.109.192644.

[31] H. Beltrán-Sánchez, M. O. Harhay, M. M. Harhay, and S. McElligott, “Prevalence and trends of metabolic syndrome in the adult U.S. population, 1999-2010,” *J Am Coll Cardiol*, vol. 62, no. 8, pp. 697–703, Aug. 2013, doi: 10.1016/J.JACC.2013.05.064.

[32] M. Li, X. Chi, Y. Wang, S. Setrerrahmane, W. Xie, and H. Xu, “Trends in insulin resistance: insights into mechanisms and therapeutic strategy,” *Signal Transduction and Targeted Therapy 2022 7:1*, vol. 7, no. 1, pp. 1–25, Jul. 2022, doi: 10.1038/s41392-022-01073-0.

[33] J. P. Després, I. Lemieux, and D. Prud’homme, “Treatment of obesity: need to focus on high risk abdominally obese patients,” *BMJ*, vol. 322, no. 7288, pp. 716–720, Mar. 2001, doi: 10.1136/BMJ.322.7288.716.

[34] N. D. Di Daniele *et al.*, “Impact of Mediterranean diet on metabolic syndrome, cancer and longevity,” *Oncotarget*, vol. 8, no. 5, pp. 8947–8979, Jan. 2017, doi: 10.18632/ONCOTARGET.13553.

[35] J. Myers, P. Kokkinos, and E. Nyelin, “Physical Activity, Cardiorespiratory Fitness, and the Metabolic Syndrome,” *Nutrients*, vol. 11, no. 7, Jul. 2019, doi: 10.3390/NU11071652.

[36] J. Rask Larsen, L. Dima, C. U. Correll, and P. Manu, “The pharmacological management of metabolic syndrome,” *Expert Rev Clin Pharmacol*, vol. 11, no. 4, pp. 397–410, Apr. 2018, doi: 10.1080/17512433.2018.1429910.

[37] A. M. Heck, J. A. Yanovski, and K. A. Calis, “Orlistat, a new lipase inhibitor for the management of obesity,” *Pharmacotherapy*, vol. 20, no. 3, pp. 270–279, 2000, doi: 10.1592/PHCO.20.4.270.34882.

[38] “Naltrexone/bupropion for obesity,” *Drug Ther Bull*, vol. 55, no. 11, pp. 126–129, 2017, doi: 10.1136/DTB.2017.11.0550.

[39] B. Elbrond *et al.*, “Pharmacokinetics, pharmacodynamics, safety, and tolerability of a single-dose of NN2211, a long-acting glucagon-like peptide 1 derivative, in healthy male subjects,” *Diabetes Care*, vol. 25, no. 8, pp. 1398–1404, Aug. 2002, doi: 10.2337/DIACARE.25.8.1398.

[40] D. J. Drucker and M. A. Nauck, “The incretin system: glucagon-like peptide-1 receptor agonists and dipeptidyl peptidase-4 inhibitors in type 2 diabetes,” *Lancet*, vol. 368, no. 9548, pp. 1696–1705, Nov. 2006, doi: 10.1016/S0140-6736(06)69705-5.

[41] S. Lear, Z. Amso, and W. Shen, “Engineering PEG-fatty acid stapled, long-acting peptide agonists for G protein-coupled receptors,” *Methods Enzymol*, vol. 622, pp. 183–200, Jan. 2019, doi: 10.1016/BS.MIE.2019.02.008.

[42] A. M. Chao, J. S. Tronieri, A. Amaro, and T. A. Wadden, “Semaglutide for the treatment of obesity,” *Trends Cardiovasc Med*, vol. 33, no. 3, pp. 159–166, Apr. 2023, doi: 10.1016/J.TCM.2021.12.008.

[43] B. Viollet, B. Guigas, N. Sanz Garcia, J. Leclerc, M. Foretz, and F. Andreelli, “Cellular and molecular mechanisms of metformin: an overview,” *Clin Sci (Lond)*, vol. 122, no. 6, pp. 253–270, Mar. 2012, doi: 10.1042/CS20110386.

[44] M. Foretz, B. Guigas, L. Bertrand, M. Pollak, and B. Viollet, “Metformin: From Mechanisms of Action to Therapies,” *Cell Metab*, vol. 20, no. 6, pp. 953–966, Dec. 2014, doi: 10.1016/J.CMET.2014.09.018.

[45] R. De Caterina, T. Salvatore, and R. Marchioli, “All cholesterol-lowering interventions are expected to reduce stroke: Confirmatory data from IMPROVE-IT,” *Data Brief*, vol. 7, pp. 1541–1550, Jun. 2016, doi: 10.1016/J.DIB.2016.04.059.

[46] K. E. Shipman, R. C. Strange, and S. Ramachandran, “Use of fibrates in the metabolic syndrome: A review,” *World J Diabetes*, vol. 7, no. 5, p. 74, 2016, doi: 10.4239/WJD.V7.I5.74.

[47] A. Pasta *et al.*, “PCSK9 inhibitors for treating hypercholesterolemia,” *Expert Opin Pharmacother*, vol. 21, no. 3, pp. 353–363, Feb. 2020, doi: 10.1080/14656566.2019.1702970.

[48] E. Ferrannini and W. C. Cushman, “Diabetes and hypertension: the bad companions,” *Lancet*, vol. 380, no. 9841, pp. 601–610, 2012, doi: 10.1016/S0140-6736(12)60987-8.

[49] N. J. Brown and D. E. Vaughan, “Angiotensin-Converting Enzyme Inhibitors,” *Circulation*, vol. 97, no. 14, pp. 1411–1420, Apr. 1998, doi: 10.1161/01.CIR.97.14.1411.

[50] E. K. Sims, A. L. J. Carr, R. A. Oram, L. A. DiMeglio, and C. Evans-Molina, “100 years of insulin: celebrating the past, present and future of diabetes therapy,” *Nat Med*, vol. 27, no. 7, p. 1154, Jul. 2021, doi: 10.1038/S41591-021-01418-2.

[51] R. Sano, Y. Shinozaki, and T. Ohta, “Sodium–glucose cotransporters: Functional properties and pharmaceutical potential,” *J Diabetes Investig*, vol. 11, no. 4, p. 770, Jul. 2020, doi: 10.1111/JDI.13255.

[52] D. Daneman, “Type 1 diabetes,” *Lancet*, vol. 367, no. 9513, pp. 847–858, Mar. 2006, doi: 10.1016/S0140-6736(06)68341-4.

[53] F. Pociot and Å. Lernmark, “Genetic risk factors for type 1 diabetes,” *Lancet*, vol. 387, no. 10035, pp. 2331–2339, Jun. 2016, doi: 10.1016/S0140-6736(16)30582-7.

[54] J. T. Warshauer, J. A. Bluestone, and M. S. Anderson, “New Frontiers in the Treatment of Type 1 Diabetes,” *Cell Metab*, vol. 31, no. 1, pp. 46–61, Jan. 2020, doi: 10.1016/J.CMET.2019.11.017.

[55] J. C. Pickup, “Insulin-pump therapy for type 1 diabetes mellitus,” *N Engl J Med*, vol. 366, no. 17, pp. 1616–1624, Apr. 2012, doi: 10.1056/NEJMCT1113948.

[56] A. Abramson *et al.*, “An ingestible self-orienting system for oral delivery of macromolecules,” *Science*, vol. 363, no. 6427, pp. 611–615, Feb. 2019, doi: 10.1126/SCIENCE.AAU2277.

[57] J. A. Bluestone, J. H. Buckner, and K. C. Herold, “Immunotherapy: Building a bridge to a cure for type 1 diabetes,” *Science*, vol. 373, no. 6554, pp. 510–516, Jul. 2021, doi: 10.1126/SCIENCE.ABH1654.

[58] W. Lv, X. Wang, Q. Xu, and W. Lu, “Mechanisms and Characteristics of Sulfonylureas and Glinides,” *Curr Top Med Chem*, vol. 20, no. 1, pp. 37–56, Dec. 2020, doi: 10.2174/1568026620666191224141617.

[59] A. M. Harmsze *et al.*, “Sulfonylureas and on-clopidogrel platelet reactivity in type 2 diabetes mellitus patients,” *Platelets*, vol. 22, no. 2, pp. 98–102, Mar. 2011, doi: 10.3109/09537104.2010.530359.

[60] K. B. Hansen, T. Vilsbøll, and F. K. Knop, “Incretin mimetics: a novel therapeutic option for patients with type 2 diabetes – a review,” *Diabetes Metab Syndr Obes*, vol. 3, p. 155, May 2010, doi: 10.2147/dmsott.s7004.

[61] D. S. Hsia, O. Grove, and W. T. Cefalu, “An Update on SGLT2 Inhibitors for the Treatment of Diabetes Mellitus,” *Curr Opin Endocrinol Diabetes Obes*, vol. 24, no. 1, p. 73, 2017, doi: 10.1097/MED.0000000000000311.

[62] J. M. Rojas-Velázquez, A. Giralt-Herrera, J. Leiva-Enríquez, and J. Leiva-Enríquez, “Role of newer antidiabetic drugs on cardiovascular prevention and heart failure,” *Clin Investig Arterioscler*, vol. 33, no. 6, pp. 314–322, Nov. 2021, doi: 10.1016/J.ARTERI.2021.02.013.

[63] R. Donnelly, A. M. Emslie-Smith, I. D. Gardner, and A. D. Morris, “ABC of arterial and venous disease: vascular complications of diabetes,” *BMJ*, vol. 320, no. 7241, pp. 1062–1066, Apr. 2000, doi: 10.1136/BMJ.320.7241.1062.

[64] P. Libby, P. M. Ridker, and G. K. Hansson, “Progress and challenges in translating the biology of atherosclerosis,” *Nature*, vol. 473, no. 7347, pp. 317–325, May 2011, doi: 10.1038/NATURE10146.

[65] K. J. Moore, F. J. Sheedy, and E. A. Fisher, “Macrophages in atherosclerosis: a dynamic balance,” *Nat Rev Immunol*, vol. 13, no. 10, pp. 709–721, Oct. 2013, doi: 10.1038/NRI3520.

[66] R. O. Tadros *et al.*, “Vascular surgeon-hospitalist comanagement improves in-hospital mortality at the expense of increased in-hospital cost,” *J Vasc Surg*, vol. 65, no. 3, pp. 819–825, Mar. 2017, doi: 10.1016/J.JVS.2016.09.042.

[67] G. Cirino, V. Vellecco, and M. Bucci, “Nitric oxide and hydrogen sulfide: the gasotransmitter paradigm of the vascular system,” *Br J Pharmacol*, vol. 174, no. 22, pp. 4021–4031, Nov. 2017, doi: 10.1111/BPH.13815.

[68] F. Santilli, D. D’Ardes, and G. Davì, “Oxidative stress in chronic vascular disease: From prediction to prevention,” *Vascul Pharmacol*, vol. 74, pp. 23–37, Nov. 2015, doi: 10.1016/J.VPH.2015.09.003.

[69] G. Cirino, C. Szabo, and A. Papapetropoulos, “Physiological roles of hydrogen sulfide in mammalian cells, tissues, and organs,” *Physiol Rev*, vol. 103, no. 1, pp. 31–276, Jan. 2023, doi: 10.1152/PHYSREV.00028.2021.

[70] R. Wang, “Two’s company, three’s a crowd: can H2S be the third endogenous gaseous transmitter?,” *FASEB J*, vol. 16, no. 13, pp. 1792–1798, Nov. 2002, doi: 10.1096/FJ.02-0211HYP.

[71] G. Caliendo, G. Cirino, V. Santagada, and J. L. Wallace, “Synthesis and biological effects of hydrogen sulfide (H2S): development of H2S-releasing drugs as pharmaceuticals,” *J Med Chem*, vol. 53, no. 17, pp. 6275–6286, Sep. 2010, doi: 10.1021/JM901638J.

[72] R. O. Beauchamp, J. S. Bus, J. A. Popp, C. J. Boreiko, D. A. Andjelkovich, and P. Leber, “A critical review of the literature on hydrogen sulfide toxicity,” *Crit Rev Toxicol*, vol. 13, no. 1, pp. 25–97, 1984, doi: 10.3109/10408448409029321.

[73] R. J. Reiffenstein, W. C. Hulbert, and S. H. Roth, “Toxicology of hydrogen sulfide,” *Annu Rev Pharmacol Toxicol*, vol. 32, pp. 109–134, 1992, doi: 10.1146/ANNUREV.PA.32.040192.000545.

[74] M. Whiteman *et al.*, “Evidence for the formation of a novel nitrosothiol from the gaseous mediators nitric oxide and hydrogen sulphide,” *Biochem Biophys Res Commun*, vol.

343, no. 1, pp. 303–310, Apr. 2006, doi: 10.1016/J.BBRC.2006.02.154.

[75] M. H. Stipanuk, “Sulfur amino acid metabolism: pathways for production and removal of homocysteine and cysteine,” *Annu Rev Nutr*, vol. 24, pp. 539–577, 2004, doi: 10.1146/ANNUREV.NUTR.24.012003.132418.

[76] K. Abe and H. Kimura, “The possible role of hydrogen sulfide as an endogenous neuromodulator,” *J Neurosci*, vol. 16, no. 3, pp. 1066–1071, Feb. 1996, doi: 10.1523/JNEUROSCI.16-03-01066.1996.

[77] E. W. Miles and J. P. Kraus, “Cystathionine beta-synthase: structure, function, regulation, and location of homocystinuria-causing mutations,” *J Biol Chem*, vol. 279, no. 29, pp. 29871–29874, Jul. 2004, doi: 10.1074/JBC.R400005200.

[78] S. Fiorucci, E. Distrutti, G. Cirino, and J. L. Wallace, “The emerging roles of hydrogen sulfide in the gastrointestinal tract and liver,” *Gastroenterology*, vol. 131, no. 1, pp. 259–271, 2006, doi: 10.1053/J.GASTRO.2006.02.033.

[79] M. Bucci *et al.*, “cGMP-dependent protein kinase contributes to hydrogen sulfide-stimulated vasorelaxation,” *PLoS One*, vol. 7, no. 12, Dec. 2012, doi: 10.1371/JOURNAL.PONE.0053319.

[80] W. Zhao, J. Zhang, Y. Lu, and R. Wang, “The vasorelaxant effect of H(2)S as a novel endogenous gaseous K(ATP) channel opener,” *EMBO J*, vol. 20, no. 21, pp. 6008–6016, Nov. 2001, doi: 10.1093/EMBOJ/20.21.6008.

[81] N. Shibuya *et al.*, “3-Mercaptopyruvate sulfurtransferase produces hydrogen sulfide and bound sulfane sulfur in the brain,” *Antioxid Redox Signal*, vol. 11, no. 4, pp. 703–714, Apr. 2009, doi: 10.1089/ARS.2008.2253.

[82] K. Módis, K. Wolanska, and R. Wozdek, “Hydrogen sulfide in cell signaling, signal transduction, cellular bioenergetics and physiology in C. elegans,” *Gen Physiol Biophys*, vol. 32, no. 1, pp. 1–22, 2013, doi: 10.4149/GPB_2013001.

[83] A. E. Braunstein, E. V. Goryachenkova, and N. D. Lac, “Reactions catalysed by serine sulfhydrase from chicken liver,” *Biochim Biophys Acta*, vol. 171, no. 2, pp. 366–368, Feb. 1969, doi: 10.1016/0005-2744(69)90173-9.

[84] K. H. Jhee and W. D. Kruger, “The role of cystathionine beta-synthase in homocysteine metabolism,” *Antioxid Redox Signal*, vol. 7, no. 5–6, pp. 813–822, May 2005, doi: 10.1089/ARS.2005.7.813.

[85] X. Cao *et al.*, “A Review of Hydrogen Sulfide Synthesis, Metabolism, and Measurement: Is Modulation of Hydrogen Sulfide a Novel Therapeutic for Cancer?,” *Antioxid Redox Signal*, vol. 31, no. 1, Jul. 2019, doi: 10.1089/ARS.2017.7058.

[86] T. Chiku, D. Padovani, W. Zhu, S. Singh, V. Vitvitsky, and R. Banerjee, “H2S biogenesis by human cystathionine gamma-lyase leads to the novel sulfur metabolites lanthionine and homolanthionine and is responsive to the grade of hyperhomocysteinemia,” *J Biol Chem*, vol. 284, no. 17, pp. 11601–11612, Apr. 2009, doi: 10.1074/JBC.M808026200.

[87] Y. Mikami, N. Shibuya, Y. Ogasawara, and H. Kimura, “Hydrogen sulfide is produced by cystathionine γ-lyase at the steady-state low intracellular Ca(2+) concentrations,” *Biochem Biophys Res Commun*, vol. 431, no. 2, pp. 131–135, Feb. 2013, doi: 10.1016/J.BBRC.2013.01.010.

[88] P. K. Yadav, K. Yamada, T. Chiku, M. Koutmos, and R. Banerjee, “Structure and kinetic analysis of H2S production by human mercaptopyruvate sulfurtransferase,” *J Biol Chem*, vol. 288, no. 27, pp. 20002–20013, Jul. 2013, doi: 10.1074/JBC.M113.466177.

[89] N. Nagahara, T. Ito, H. Kitamura, and T. Nishino, “Tissue and subcellular distribution of mercaptopyruvate sulfurtransferase in the rat: confocal laser fluorescence and immunoelectron microscopic studies combined with biochemical analysis,” *Histochem Cell Biol*, vol. 110, no. 3, pp. 243–250, 1998, doi: 10.1007/S004180050286.

[90] N. Nagahara, “Regulation of mercaptopyruvate sulfurtransferase activity via intrasubunit and intersubunit redox-sensing switches,” *Antioxid Redox Signal*, vol. 19, no. 15, pp. 1792–1802, Nov. 2013, doi: 10.1089/ARS.2012.5031.

[91] J. W. Calvert, W. A. Coetzee, and D. J. Lefer, “Novel insights into hydrogen sulfide--mediated cytoprotection,” *Antioxid*

Redox Signal, vol. 12, no. 10, pp. 1203–1217, May 2010, doi: 10.1089/ARS.2009.2882.

[92] H. Kimura, "Hydrogen sulfide: from brain to gut," *Antioxid Redox Signal*, vol. 12, no. 9, pp. 1111–1123, May 2010, doi: 10.1089/ARS.2009.2919.

[93] "Sulfur reduction by human erythrocytes - PubMed." Accessed: Jan. 18, 2024. [Online]. Available: https://pubmed.ncbi.nlm.nih.gov/9755482/

[94] M. D. Levitt, J. Furne, J. Springfield, F. Suarez, and E. DeMaster, "Detoxification of hydrogen sulfide and methanethiol in the cecal mucosa," *J Clin Invest*, vol. 104, no. 8, pp. 1107–1114, 1999, doi: 10.1172/JCI7712.

[95] R. Picton, M. C. Eggo, G. A. Merrill, M. J. S. Langman, and S. Singh, "Mucosal protection against sulphide: importance of the enzyme rhodanese," *Gut*, vol. 50, no. 2, pp. 201–205, 2002, doi: 10.1136/GUT.50.2.201.

[96] G. P. Kurzban, L. Chu, J. L. Ebersole, and S. C. Holt, "Sulfhemoglobin formation in human erythrocytes by cystalysin, an L-cysteine desulfhydrase from Treponema denticola," *Oral Microbiol Immunol*, vol. 14, no. 3, pp. 153–164, Jun. 1999, doi: 10.1034/J.1399-302X.1999.140303.X.

[97] M. R. Filipovic, J. Zivanovic, B. Alvarez, and R. Banerjee, "Chemical Biology of H2S Signaling through Persulfidation," *Chem Rev*, vol. 118, no. 3, pp. 1253–1337, Feb. 2018, doi: 10.1021/ACS.CHEMREV.7B00205.

[98] M. Fu, W. Zhang, L. Wu, G. Yang, H. Li, and R. Wang, "Hydrogen sulfide (H2S) metabolism in mitochondria and its regulatory role in energy production," *Proc Natl Acad Sci U S A*, vol. 109, no. 8, pp. 2943–2948, Feb. 2012, doi: 10.1073/PNAS.1115634109.

[99] W. Zhao, J. Zhang, Y. Lu, and R. Wang, "The vasorelaxant effect of H2S as a novel endogenous gaseous KATP channel opener," *EMBO Journal*, vol. 20, no. 21, pp. 6008–6016, Nov. 2001, doi: 10.1093/emboj/20.21.6008.

[100] J. Elies *et al.*, "Hydrogen sulfide inhibits Cav3.2 T-type Ca2+ channels," *FASEB J*, vol. 28, no. 12, pp. 5376–5387, Dec. 2014, doi: 10.1096/FJ.14-257113.

[101] A. Martelli *et al.*, "Vasorelaxation by hydrogen sulphide involves activation of Kv7 potassium channels," *Pharmacol*

Res, vol. 70, no. 1, pp. 27–34, Apr. 2013, doi: 10.1016/J.PHRS.2012.12.005.

[102] L. Testai *et al.*, "Persulfidation of mitoKv7.4 channels contributes to the cardioprotective effects of the H2S-donor Erucin against ischemia/reperfusion injury," *Biochem Pharmacol*, vol. 215, Sep. 2023, doi: 10.1016/J.BCP.2023.115728.

[103] D. Avanzato, A. Merlino, S. Porrera, R. Wang, L. Munaron, and D. Mancardi, "Role of calcium channels in the protective effect of hydrogen sulfide in rat cardiomyoblasts," *Cell Physiol Biochem*, vol. 33, no. 4, pp. 1205–1214, 2014, doi: 10.1159/000358690.

[104] A. K. Mustafa *et al.*, "Hydrogen sulfide as endothelium-derived hyperpolarizing factor sulfhydrates potassium channels," *Circ Res*, vol. 109, no. 11, pp. 1259–1268, Nov. 2011, doi: 10.1161/CIRCRESAHA.111.240242.

[105] M. Lu *et al.*, "Hydrogen sulfide inhibits plasma renin activity," *J Am Soc Nephrol*, vol. 21, no. 6, pp. 993–1002, Jun. 2010, doi: 10.1681/ASN.2009090949.

[106] C. C. Bauer, J. P. Boyle, K. E. Porter, and C. Peers, "Modulation of Ca(2+) signalling in human vascular endothelial cells by hydrogen sulfide," *Atherosclerosis*, vol. 209, no. 2, pp. 374–380, Apr. 2010, doi: 10.1016/J.ATHEROSCLEROSIS.2009.10.004.

[107] G. H. Liang, Q. Xi, C. W. Leffler, and J. H. Jaggar, "Hydrogen sulfide activates Ca^{2+} sparks to induce cerebral arteriole dilatation," *J Physiol*, vol. 590, no. 11, pp. 2709–2720, Jun. 2012, doi: 10.1113/JPHYSIOL.2011.225128.

[108] M. Bucci *et al.*, "Hydrogen sulfide is an endogenous inhibitor of phosphodiesterase activity," *Arterioscler Thromb Vasc Biol*, vol. 30, no. 10, pp. 1998–2004, Oct. 2010, doi: 10.1161/ATVBAHA.110.209783.

[109] Z. T. Kelleher, A. Matsumoto, J. S. Stamler, and H. E. Marshall, "NOS2 regulation of NF-kappaB by S-nitrosylation of p65," *J Biol Chem*, vol. 282, no. 42, pp. 30667–30672, Oct. 2007, doi: 10.1074/JBC.M705929200.

[110] D. Zhang, J. Du, C. Tang, Y. Huang, and H. Jin, "H2S-Induced Sulfhydration: Biological Function and Detection Methodology," *Front Pharmacol*, vol. 8, no. SEP, Sep. 2017, doi: 10.3389/FPHAR.2017.00608.

[111] G. Yang *et al.*, "Hydrogen sulfide protects against cellular senescence via S-sulfhydration of Keap1 and activation of Nrf2," *Antioxid Redox Signal*, vol. 18, no. 15, pp. 1906–1919, May 2013, doi: 10.1089/ARS.2012.4645.

[112] S. K. Yan, T. Chang, H. Wang, L. Wu, R. Wang, and Q. H. Meng, "Effects of hydrogen sulfide on homocysteine-induced oxidative stress in vascular smooth muscle cells," *Biochem Biophys Res Commun*, vol. 351, no. 2, pp. 485–491, Dec. 2006, doi: 10.1016/J.BBRC.2006.10.058.

[113] O. Kabil and R. Banerjee, "Characterization of patient mutations in human persulfide dioxygenase (ETHE1) involved in H2S catabolism," *J Biol Chem*, vol. 287, no. 53, pp. 44561–44667, Dec. 2012, doi: 10.1074/JBC.M112.407411.

[114] G. Yang, G. Tang, L. Zhang, L. Wu, and R. Wang, "The pathogenic role of cystathionine γ-lyase/hydrogen sulfide in streptozotocin-induced diabetes in mice," *Am J Pathol*, vol. 179, no. 2, pp. 869–879, Aug. 2011, doi: 10.1016/J.AJPATH.2011.04.028.

[115] M. I. Hassan *et al.*, "Platelet-derived growth factor-BB induces cystathionine γ-lyase expression in rat mesangial cells via a redox-dependent mechanism," *Br J Pharmacol*, vol. 166, no. 8, pp. 2231–2242, Aug. 2012, doi: 10.1111/J.1476-5381.2012.01949.X.

[116] B. Renga, A. Mencarelli, M. Migliorati, E. Distrutti, and S. Fiorucci, "Bile-acid-activated farnesoid X receptor regulates hydrogen sulfide production and hepatic microcirculation," *World J Gastroenterol*, vol. 15, no. 17, pp. 2097–2108, May 2009, doi: 10.3748/WJG.15.2097.

[117] G. Yang *et al.*, "Increased neointimal formation in cystathionine gamma-lyase deficient mice: role of hydrogen sulfide in α5β1-integrin and matrix metalloproteinase-2 expression in smooth muscle cells," *J Mol Cell Cardiol*, vol. 52, no. 3, pp. 677–688, Mar. 2012, doi: 10.1016/J.YJMCC.2011.12.004.

[118] U. Sen *et al.*, "Increased endogenous H2S generation by CBS, CSE, and 3MST gene therapy improves ex vivo renovascular relaxation in hyperhomocysteinemia," *Am J Physiol Cell Physiol*, vol. 303, no. 1, Jul. 2012, doi: 10.1152/AJPCELL.00398.2011.

[119] R. Wang, “Physiological implications of hydrogen sulfide: a whiff exploration that blossomed,” *Physiol Rev*, vol. 92, no. 2, pp. 791–896, Apr. 2012, doi: 10.1152/PHYSREV.00017.2011.
[120] K. R. Olson, “The therapeutic potential of hydrogen sulfide: separating hype from hope,” *Am J Physiol Regul Integr Comp Physiol*, vol. 301, no. 2, Aug. 2011, doi: 10.1152/AJPREGU.00045.2011.
[121] Y. Cheng, J. F. Ndisang, G. Tang, K. Cao, and R. Wang, “Hydrogen sulfide-induced relaxation of resistance mesenteric artery beds of rats,” *Am J Physiol Heart Circ Physiol*, vol. 287, no. 5, Nov. 2004, doi: 10.1152/AJPHEART.00331.2004.
[122] M. Wang, Z. Guo, and S. Wang, “Regulation of cystathionine γ-lyase in mammalian cells by hypoxia,” *Biochem Genet*, vol. 52, no. 1–2, pp. 29–37, Feb. 2014, doi: 10.1007/S10528-013-9624-7.
[123] N. Siebert, D. Cantré, C. Eipel, and B. Vollmar, “H2S contributes to the hepatic arterial buffer response and mediates vasorelaxation of the hepatic artery via activation of K(ATP) channels,” *Am J Physiol Gastrointest Liver Physiol*, vol. 295, no. 6, Dec. 2008, doi: 10.1152/AJPGI.90484.2008.
[124] G. Tang, L. Wu, and R. Wang, “Interaction of hydrogen sulfide with ion channels,” *Clin Exp Pharmacol Physiol*, vol. 37, no. 7, pp. 753–763, 2010, doi: 10.1111/J.1440-1681.2010.05351.X.
[125] G. Tang, L. Wu, W. Liang, and R. Wang, “Direct stimulation of K(ATP) channels by exogenous and endogenous hydrogen sulfide in vascular smooth muscle cells,” *Mol Pharmacol*, vol. 68, no. 6, pp. 1757–1764, Dec. 2005, doi: 10.1124/MOL.105.017467.
[126] R. Fitzgerald *et al.*, “H2S relaxes isolated human airway smooth muscle cells via the sarcolemmal K(ATP) channel,” *Biochem Biophys Res Commun*, vol. 446, no. 1, pp. 393–398, Mar. 2014, doi: 10.1016/J.BBRC.2014.02.129.
[127] B. Jiang, G. Tang, K. Cao, L. Wu, and R. Wang, “Molecular mechanism for H(2)S-induced activation of K(ATP) channels,” *Antioxid Redox Signal*, vol. 12, no. 10, pp. 1167–1178, May 2010, doi: 10.1089/ARS.2009.2894.

[128] S. W. Lee, Y. Cheng, P. K. Moore, and J. S. Bian, “Hydrogen sulphide regulates intracellular pH in vascular smooth muscle cells,” *Biochem Biophys Res Commun*, vol. 358, no. 4, pp. 1142–1147, Jul. 2007, doi: 10.1016/J.BBRC.2007.05.063.

[129] Y. H. Liu, C. D. Yan, and J. S. Bian, “Hydrogen sulfide: a novel signaling molecule in the vascular system,” *J Cardiovasc Pharmacol*, vol. 58, no. 6, pp. 560–569, Dec. 2011, doi: 10.1097/FJC.0B013E31820EB7A1.

[130] M. Bucci *et al.*, “Hydrogen sulfide is an endogenous inhibitor of phosphodiesterase activity,” *Arterioscler Thromb Vasc Biol*, vol. 30, no. 10, pp. 1998–2004, Oct. 2010, doi: 10.1161/ATVBAHA.110.209783.

[131] S. Kubo, Y. Kurokawa, I. Doe, T. Masuko, F. Sekiguchi, and A. Kawabata, “Hydrogen sulfide inhibits activity of three isoforms of recombinant nitric oxide synthase,” *Toxicology*, vol. 241, no. 1–2, pp. 92–97, Nov. 2007, doi: 10.1016/J.TOX.2007.08.087.

[132] M. Y. Ali *et al.*, “Regulation of vascular nitric oxide in vitro and in vivo; a new role for endogenous hydrogen sulphide?,” *Br J Pharmacol*, vol. 149, no. 6, pp. 625–634, Nov. 2006, doi: 10.1038/SJ.BJP.0706906.

[133] J. L. Jia, Y. H. Liu, E. S. W. Khin, and J. S. Bian, “Vasoconstrictive effect of hydrogen sulfide involves downregulation of cAMP in vascular smooth muscle cells,” *Am J Physiol Cell Physiol*, vol. 295, no. 5, Nov. 2008, doi: 10.1152/AJPCELL.00195.2008.

[134] M. N. Hughes, M. N. Centelles, and K. P. Moore, “Making and working with hydrogen sulfide: The chemistry and generation of hydrogen sulfide in vitro and its measurement in vivo: a review,” *Free Radic Biol Med*, vol. 47, no. 10, pp. 1346–1353, Nov. 2009, doi: 10.1016/J.FREERADBIOMED.2009.09.018.

[135] C. R. Powell, K. M. Dillon, and J. B. Matson, “A Review of Hydrogen Sulfide (H2S) Donors: Chemistry and Potential Therapeutic Applications,” *Biochem Pharmacol*, vol. 149, p. 110, Mar. 2018, doi: 10.1016/J.BCP.2017.11.014.

[136] J. D. Clarke *et al.*, “Bioavailability and inter-conversion of sulforaphane and erucin in human subjects consuming broccoli sprouts or broccoli supplement in a cross-over study

design," *Pharmacol Res*, vol. 64, no. 5, pp. 456–463, 2011, doi: 10.1016/J.PHRS.2011.07.005.
[137] V. Citi *et al.*, "Anticancer properties of erucin, an H2 S-releasing isothiocyanate, on human pancreatic adenocarcinoma cells (AsPC-1)," *Phytother Res*, vol. 33, no. 3, pp. 845–855, Mar. 2019, doi: 10.1002/PTR.6278.
[138] A. Martelli *et al.*, "Erucin exhibits vasorelaxing effects and antihypertensive activity by H2 S-releasing properties," *Br J Pharmacol*, vol. 177, no. 4, pp. 824–835, Feb. 2020, doi: 10.1111/BPH.14645.
[139] K. Suzuki, M. Sagara, C. Aoki, S. Tanaka, and Y. Aso, "Clinical Implication of Plasma Hydrogen Sulfide Levels in Japanese Patients with Type 2 Diabetes," *Intern Med*, vol. 56, no. 1, pp. 17–21, 2017, doi: 10.2169/INTERNALMEDICINE.56.7403.
[140] H. Zhao *et al.*, "Hydrogen sulfide improves diabetic wound healing in ob/ob mice via attenuating inflammation," *J Diabetes Complications*, vol. 31, no. 9, pp. 1363–1369, Sep. 2017, doi: 10.1016/J.JDIACOMP.2017.06.011.
[141] V. Brancaleone, F. Roviezzo, V. Vellecco, L. De Gruttola, M. Bucci, and G. Cirino, "Biosynthesis of H2S is impaired in non-obese diabetic (NOD) mice," *Br J Pharmacol*, vol. 155, no. 5, pp. 673–680, Nov. 2008, doi: 10.1038/BJP.2008.296.
[142] M. Bucci *et al.*, "Hydrogen sulfide accounts for the peripheral vascular effects of zofenopril independently of ACE inhibition," *Cardiovasc Res*, vol. 102, no. 1, pp. 138–147, 2014, doi: 10.1093/CVR/CVU026.
[143] N. Liu *et al.*, "Hydrogen Sulphide modulating mitochondrial morphology to promote mitophagy in endothelial cells under high-glucose and high-palmitate," *J Cell Mol Med*, vol. 21, no. 12, pp. 3190–3203, Dec. 2017, doi: 10.1111/JCMM.13223.
[144] V. Vellecco *et al.*, "Vascular effects of linagliptin in non-obese diabetic mice are glucose-independent and involve positive modulation of the endothelial nitric oxide synthase (eNOS)/caveolin-1 (CAV-1) pathway," *Diabetes Obes Metab*, vol. 18, no. 12, pp. 1236–1243, Dec. 2016, doi: 10.1111/DOM.12750.

[145] A. Katsouda *et al.*, “CTH/MPST double ablation results in enhanced vasorelaxation and reduced blood pressure via upregulation of the eNOS/sGC pathway,” *Front Pharmacol*, vol. 14, 2023, doi: 10.3389/FPHAR.2023.1090654.
[146] N. A. Sallam and I. Laher, “Redox Signaling and Regional Heterogeneity of Endothelial Dysfunction in db/db Mice,” *Int J Mol Sci*, vol. 21, no. 17, pp. 1–20, Sep. 2020, doi: 10.3390/IJMS21176147.
[147] M. Bucci *et al.*, “In vivo delivery of the caveolin-1 scaffolding domain inhibits nitric oxide synthesis and reduces inflammation,” *Nat Med*, vol. 6, no. 12, pp. 1362–1367, 2000, doi: 10.1038/82176.
[148] T. Y. Lam *et al.*, “Impairment of the vascular relaxation and differential expression of caveolin-1 of the aorta of diabetic +db/+db mice,” *Eur J Pharmacol*, vol. 546, no. 1–3, pp. 134–141, Sep. 2006, doi: 10.1016/J.EJPHAR.2006.07.003.
[149] M. Bucci *et al.*, “Diabetic mouse angiopathy is linked to progressive sympathetic receptor deletion coupled to an enhanced caveolin-1 expression,” *Arterioscler Thromb Vasc Biol*, vol. 24, no. 4, pp. 721–726, Apr. 2004, doi: 10.1161/01.ATV.0000122362.44628.09.
[150] V. Vellecco *et al.*, “Anomalous Kv 7 channel activity in human malignant hyperthermia syndrome unmasks a key role for H2 S and persulfidation in skeletal muscle,” *Br J Pharmacol*, vol. 177, no. 4, pp. 810–823, Feb. 2020, doi: 10.1111/BPH.14700.
[151] V. Vellecco *et al.*, “Phosphodiesterases S-sulfhydration contributes to human skeletal muscle function,” *Pharmacol Res*, vol. 177, Mar. 2022, doi: 10.1016/J.PHRS.2022.106108.
[152] V. Ciccone *et al.*, “Anti-Inflammatory Effect of the Natural H2S-Donor Erucin in Vascular Endothelium,” *Int J Mol Sci*, vol. 23, no. 24, Dec. 2022, doi: 10.3390/IJMS232415593.
[153] C. E. Alpers and K. L. Hudkins, “Mouse models of diabetic nephropathy,” *Curr Opin Nephrol Hypertens*, vol. 20, no. 3, pp. 278–284, May 2011, doi: 10.1097/MNH.0B013E3283451901.
[154] S. Banquet *et al.*, “Role of G(i/o)-Src kinase-PI3K/Akt pathway and caveolin-1 in β_2-adrenoceptor coupling to endothelial NO synthase in mouse pulmonary artery,” *Cell*

Signal, vol. 23, no. 7, pp. 1136–1143, Jul. 2011, doi: 10.1016/J.CELLSIG.2011.02.008.

[155] V. Vellecco *et al.*, "Biphasic inflammatory response induced by intra-plantar injection of L-cysteine: Role of CBS-derived H2S and S1P/NO signaling," *Biomed Pharmacother*, vol. 167, Nov. 2023, doi: 10.1016/J.BIOPHA.2023.115536.

[156] E. Mitidieri *et al.*, "β3 adrenergic receptor activation relaxes human corpus cavernosum and penile artery through a hydrogen sulfide/cGMP-dependent mechanism," *Pharmacol Res*, vol. 124, pp. 100–104, Oct. 2017, doi: 10.1016/J.PHRS.2017.07.025.

[157] Z. Zhou *et al.*, "Regulation of soluble guanylyl cyclase redox state by hydrogen sulfide," *Pharmacol Res*, vol. 111, pp. 556–562, Sep. 2016, doi: 10.1016/J.PHRS.2016.06.029.

[158] M. A. Olivencia *et al.*, "Hydrogen sulfide regulates the redox state of soluble guanylate cyclase in CSE-/- mice corpus cavernosum microcirculation," *Pharmacol Res*, vol. 194, Aug. 2023, doi: 10.1016/J.PHRS.2023.106834.

[159] S. I. Bibli and I. Fleming, "Oxidative Post-Translational Modifications: A Focus on Cysteine S- Sulfhydration and the Regulation of Endothelial Fitness," *Antioxid Redox Signal*, vol. 35, no. 18, pp. 1494–1514, Dec. 2021, doi: 10.1089/ARS.2021.0162.

[160] B. D. Paul and S. H. Snyder, "H_2S signalling through protein sulfhydration and beyond," *Nat Rev Mol Cell Biol*, vol. 13, no. 8, pp. 499–507, Aug. 2012, doi: 10.1038/NRM3391.

[161] S. Makino, K. Kunimoto, Y. Muraoka, Y. Mizushima, K. Katagiri, and Y. Tochino, "Breeding of a non-obese, diabetic strain of mice," *Jikken Dobutsu*, vol. 29, no. 1, pp. 1–13, 1980, doi: 10.1538/EXPANIM1978.29.1_1.

[162] S. Kawamoto *et al.*, "Suppression of T(h)1 cell activation and prevention of autoimmune diabetes in NOD mice by local expression of viral IL-10," *Int Immunol*, vol. 13, no. 5, pp. 685–694, 2001, doi: 10.1093/INTIMM/13.5.685.

[163] S. Shao, F. He, Y. Yang, G. Yuan, M. Zhang, and X. Yu, "Th17 cells in type 1 diabetes," *Cell Immunol*, vol. 280, no. 1, pp. 16–21, Nov. 2012, doi: 10.1016/J.CELLIMM.2012.11.001.

[164] S. Dong *et al.*, "The effect of low-dose IL-2 and Treg adoptive cell therapy in patients with type 1 diabetes," *JCI*

Insight, vol. 6, no. 18, Sep. 2021, doi: 10.1172/JCI.INSIGHT.147474.

[165] D. Mozaffarian *et al.*, "Heart Disease and Stroke Statistics-2016 Update: A Report From the American Heart Association," *Circulation*, vol. 133, no. 4, pp. e38–e48, Jan. 2016, doi: 10.1161/CIR.0000000000000350.

[166] L. Sasset, Y. Zhang, T. M. Dunn, and A. Di Lorenzo, "Sphingolipid De Novo Biosynthesis: A Rheostat of Cardiovascular Homeostasis," *Trends Endocrinol Metab*, vol. 27, no. 11, pp. 807–819, Nov. 2016, doi: 10.1016/J.TEM.2016.07.005.

[167] D. Siow, M. Sunkara, A. Morris, and B. Wattenberg, "Regulation of de novo sphingolipid biosynthesis by the ORMDL proteins and sphingosine kinase-1," *Adv Biol Regul*, vol. 57, pp. 42–54, Jan. 2015, doi: 10.1016/J.JBIOR.2014.09.002.

[168] A. Cantalupo *et al.*, "Nogo-B regulates endothelial sphingolipid homeostasis to control vascular function and blood pressure," *Nat Med*, vol. 21, no. 9, pp. 1028–1037, Sep. 2015, doi: 10.1038/NM.3934.

[169] A. Marino, Y. Zhang, L. Rubinelli, M. A. Riemma, J. E. Ip, and A. Di Lorenzo, "Pressure overload leads to coronary plaque formation, progression, and myocardial events in ApoE-/- mice," *JCI Insight*, vol. 4, no. 9, May 2019, doi: 10.1172/JCI.INSIGHT.128220.

[170] J. F. Bentzon and E. Falk, "Atherosclerotic lesions in mouse and man: is it the same disease?," *Curr Opin Lipidol*, vol. 21, no. 5, pp. 434–440, Oct. 2010, doi: 10.1097/MOL.0B013E32833DED6A.

[171] P. Duewell *et al.*, "NLRP3 inflammasomes are required for atherogenesis and activated by cholesterol crystals," *Nature*, vol. 464, no. 7293, pp. 1357–1361, Apr. 2010, doi: 10.1038/NATURE08938.

[172] P. Tiwari, B. N. Mishra, and N. S. Sangwan, "Phytochemical and pharmacological properties of Gymnema sylvestre: an important medicinal plant," *Biomed Res Int*, vol. 2014, 2014, doi: 10.1155/2014/830285.

[173] A. F. G. Cicero, F. Fogacci, and M. Banach, "Red Yeast Rice for Hypercholesterolemia," *Methodist Debakey Cardiovasc*

J, vol. 15, no. 3, pp. 192–199, Jul. 2019, doi: 10.14797/MDCJ-15-3-192.

[174] G. Klein, J. Kim, K. Himmeldirk, Y. Cao, and X. Chen, "Antidiabetes and Anti-obesity Activity of Lagerstroemia speciosa," *Evid Based Complement Alternat Med*, vol. 4, no. 4, pp. 401–407, Dec. 2007, doi: 10.1093/ECAM/NEM013.

[175] M. Z. De Souza Zanchet, G. M. Nardi, L. De Oliveira Souza Bratti, F. B. Filippin-Monteiro, and C. Locatelli, "Lycium barbarum Reduces Abdominal Fat and Improves Lipid Profile and Antioxidant Status in Patients with Metabolic Syndrome," *Oxid Med Cell Longev*, vol. 2017, 2017, doi: 10.1155/2017/9763210.

[176] N. L. Urizar and D. D. Moore, "GUGULIPID: a natural cholesterol-lowering agent," *Annu Rev Nutr*, vol. 23, pp. 303–313, 2003, doi: 10.1146/ANNUREV.NUTR.23.011702.073102.

[177] C. Carresi *et al.*, "The Effect of Natural Antioxidants in the Development of Metabolic Syndrome: Focus on Bergamot Polyphenolic Fraction," *Nutrients*, vol. 12, no. 5, May 2020, doi: 10.3390/NU12051504.

[178] A. Melchini and M. H. Traka, "Biological profile of erucin: a new promising anticancer agent from cruciferous vegetables," *Toxins (Basel)*, vol. 2, no. 4, pp. 593–612, Apr. 2010, doi: 10.3390/TOXINS2040593.

[179] M. Villatoro-Pulido *et al.*, "An approach to the phytochemical profiling of rocket [Eruca sativa (Mill.) Thell]," *J Sci Food Agric*, vol. 93, no. 15, pp. 3809–3819, Dec. 2013, doi: 10.1002/JSFA.6286.

[180] A. Martelli *et al.*, "The H2S-Donor Erucin Exhibits Protective Effects against Vascular Inflammation in Human Endothelial and Smooth Muscle Cells," *Antioxidants (Basel)*, vol. 10, no. 6, Jun. 2021, doi: 10.3390/ANTIOX10060961.

[181] A. E. Wagner, A. M. Terschluesen, and G. Rimbach, "Health promoting effects of brassica-derived phytochemicals: from chemopreventive and anti-inflammatory activities to epigenetic regulation," *Oxid Med Cell Longev*, vol. 2013, 2013, doi: 10.1155/2013/964539.